High Dimensional Modulation and MIMO Techniques for Access Networks

Binti Othman, Maisara

Publication date:
2012

Document Version
Publisher's PDF, also known as Version of record

High Dimensional Modulation and MIMO Techniques for Access Networks

Maisara Binti Othman

Supervisors:
Professor Idelfonso Tafur Monroy
Assistant Professor Jesper Bevensee Jensen

Delivery Date: 1st October 2012

DTU Fotonik
Department of Photonics Engineering
Technical University of Denmark
2800 Kgs. Lyngby
DENMARK

DTU Fotonik
Institut for Fotonik

Abstract

Exploration of advanced modulation formats and multiplexing techniques for next generation optical access networks are of interest as promising solutions for delivering multiple services to end-users. This thesis addresses this from two different angles: high dimensionality carrierless amplitude-phase (CAP) and multiple-input multiple-output (MIMO) radio-over-fiber (RoF) systems.

High dimensionality CAP modulation has been investigated in optical fiber systems. In this project we conducted the first experimental demonstration of 3 and 4 dimensional CAP with bit rates up to 10 Gb/s. These results indicate the potentiality of supporting multiple users with converged services. At the same time, orthogonal division multiple access (ODMA) systems for multiple possible dimensions of CAP modulation has been demonstrated for user and service allocation in wavelength division multiplexing (WDM) optical access network.

2×2 MIMO RoF employing orthogonal frequency division multiplexing (OFDM) with 5.6 GHz RoF signaling over all-vertical cavity surface emitting lasers (VCSEL) WDM passive optical networks (PONs). We have employed polarization division multiplexing (PDM) to further increase the capacity per wavelength of the femto-cell network. Bit rate up to 1.59 Gbps with fiber-wireless transmission over 1 m air distance is demonstrated.

The results presented in this thesis demonstrate the feasibility of high dimensionality CAP in increasing the number of dimensions and their potentially to be utilized for multiple service allocation to different users. MIMO multiplexing techniques with OFDM provides the scalability in increasing spectral efficiency and bit rates for RoF systems.

High dimensional CAP and MIMO multiplexing techniques are two promising solutions for supporting wired and hybrid wired-wireless access networks.

Resumé

Udnyttelse af avancerede modulationformater og multipleksningsteknikker til næste generations optiske access netværker er lovende løsninger, som kan levere multiple funktionaliteter til slutbrugerne. Denne afhandling anskuer dette fra to vinkler: Høj-dimensionel 'carrierless' amplitude- og fase-modulation (CAP) samt multipelt input multipelt output (MIMO) radio-over-fiber (RoF) systemer.

CAP med højere dimensionalitet end 2 er blevet undersøgt med henblik på brug i fiberoptiske systemer. I dette projekt har vi gennemført den første eksperimentelle demonstration af 3- og 4- dimensional CAP med bit rater op til 10 Gb/s. Disse resultater indikerer et potentiale til at levere konvergerede ydelser til flere brugere ved høje bit rater. 'Orthogonal division multiple access' (ODMA) systemer hvor de mulige multiple CAP-dimensioner er blevet distribueret til slutbrugerne i et bølgelængde multiplekset (WDM) netværk er blevet demonstreret.

Et andet vigtigt resultat fra denne afhandling er den første demonstration af et 2×2 MIMO OFDM fiber/5.6 GHz trådløst passivt optisk netværk (PON), der udelukkende anvender VCSELs som optiske kilder. Baseret på dette koncept har vi anvendt polarisations division multipleksning (PDM) til yderligere at øge kapaciteten per bølgelængde i femtocelle netværk. Bit rater op til 1.59 Gb/s med fibertransmission og trådløs transmission over 1 m er blevet demonstreret eksperimentelt.

Resultaterne, der er præsenteret I denne afhandling, demonstrerer mulighederne i høj-dimensional CAP til at allokere forskellige ydelser til forskellige brugere. MIMO multipleksning med OFDM tilbyder skalerbarhed samt øget spektral effektivitet og bit rate i RoF systemer.

De to teknologier kan ses som to mulige løsninger til næste generations hybride trådløse/optiske access netværk.

Acknowledgements

First of all, I would like to attribute my sincere gratitude to my supervisor and co-supervisor, Professor Idelfonso Tafur Monroy and Assistant Professor Jesper Bevensee Jensen for their encouragement, support and enthusiasm. They always spent time with me and guided me through the problems that I have encountered. It is a privilege to work with them. Thanks a lot from my heart.

I am very grateful to the Ministry of Higher Education of Malaysia (MOHE) and University of Tun Hussein Onn Malaysia (UTHM) for providing me with a scholarship. I would not have completed a Ph.D without this financial assistance.

My warmest thanks are extended to my closest friend Lei, Xu, Xiaodan, and Ying. We have spent time together in the lab doing the experiment with a very good team working spirit. My sincere thanks to Kamau and Xianbin for their practical assistance. I would also like to thank all my colleagues at Metro-Access group, Darko, JJ, Neil, Alexey, Thang, Valeria, Roberto, Robert, Silvia, Alexander, Bomin, Miguel, David and also my colleagues in DTU Fotonik. I must also thank Evarist my ex-officemate in building 343 DTU Fotonik for sharing all the good food recipes.

I want to thank to all my Malaysian friends in Denmark for friendship through all these years. Many thanks for supporting each other, and I really hope this friendship will last forever.

The last, and foremost, I would like to thank my parents, mother in law, my brothers, my husband, Shamsudin Bin Awang and my two handsome heroes: Muhammad Hazlam and Muhammad Hulaif. Thanks for their 'dua', love, patience, and encouragement. This made my Ph.D study possible and joyful at DTU Fotonik.

Summary of Original Work

This thesis is based on the following original publications:

PAPER 1 M. B. Othman, X. Zhang, L. Deng, M. Wieckowski, J. Bevensee Jensen, and I. Tafur Monroy, "Experimental Investigations Demonstration of 3D/4D-CAP Modulation with DM-VCSELs," *Photonic Technology Letters*, accepted for publication, 2012.

PAPER 2 M. B. Othman, X. Zhang, L. Deng, J. Bevensee Jensen, and I. Tafur Monroy, "Experimental Demonstration of 3D/4D-CAP Modulation Employing CT-CMA Channel Estimation," submitted to *Journal of Lightwave Technology*, 2012.

PAPER 3 M. B. Othman, J. Bevensee Jensen, Xu Zhang, and I. Tafur Monroy, "Performance Evaluation of Spectral Amplitude Codes for OCDMA PON," in *(15th International Conference on Optical Network Design and Modeling (ONDM)*, 2011.

PAPER 4 M. B. Othman, X. Zhang, J. Bevensee Jensen, and I. Tafur Monroy, "Using CAP Dimensionality for Service and User Allocation for Optical Access Networks ," in *Asia Communications and Photonics Conference (ACP)*, Guangzhou, China, accepted for publication, 2012.

PAPER 5 X. Zhang, M. B. Othman, X. Pang, J. Bevensee Jensen, and I. Tafur Monroy, "Bi-directional Multi Dimension CAP Transmission for Smart Grid Communication Services," in *Asia Communications*

and Photonics Conference (ACP), Guangzhou, China, accepted for publication, 2012.

PAPER 6 M. B. Othman, L. Deng, X. Pang, J. Caminos, W. Kozuch, K. Prince, J. Bevensee Jensen, and I. Tafur Monroy, "Directly modulated VCSELs for 2×2 MIMO-OFDM radio over fiber in WDM-PON," in *37th European Conference and Exhibition on Optical Communication (ECOC)*, Geneva, Switzerland, paper We.10.P1.119, 2011.

PAPER 7 M. B. Othman, L. Deng, X. Pang, J. Caminos, W. Kozuch, K. Prince, X. Yu, J. Bevensee Jensen, and I. Tafur Monroy, "MIMO-OFDM WDM PON with DM-VCSEL for femtocells application," *Optics Express* , vol. 19, no. 26, pp. B537—B542, 2011.

PAPER 8 X. Pang, L. Deng, Y. Zhao, M. B. Othman, X. Yu, J. Bevensee Jensen, D. Zibar, and I. Tafur Monroy, "Seamless Translation of Optical Fiber PolMux-OFDM into a 2×2 MIMO Wireless Transmission Enabled by Digital Training-Based Fiber-Wireless Channel Estimation," in *Asia Communications and Photonics Conference and Exhibition*, Proceedings of SPIE, 2011.

PAPER 9 L. Deng, X. Pang, Y. Zhao, M. B. Othman, J. Bevensee Jensen, Darko Zibar, Xianbin Yu, Deming Liu, and I. Tafur Monroy, "2×2 MIMO-OFDM Gigabit fiber-wireless access system based on polarization division multiplexed WDM-PON," *Optics Express.* vol. 20, no. 4, pp. 4369-4375, 2012.

PAPER 10 X. Pang, Y. Zhao, L. Deng, M. B. Othman, X. Yu, J. Bevensee Jensen, and I. Tafur Monroy, "A Spectral Efficient PoIMux-QPSK-RoF System with CMA-Based Blind Estimation of a 2×2 MIMO Wireless Channel," in *IEEE Photonics Conference, (IPO)*, paper TuM2, pp. 296–297, 2011.

PAPER 11 Y. Zhao, X. Pang, L. Deng, M. B. Othman, X. Yu, X. Zheng, H. Zhang and I. Tafur Monroy, "Experimental Demonstration of 5-Gb/s Polarization-Multiplexed Fiber-Wireless MIMO Systems," in

International Topical Meeting on & Microwave Photonics Conference (MWP/APMP), pp. 13–16, 2011.

Other scientific reports:

[C1] N. Guerrero Gonzalez, A. Caballero, R. Borkowski, V. Arlunno, T. T. Pham, R. Rodes, X. Zhang, M. B. Othman, K. Prince, X. Yu, J. B. Jensen, D. Zibar, and I. Tafur Monroy, "Reconfigurable digital coherent receiver for metro-access networks supporting mixed modulation formats and bit-rates," in *Proc. Optical Fiber Communication Conference and Exposition, OFC/NFOEC*, Los Angeles, CA, paper OMW7, 2011, .

[C2] V. Arlunno, N. Guerrero Gonzalez, A. Caballero, Antonio; R. Borkowski, T. T. Pham, R. Rodes, X. Zhang, M. B. Othman, K. Prince, X. Yu, J. B. Jensen, D. Zibar, and I. Tafur Monroy, "Reconfigurable Digital Coherent Receiver for Hybrid Optical Fiber/Wireless Metro-Access Networks," in *Poster session presented at 2nd Annual Workshop on Photonic Technologies for Access and Biophotonics*, Stanford, CA, 2011.

[C3] K. Prince, X. Yu, N. Guerrero Gonzalez, A. Caballero, X. Zhang, R. Rodes, V. Arlunno, M. B. Othman, J. B. Jensen, D. Zibar, and I. Tafur Monroy,"Ultra-high throughput converged optical wireless links: challenges and opportunities : [invited]" in *8th Conference of Finnish-Russian University Cooperation in Telecommunications*, 2011.

Contents

Chapter 1

Introduction

This chapter provides an introduction to the topics of this thesis. An overview of the covered topics is presented in sections 1.3 and 1.4, and state-of the-art and beyond in sections 1.5 and 1.6. The contributions of this project are described in section 1.7. The introduction is structured into two main categories: multi-level, multi-dimensional carrierless amplitude-phase (CAP) modulation for access and in-home networks applications; and multi-input multi-output (MIMO) multiplexing schemes for radio-over-fiber networks.

1.1 Outline of the Thesis

This thesis is structured as follows: Chapter 1 introduces the context of the main research papers included in this thesis. It provides a short overview on high dimensionality CAP as one of the advanced modulation formats in optical fiber system and MIMO multiplexing techniques as a promising method to increase the data throughput and link range compared to the traditional single-input single-output (SISO) method. The impact of these two main fields is to support the next generation access network in wired and wireless link.

Chapter 2 describes the main contributions of the thesis. To conclude, Chapter 3 summarizes the main achievements of this thesis and provides an outlook on the prospects of the CAP modulation format and MIMO multiplexing techniques.

1.2 Optical Transmission for Next Generation Access and In-home Network

In the last few years attention has turned to the developments of so-called next generation telecommunication networks [1]. These networks comprise two segments: the next generation core (NGN), or backbone, and the next generation access (NGA) networks. Next generation core refers to the core internet protocol (IP) network and is characterized by the replacement of legacy transmission and switching equipment with IP technology in the core network. Next generation access refers to the access technology (optical fibre, copper or wireless) and its deployment, either to a street cabinet close to the customer premises in conjunction with copper-based infrastructure such as x-digital subscriber line (x-DSL), or with the deployment of fibre or wireless systems directly to the customer premises [2].

The term NGA is often used to describe fibre connections coming closer to the end-user, which may be typically characterized by significantly higher bandwidth than currently available technology, while providing better quality of service and greater uplink/downlink symmetry in data rates. As a result, the copper or cable wire is to an increasing extent replaced with fibre-optic technology. Wireless technologies can also be considered as NGA, indeed, wireless technologies can provide a vital option to extend and improve broadband coverage in particular scenarios.

Next generation access services facilitate network access while the applications provide an interface for information exchange. They differ from traditional access services as they are 'always on' and enable the integration of voice, data, images and video applications. Fig. 1.1 depicts the traditional access with dedicated services and next generation structure that enables the hosting of converged applications in a shared environment taken from [3].

Home access networks (HANs) are vital to end-to-end multimedia broadband service provisioning. The emerging services that end users are demanding, such as high-definition video streaming, video-calls and access to cloud computing, have put severe pressure on the telecommunication network infrastructure to provide high capacity links capable of supporting diverse service requirements in different customer-premises environments and at low cost. This demand has resulted in an evolution of short-range and wired access networks from the copper-based transmission systems with limited coverage and bandwidth to the use of photonic technologies achieving high capacity and long reach links [4, 5]. Fig. 1.2 shows the scenario

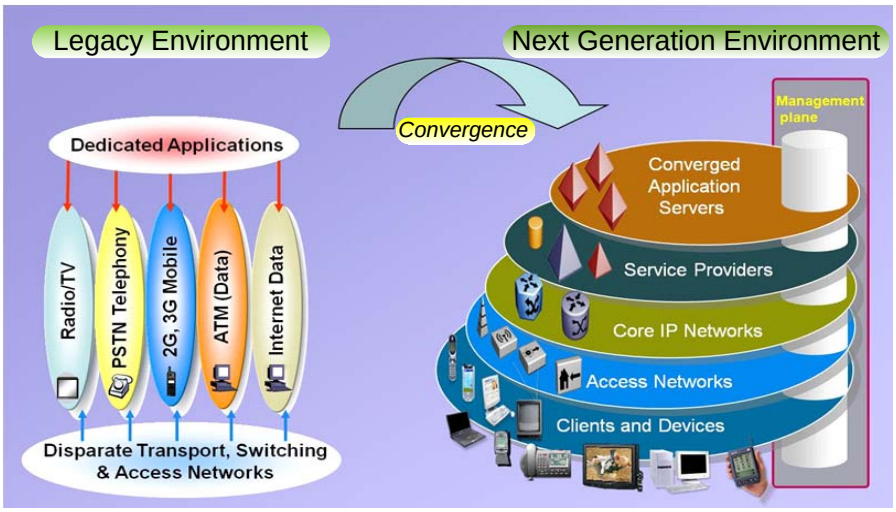

Figure 1.1: Traditional access environment with dedicated services (on the left) and next generation service environment (on the right) [3].

in home access network (HAN) with varieties of multimedia services with wired and wireless network for fiber-to-the-home (FTTH). To increase flexibility in the HAN, multiplexing and transparency to different transmission and modulation formats would be beneficial. Optical technologies give solutions for such architectures, with multipoint transparent architectures that can eventually use the wavelength domain to achieve multiplexing.

This Ph.D thesis focuses on the applications of high dimensionality CAP modulation in wired transmission for access and in-home networks. In addition, MIMO multiplexing scheme has been used for RoF wireless transmission for HAN with different multiplexing solutions such as wavelength division multiplexing (WDM) and polarization division multiplexing (PDM).

1.3 Advanced Modulation Formats for Optical Communication System

Historically, optical communication systems used a simple modulation format, where logical "1" was represented by the presence of light, and a logical "0" was represented by the absence of light. This modulation scheme is known as on-off keying (OOK). However, as the transmission distances and the bit rate per channel increase, and the channel spacing decreases, more

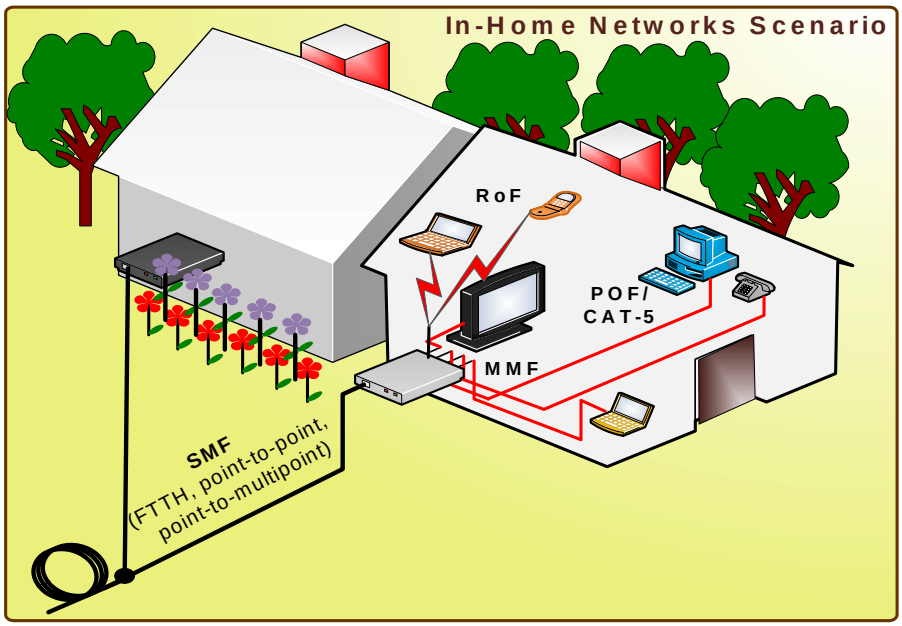

Figure 1.2: Fiber-to-the-home home access network with varieties of multimedia services supported with wired and wireless network in customer premises.

advanced modulation formats have been suggested to mitigate nonlinear transmission impairments, to improve receiver sensitivity and facilitate a per channel bit rate increase beyond the limits of binary systems [6, 7].

Multi-level modulation formats such as quadrature amplitude modulation (QAM) and differential quadrature phase shift keying (DQPSK) have received appreciable attention widely in optical communications [8]. In order to further increase spectral efficiency, even more advanced modulation formats are required. New formats have been proposed in [6]; combinations of amplitude shift keying (ASK) and DQPSK, DQPSK with inverse-return-to-zero (RZ) pulse shape and differential 8-ary phase shift keying (D8PSK). Besides increasing the number of levels, the number of dimensions also can be increased in order to increase the spectral utilization [9] and to support multiple service applications [10]. Therefore multi-level multi-dimensional carrierless amplitude-phase (CAP) have been proposed for digital subscriber line (DSL) during early and mid 1990s by the Bell Labs [11, 12]. Besides CAP, there is another competing and incompatible standard for modulating the asymmetrical digital subscriber line (ADSL) signal, known as discrete multitone (DMT). CAP treats the entire frequency spectrum as

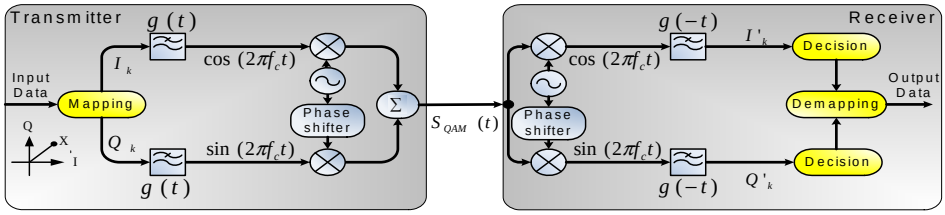

Figure 1.3: Block diagram of the QAM transceiver.

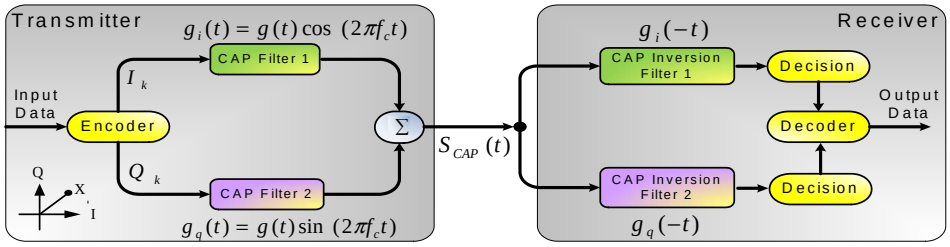

Figure 1.4: Block diagram of the CAP transceiver.

a single channel and optimizes the data rate over that channel. In contrast, DMT divides the bandwidth into sub-channels and optimizes the data rate for each sub-channel. DMT has been accepted as the standard by the American national standards institute (ANSI) and the European telecommunications standards institute (ETSI) [13, 14] due to the communications speed, bandwidth efficiency, spectral compatibility, robustness and power consumption.

1.3.1 Carrierless Amplitude-Phase Modulation (CAP)

CAP is a multi-dimensional and multi-level signal format employing orthogonal waveforms; one for each dimension. These waveforms are obtained from frequency domain filters with orthogonal impulse responses. In its principle, it is akin to QAM in the sense that both CAP and QAM supports multiple levels and modulation in more than one dimension. Contrary to QAM, however, CAP does not require the generation of sinusoidal carriers at the transmitter-receiver (transceiver) as shown in Fig. 1.3 and 1.4. Avoiding the carrier has two distinct advantages. First, less expensive digital transceiver implementation is required as the computation intensive multiplication operations needed for carrier modulation and demodulation becomes unnecessary. Secondly, the carrier's absence increases flexibility, such as changing the spectrum's properties, center frequency and shape.

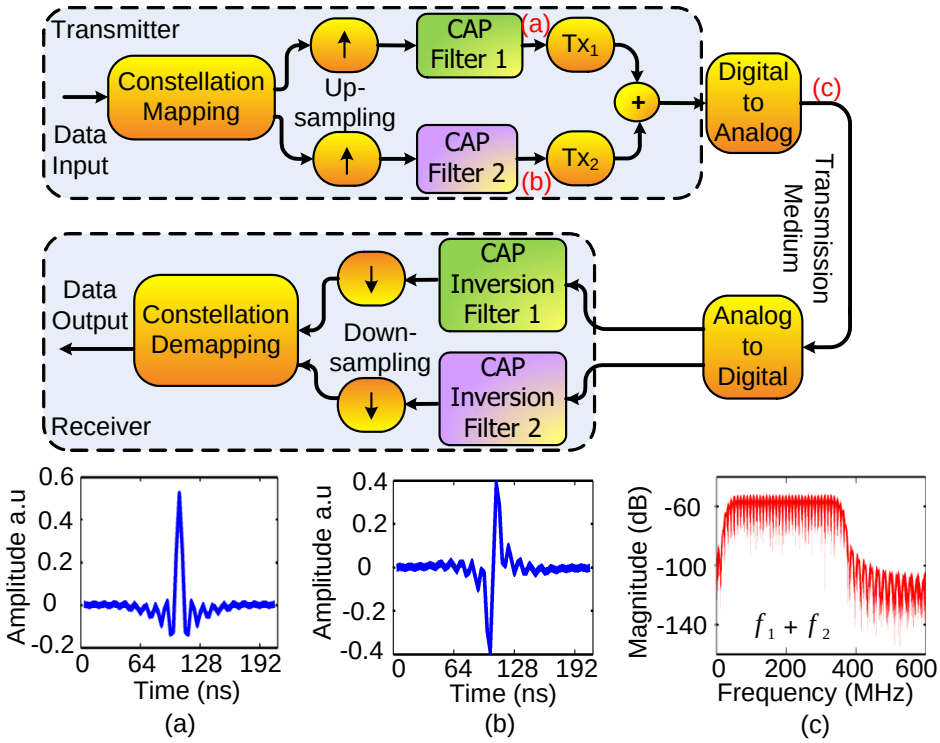

Figure 1.5: CAP transmitter and receiver for 2D CAP system.

CAP has been widely used for ADSL and asynchronous transfer mode (ATM) local area networks (LANs) [15]. In both of these applications, CAP modulation has been adopted primarily because of its high bandwidth efficiency and low implementation costs. Additionally, CAP supports modulation in more than 2 dimensions, provided that orthogonal pulse shapes can be identified [10]. This possibility of multi-dimensional modulation makes CAP an attractive modulation format to support multiple services for next generation access networks and in-home networks [16].

The basic idea of the CAP system is to use different signals as signature waveforms, forming a Hilbert pair (e.g. sine and cosine waveforms) to modulate different data streams. A block diagram of the CAP transmitter and receiver is shown in Fig.1.5. Data in the transmitter is mapped according to the given constellation by converting a number of raw data bits into a number of multi-level symbols. These symbols are upsampled and shaped by the CAP filters in order to achieve square-root raised cosine (SRRC) waveforms. These waveforms are multiplied by sine or cosine waveforms

to achieve orthogonality between them and move them from baseband to passband. The resultant waveforms are given by:

$$f_1(t) = h_{SRRC}(t) \cos 2\pi f_c t \tag{1.1}$$

$$f_2(t) = h_{SRRC}(t) \sin 2\pi f_c t \tag{1.2}$$

where f_c is a frequency suitable for the passband filters. The pair of modulated waveforms f_1 and f_2 constitute a Hilbert pair. A Hilbert pair is two signals of the same magnitude response but with phase responses shifted by 90^o. Fig.1.5 (a) and (b) presents the impulse response of the CAP filters in time domain. The two orthogonal signals are added and converted from digital to analog form. The combined frequency spectrum of CAP is shown in Fig. 1.5(c). At the receiver, the signals are converted back to digital form. The time-inversion of the transmission filters, i.e. matched filtering, is implemented to retrieve the original sequence of symbols; the symbols are downsampled and demapped, and the original data can be recovered. For higher dimensionality CAP, the required sample/symbol ratio is linearly proportional to the number of dimensions [10]. The upsampling factor therefore must be increased in order to support an increased number of dimensions. This means that the spectral efficiency has not been improved by increasing the number of dimensions. However, the additional dimensions can be used to support multiple access applications.

The Hilbert pair which are sine and cosine waveforms used for 2D-CAP can not be used for 3D or 4D, so a new set of filters needs to be designed. The 3D/4D CAP systems are shown in Fig. 1.6. The filters are added according to the dimensions that are required in the system. To avoid inter-dimensional crosstalk; it is vital that the transmitter-receiver filter combinations satisfy the orthogonality or perfect reconstruction (PR) criteria. In the experiment, the optimization algorithm (OA) described in [17] has been applied to extend the conventional 2D-CAP scheme to higher dimensionality and to assure the PR of the filters. The advantage of this formulation is that the frequency magnitude response of the transmitter and receiver filters will be identical. Additionally, it is a straight-forward method to extend the design to higher dimensionality CAP systems. In equation (1.3) the variables f_i and g_j represents the CAP transmitter and receiver finite impulse response (FIR) filters respectively.

$$\begin{aligned} P(f_i)g_j &= \tilde{\delta}, \quad i,j \in \{1,2,3,4\} \\ P(f_i)g_j &= \tilde{0}, \quad i,j \in \{1,2,3,4\} \text{ and } i \neq j \end{aligned} \tag{1.3}$$

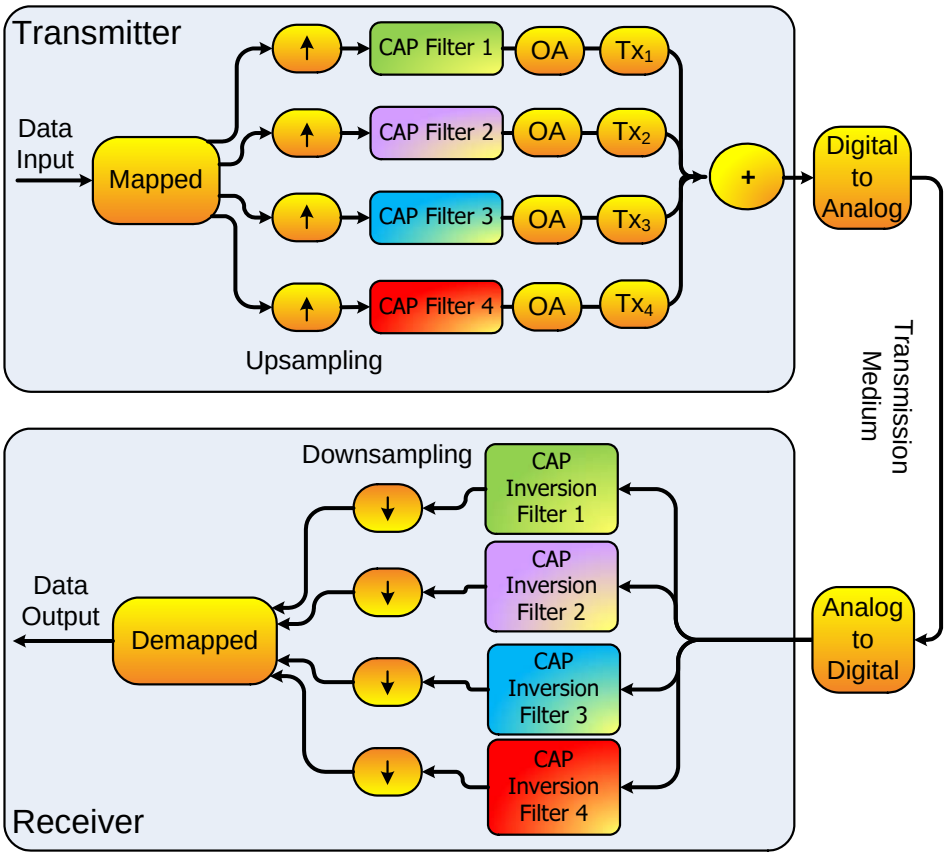

Figure 1.6: CAP transmitter and receiver for 3D or 4D CAP system.

where $P(f_i)$ is a shift matrix that operates on vector f_i, $\tilde{\delta}$ is a vector with one unity element and $\tilde{0}$ is a vector of all zeros.

The optimization algorithm for high dimensionality CAP is described as follows

$$\min_{f_1,f_2,f_3,...f_N} \max\left(|F_{1,HP}|, |F_{2,HP}|, |F_{3,HP}|, ...|F_{N,HP}|\right) \tag{1.4}$$

subject to the PR condition in (1.3) and

$$g_i = \text{inverse}\left[F_i\right], i \in \{1, 2, 3, ..N\} \tag{1.5}$$

where F_i is the discrete Fourier transform (DFT) of vector f_i. The $F_{i,HP}$ is the out-of-band portion of the transmitter response above the f_B. The

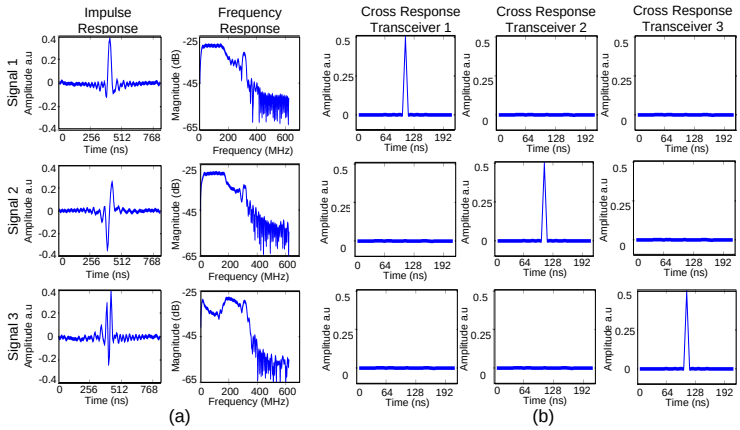

Figure 1.7: 3D-CAP (a) impulse responses and frequency responses; (b) cross responses of transceiver filters.

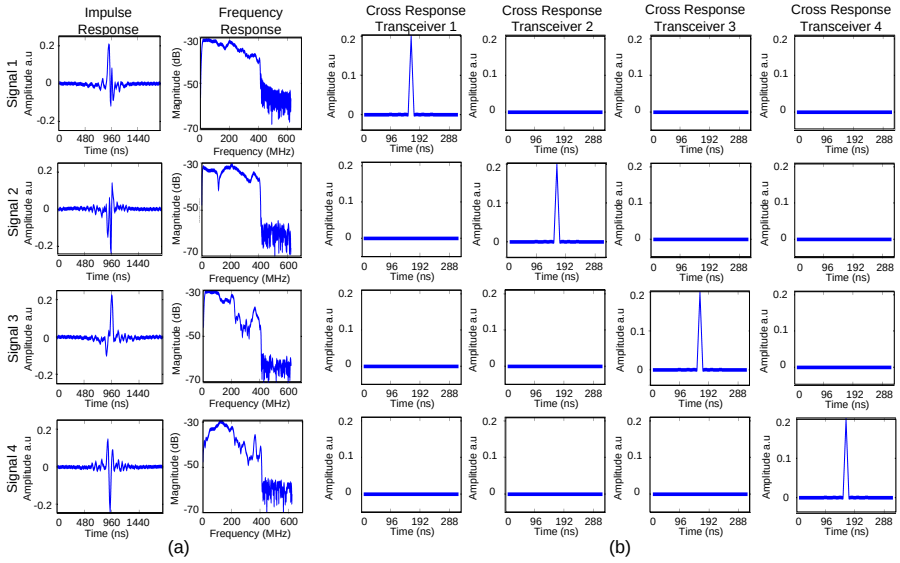

Figure 1.8: 4D-CAP (a) impulse responses and frequency responses; (b) cross responses of transceiver filters.

boundary frequency f_B is to ensure the receivers frequency magnitude response will be exactly the same as the transmitters. This means that the out-of-band spectral content of the filters is zero. For 1D pulse amplitude modulation (PAM), Nyquist has proved that to avoid inter symbol interference (ISI), i.e., PR condition for one dimension, a minimum bandwidth

of $\frac{1}{2T}$ is needed, where $\frac{1}{T}$ is the baud rate. Similarly, for the 3D-CAP system, there is a minimum bandwidth ($f_{B,min}$) value that will achieve the PR condition. It has been proven in [17], that f_B for the 3D-CAP system is at least equal to or greater than $\frac{3}{2T}$ to preserve the PR condition. In the experiments, the band limiting condition f_B is set to $\frac{2}{3}(2 \times f_s)$, where f_s is the highest frequency component of the 3D/4D-CAP signals.

Fig. 1.7 and 1.8 show the responses of the digital filters at the transmitter and receiver for 3D-CAP and 4D-CAP respectively. Fig. 1.7(a) and 1.8(a) show the impulse response and the frequency response for each of the signals. Fig. 1.7(b) and 1.8(b) shows the cross responses of the transmitter-receiver (transceiver) filters. The impulse only exists at the cross responses of f_1 and g_1, f_2 and g_2, f_3 and g_3, f_4 and g_4 (extra dimension for 4D-CAP), with zeros at the other transmitter-receiver pairs, for example f_1 and g_2, f_1 and g_3 and etc. The transmitter-receiver filter combinations are orthogonal and satisfy the perfect reconstruction criteria.

The generation and experimental demonstration of high dimensionality CAP is reported in **PAPER 1** for the first time in optical fiber systems. In **PAPER 2**, the high dimensionality CAP is demonstrated and investigated at higher bit rate up to 10 Gb/s with 1310 nm DM-VCSELs.

1.3.2 Multiplexing Scheme for High Dimensionality CAP

Spread spectrum communication in the form of code division multiple access (CDMA) offered large advantages to the wireless communication industry in the 1970s [18] in terms of cellular telephony network, global positioning system (GPS), etc. The success of this technique has also motivated interest for applications in optical communication networks under the name of optical code division multiple access (OCDMA). **PAPER 3** presents the principle of OCDMA with simulation evaluation of three different codes that have been developed for spectral amplitude coding - optical code division multiple access (SAC-OCDMA) systems.

All-optical 2 dimensional (2D) OCDMA has been proposed for next generation access network (NGAN) for multimedia applications [19] and increased spectral efficiency in FTTH [20]. Due to the limited coding space, incoherent 1 dimensional (1D) optical coding technology (either in the time or wavelength domain) is not feasible for future access networks which are required to support a large number of end users. Both 2D and 3 dimensional (3D) encoding techniques require multiple domains to realize optical codes. Therefore, it is difficult to smoothly upgrade the capacity of an access network where 2D or 3D encoders/decoders are employed [20]. In

order to overcome this problem the encoder and decoder can be designed in the electrical domain. The orthogonal division multiple access (ODMA) systems for multiple possible dimensions of CAP modulation [10, 21] has been proposed for multiple services application.

ODMA can be classified under the CDMA concept, with orthogonality imposed on the set of signals. Although the ODMA looks similar to the well-known CDMA, there is a fundamental difference between these two techniques. CDMA is generated using a pseudo-random generator, while the ODMA is generated by employing the optimization algorithm.

In this thesis, **PAPER 4** presents the first experimental demonstration of a 2x2D-ODMA configuration in a WDM access network. A bi-directional fiber optical link using 3D-CAP and employing DM-VCSELs operating around 1550 nm is demonstrated in **PAPER 5**.

1.4 Hybrid Wireless-Optical Links for Next Generation Access Networks

Next generation broadband access networks will provide heterogeneous services, wired and wireless. The inclusion of wireless, in the form of radio-over-fiber (RoF), into access networks needs to be compatible with existing access architectures and coexist with baseband signals. The most promising architecture for optical access networks is passive optical network (PON) because of low cost, simple maintenance and operation, and high-bandwidth provisioning [4, 22]. Several architectures, called hybrid PONs, have been proposed in order to include optical wireless signal distribution in PON. Among the different multiplexing techniques for PON, WDM is the most promising solution for future broadband access networks, as it can accommodate exponential traffic growth, support different broadband services and allow fast network reconfiguration due to the flexibility in wavelength allocation [22–25].

The application of wireless links for access networks takes place in the last mile segment of the data transport, providing high capacity links to the end-user. One type of wireless signal distribution concerns cellular networks, where a certain geographical area needs wireless coverage, provided by a number of antennas base station (BS). For next generation cellular networks with increased capacity, the reach of the wireless link will be short as a consequence of the higher radio frequency (RF) carriers and the use of higher modulation formats needed to achieve high capacity links. To provide proper coverage, the density of antennas per area needs to be

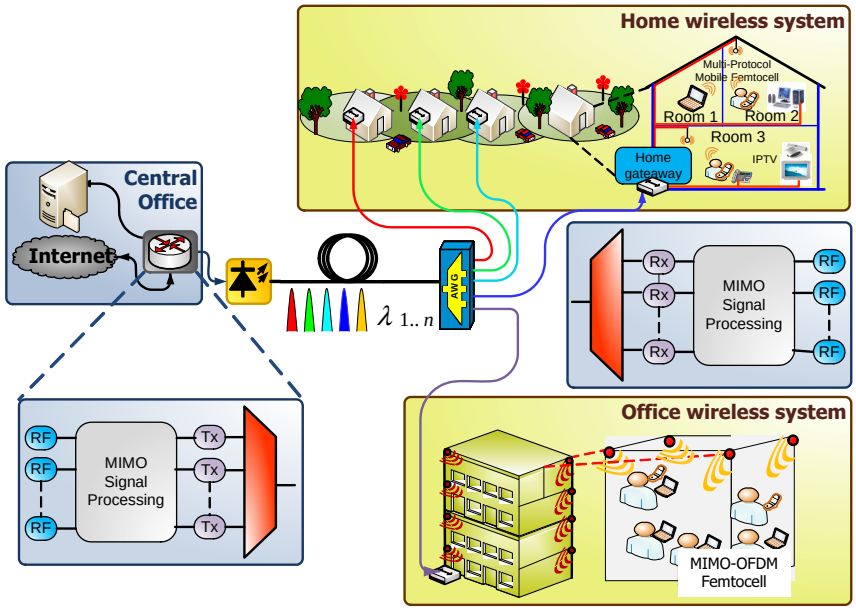

Figure 1.9: MIMO implementation for in-home and in-office scenarios for WDM-PON applications.

increased, resulting in a large number of nodes to be distributed and controlled by the network. The new architecture shall support high number of BS, with possibly high number of antennas per BS, to support MIMO.

1.4.1 MIMO Multiplexing Scheme for RoF Networks

In the next generation wireless access network, various kinds of high–throughput internet services are to be provided at any time and any place. Recently, wireless radio systems using multi-antenna technology are used in new wireless radio communication such as MIMO towards highly reliable communications [26]. Furthermore MIMO technology has improved transmission distances and increased the data rates supported by modern wireless networks without any additional power or bandwidth expenditure [27]. Fig. 1.9 shows integration of MIMO wireless systems into RoF networks implementing WDM-PON architecture. Such multiple antenna techniques, however, present a challenge for RoF systems, which have to ensure clean transmission of multiple signals between elements of the antenna array, and must mitigate signal path impairments which introduce crosstalk, attenuation and multipath fading [28]. Sophisticated receiver algorithms may be

implemented to overcome these path-dependent effects.

Orthogonal frequency-division multiplexing (OFDM) has emerged as one of the leading modulation techniques in the wireless domain. The combination of OFDM with MIMO provides an attractive solution because of the simple implementation, and potentially high spectral efficiency.

First experimental demonstration of MIMO for WDM-PON application is presented in **PAPER 6** with 4-QAM-OFDM modulation scheme. These results were extended by using a training sequence algorithm to reduce computational complexity at the receiver, this work was reported in **PAPER 7**.

PDM have been implemented in **PAPER 8** and **PAPER 9** in order to increased the spectral efficiency in MIMO systems and WDM-PON networks. The 4-QAM-OFDM and 16-QAM-OFDM have been transmitted over 22.8 km of single mode fibre (SMF). Furthermore the constant modulus algorithm (CMA) has been implemented in **PAPER 10** and **PAPER 11** with 4 bit/s/Hz spectral efficiency has been achieved in both papers.

1.5 State-of-the-Art Analysis

In this section the state-of the-art results are divided into two categories; CAP modulation format and MIMO multiplexing techniques.

1.5.1 Carrierless Amplitude-Phase Modulation

CAP modulation originally called carrierless AM/PM was proposed in mid 1975s by the Bell Labs as a viable modulation technique for high-speed communication links over copper wires [29]. It was derived from QAM and might be conceded its variation, even though there is a fundamental difference in the way the signal is generated. CAP has received most of its attention during early and mid 1990s with the dawn of the DSL techniques that were aimed for private consumers ADSL [11, 12]. Continuous effort from Bell Labs led to CAP being a part of early DSL and ATM specification [15], almost always proposed as optional to discrete multi-tone modulation (DMT). The proposals of 3D, 4 dimensional (4D) and 6 dimensional (6D) CAP modulation have been presented in [10, 21, 30] for DSL application. For high dimensionality CAP the optimization algorithm (OA) described in [10, 17, 31] has been used to extend the conventional 2D-CAP scheme to higher dimensionality and to assure perfect filter reconstruction. However

published work on high dimensional CAP up to year 2007 [15], just focused on simulation results rather than realistic practical experiments. Possible limitations of multi-dimensional CAP systems in practice have not been reported so far.

Recently, CAP modulation has received attention in the research of optical communication [32–34] due to the potential high spectral efficiency and the possibility of generating the required orthogonal pulses by means of transversal filters. In [33] 2D-CAP 8-levels per dimension (L/D) over 50 m polymer optical fiber (POF) has been demonstrated with resonance cavity light emitting diodes resonant cavity light emitting diodes (RC-LEDs) with a spectral efficiency of 4.6 bit/s/Hz. Directly modulated vertical cavity surface emitting lasers (DM-VCSELs) for wavelength division multiplexing (WDM) application with 2D-CAP 4-L/D has been experimentally demonstrated in [34, 35], reporting transmission of up to 1.25 Gbps over 26 km standard single mode fiber standard single mode fibre (SSMF). A spectral efficiency of 4 bit/s/Hz is reported in both papers. In [36] and [32], 10 Gb/s and 40 Gb/s 2D-CAP 4-L/D has been successfully generated with analogue transversal filters. However, all of these reports are focused only on 2D-CAP at different L/D. A detailed explanation of the relationship between levels per dimension, bits/symbol and total number of levels of CAP can be found in **PAPER 1** and **PAPER 2**.

1.5.2 Multiple-Input Multiple-Output Multiplexing Technique

MIMO technology has attracted attention in wireless communications, because it offers significant increase in data throughput and link range without requiring additional wireless transmission bandwidth or increased transmission power. It achieves this goal by utilizing multiple transceiver antennas to achieve an array gain that improves the spectral efficiency (measured in bits per second per hertz of bandwidth) or to achieve a diversity gain that improves the link reliability (improved transmission robustness to wireless channel fading effects).

MIMO wireless systems implement antenna arrays at both transmitter and receiver. First simulation studies that reveal the potentially large capacities of those systems were already done in the 1980s [37], and later papers explored the capacity from an analytical point of view [38,39]. Since that time, interest in MIMO systems has exploded [40].

The combination of MIMO with orthogonal frequency division multiplexing (MIMO-OFDM) gives an attractive air-interface solution for wire-

less local area networks (WLANs), wireless metropolitan area networks (WMANs), and fourth-generation mobile cellular wireless systems [41–43].

Previous simulation work has been done towards integrating MIMO-OFDM technology with RoF [28], and integrating dense wavelength division multiplexing (DWDM) with MIMO-OFDM [44]. The bi-directional experimental work of MMF bandwidth investigations are presents for RoF picocellular network architectures with 850 nm and 1300 nm VCSELs [27]. The MIMO-RoF concepts with 16-QAM-OFDM is demonstrated in [45], but that analysis implements separate fibers for each remote antenna unit (RAU). The wireless transmission distance is up to 8 m with optimum of 1 m antenna separation.

Recent proposals have aimed to provide current wireless and/or wired services over WDM passive optical network (WDM-PON) [46–49]. However, in order to increase the throughput of the wireless access, the strict limitation imposed by the radio frequency spectrum leads to the reduction of cell size and the use of higher radio frequency bands, and thus a huge number of base stations (BSs) are needed to cover a wide area. The femto-cell architecture provided by broadband optical access network is a promising approach to realize the next generation wireless access. A novel architecture of broadband ubiquitous femto-cell networks with RoF distributed antenna system (DAS) systems over WDM-PON have been reported in [49, 50]. However, these works implemented back-to-back (B2B) signalling using 64-QAM-OFDM modulation without any wireless transmission. Further experimental investigation by deploying 20 km and 40 km SMF has been reported in [51] for 2.4 GHz but still without wireless transmission. The 2×2 MIMO technique has also been explored at 60 GHz RoF system [52]. A 27.15 Gb/s bit rate is achieved by employing 16-QAM modulation format transmitted over 25 km of standard single-mode fiber and 3 m wireless distance. Frequency domain equalizer (FDE) has been used to estimate the MIMO channel response .

Polarization division multiplexing (PDM) allows doubling of the spectral efficiency of a transmission system [53]. A 5 Gb/s PDM wireless MIMO transmission over 60 GHz wireless link has also been reported in [54], however employing OOK modulation. Moreover, high speed PDM-OFDM transmission system have been realized in [55, 56] without wireless transmission.

For wireless MIMO systems, channel estimation is essential for signal demodulation. For multi-carrier systems like OFDM, a large computational complexity will be introduced by using the classical MIMO channel

estimation method based on the butterfly structure because an adaptive filter needs to be assigned for each OFDM subcarrier. Consequently, a training-based channel estimation method has the relatively low computational complexity at the receiver [57]. However, a large signaling overhead is often required to extract the channel response, resulting in the decrease of the net data rate in the system. Furthermore, to obtain preamble or training symbols in the receiver, precise synchronization or timing recovery is essential [58, 59] since preamble-based approaches are all decision-directed. In contrast, CMA based equalizer is able to make blind estimation when transmitting constant envelope signals, e.g. QPSK [60]. Meanwhile, CMA could also treat the polarization rotation in the fiber together with the wireless crosstalk when combining the PDM-RoF system with MIMO technique.

1.6 Beyond the State-of-the-Art

The work presented in this thesis has significantly extended the state-of-the-art of the CAP modulation format in optical fiber systems and MIMO multiplexing techniques. Recent work has focused only on 2D-CAP in optical fibers and no experimental work has investigated for high dimensionality CAP. We have successfully demonstrated the 3D-CAP and 4D-CAP at different bit rates and transmission distance at different VCSELs wavelengths. For MIMO multiplexing we have successfully demonstrated 2×2 MIMO by employing OFDM with various wireless transmission for WDM-PON. In order to increase spectral efficiency, we have implemented PDM in combination with MIMO systems. In this section we divided the achievements into two subsections in conjunction with the previous state-of-the-art.

1.6.1 High Dimensionality CAP

Fig. 1.10 shows the previous work that has been proposed and demonstrated in DSL and optical fiber systems. Details of the extension of this work beyond the state-of-the-art are also highlighted and illustrated in the schematic diagram.

At the start of this Ph.D work, we initially examined the codes that have been developed for OCDMA for RoF PON systems. **PAPER 3** presents the principle of the OCDMA with simulation evaluation of three different codes that have been developed for SAC-OCDMA systems. However to implement all of these codes extra filters need to be added both at the

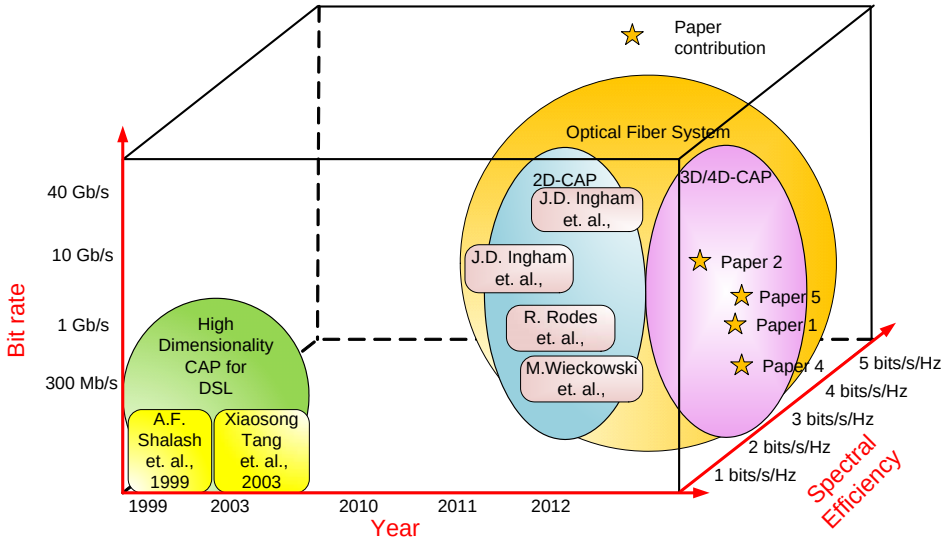

Figure 1.10: Illustration of the state-of-the-art and further achievement in the state-of-the-art of CAP modulation format.

encoder and decoder side in real implementations. After a further discussion with the supervisor and co-supervisor, we decided to change the scope of the study for investigating higher dimensionality CAP. Previous reports just focused on simulation work [10, 17, 21].

PAPER 1 demonstrates the first experimental investigation of 3D-CAP and 4D-CAP for optical fiber transmission systems with 1550 nm DM-VCSELs. The signals are transmitted over 20 km standard single-mode fiber (SSMF). For multi-level 3D-CAP, bit rates of 468.75 Mb/s and 937.5 Mb/s are achieved at 2-levels/dimension (2-L/D) and 4-levels/dimension (4-L/D) respectively. For 4D-CAP, bit rates of 416.67 Mb/s and 833.3 Mb/s are achieved at (2-L/D) and (4-L/D) respectively. Spectral efficiencies of 2.68 bits/s/Hz and 2.08 bits/s/Hz are reported for 3D-CAP and 4D-CAP respectively at 4-L/D. Furthermore, CAP has also been investigated at higher bit rates with directly-modulated 1310 nm VCSELs in **PAPER 2**. The signals are transmitted over 10 km SSMF. For multi-level 3D-CAP, bit rates of 6 Gb/s and 10.2 Gb/s are achieved at 2-L/D and 4-L/D respectively with 4 GHz bandwidth. For 4D-CAP, bit rates of 6.85 Gb/s and 10.66 Gb/s are achieved at 2-L/D and 4-L/D respectively with 8 GHz bandwidth. Spectral efficiencies of 2.44 bits/s/Hz and 1.33 bits/s/Hz are reported for 3D-CAP and 4D-CAP respectively at 4-

L/D. Coordinate transformed constant modulus algorithm (CT-CMA) channel estimation employed in order to combat the inter symbol interference (ISI) and inter dimensional crosstalk is investigated as an added value of this work.

The usability of CAP modulation dimensions for service and user allocation for WDM optical access has been experimentally demonstrated in a 2x2D-orthogonal division multiple access (ODMA) configuration **PAPER 4**. The spectral efficiency for 4-L/D is 2.08 bits/s/Hz with bit rate of 833.3 MHz is presented in this work. The flexibility of the 4D-CAP in dividing the dimensions in the optical fiber systems is successfully demonstrated.

A bi-directional optical transmission using 3D-CAP at 2-L/D and 4-L/D modulation has been successfully demonstrated in **PAPER 5**. The spectral efficiency achievements of 2.25 bits/s/Hz and 3.6 bits/s/Hz for 3D-CAP 2-L/D and 3D-CAP 4-L/D are achieved at bit rate of 4.5 Gb/s and 7.2 Gb/s respectively. This demonstrative work is a promising solution to enable the Gigabits passive optical networks (PON) transmission.

1.6.2 2x2 MIMO Multiplexing Techniques

Fig. 1.11 shows the previous work that has been proposed and demonstrated for MIMO RoF systems. The extended work to the state of the art is also highlighted and illustrated in the schematic diagram.

PAPER 6 presents the first experimental demonstration of all-VCSEL 2×2 MIMO OFDM with 5.6 GHz RoF signaling over WDM-PON systems. The 4-QAM-OFDM signals modulated at 198.5 Mb/s net bit rate are achieved after fiber and 2 m indoor wireless transmission. A further investigation of this system has been presented in **PAPER 7** with 16-QAM-OFDM signal. Furthermore, this work has been proposed for in-home and in-office femto-cell networks. For both papers the training symbols algorithm is employed to compensate the multipath fading in the RoF system.

Because of the significantly low net bit rate, in **PAPER 8** and **PAPER 9** PDM has been proposed and applied to the rest of the experimental work. **PAPER 8** demonstrates a hybrid fiber wireless system by using a PDM 4-quadrature amplitude modulation (4-QAM)-OFDM signal, which is translated into a 2×2 MIMO wireless transmission, using training-based OFDM-MIMO channel estimation. The net bit rate of 795.5 Mbps is achieved with 2.55 bit/s/Hz spectral efficiency over 22.8 km SSMF and 3 m wireless distance. An extension work of 16-QAM-OFDM signals has been further investigated in **PAPER 9** with 1.59 Gb/s net bit rate obtained for PDM WDM-PON systems.

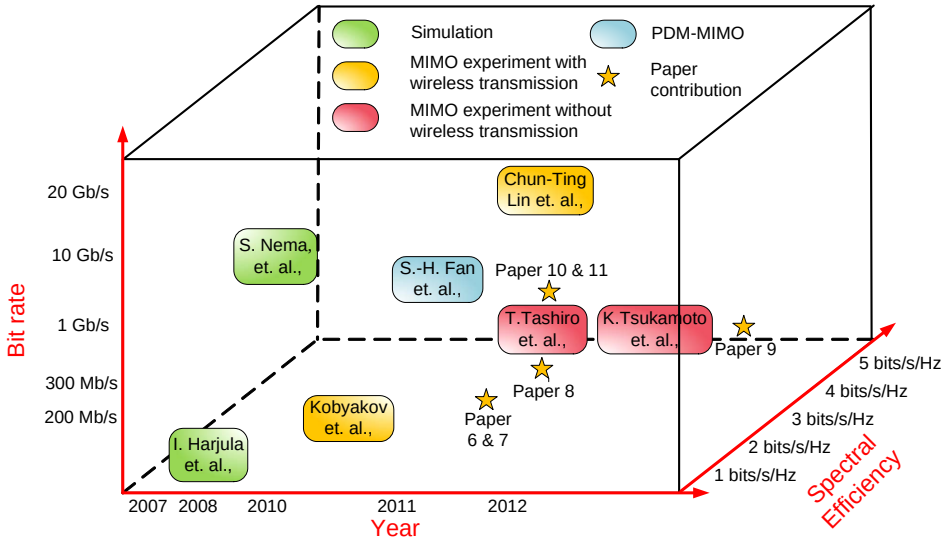

Figure 1.11: Illustration of the state-of-the-art and further achievement in the state-of-the-art of MIMO techniques.

PAPER 10 presents and experimentally demonstrate a PDM-RoF system with 1.25 Gbaud/s QPSK sequence on each polarization state and followed by a 2×2 MIMO wireless link. In the experiment, a 2 m wireless distance and 10 km SMF transmission of 5.4 GHz QPSK with bit rate up to 5 Gbps, and hence 4 bits/s/Hz spectral efficiency was successfully achieved. An extended reach up to 26 km SMF transmission has been demonstrated in **PAPER 11**. The CMA blind channel estimation has been employed in the 2×2 MIMO wireless channel for characterization and adaptive equalization of the demodulated signal.

1.7 Main Contribution

The main contributions of this thesis are the high dimensionality CAP modulation format in optical fiber systems and MIMO multiplexing techniques for next generation access network.

Firstly, this thesis proposes, studies and experimentally demonstrates the use of high dimensionality CAP at different bit rates. The ODMA multiplexing technique that has also been proposed for high dimensionality CAP combined with WDM is an alternative solution for 2D-code in OCDMA systems.

Secondly, this Ph.D project contributes on the MIMO multiplexing techniques by employing OFDM and two different channel estimation techniques for equalization of the 2×2 MIMO signals. For the first time it has been proposed for femto-cell WDM PON with wireless transmission. In addition the utilization of PDM would increase the bit rate up to gigabit per fiber-wireless access system.

Chapter 2

Description of Papers

This thesis is based on a set of articles already published or submitted for publication in peer-reviewed journals and conference proceedings. These articles present the results obtained during the course of my doctoral studies combining theoretical analysis, simulation and experimental results. The papers are grouped in two categories, dealing with the high dimensionality of CAP modulation and MIMO multiplexing techniques in radio-over-fiber (RoF) links. The CAP modulation format is studied and demonstrated experimentally in **PAPER 1**, **PAPER 2**, **PAPER 4** and **PAPER 5**. The theoretical analysis and numerical simulation are performed in **PAPER 3** for OCDMA PON system. **PAPER 6** and **PAPER 7** present the experimental results for 2×2 MIMO multiplexing technique for WDM-PON system. The PDM is proposed and demonstrated in **PAPER 8** to **PAPER 11** for 2×2 MIMO wireless channels.

2.1 High Dimensionality CAP and OCDMA Multiplexing for Next Generation Networks

PAPER 1 demonstrates the first reported experimental results for 3D-CAP and 4D-CAP using 1550 nm DM-VCSELs. The main novelty of this paper is the investigation and demonstration of high dimensionality CAP which before this just focused on the numerical simulation work for ADSL. The optimization algorithm for generating the CAP orthogonal filters is also explained in this paper. The signals are successfully transmitted over 20 km of SSMF. For both 3D-CAP and 4D-CAP signals, bit error rate (BER) below the forward error correction (FEC) limit of 2.8×10^{-3} was

achieved after 20 km of SSMF. For 3D/4D-CAP signals at 4-L/D, a bit rate BR)of 937.5 Mb/s and 833.3 Mb/s (including 7% forward error correction (FEC) overhead) is obtained in the system, while spectral efficiencies of 2.68 bits/s/Hz and 2.08 bits/s/Hz are achieved for 3D-CAP and 4D-CAP respectively at 4-L/D.

PAPER 2 presents a further demonstration of 3D-CAP and 4D-CAP at higher bit rates. The signals are successfully transmitted over 10 km SSMF. For both 3D-CAP and 4D-CAP signals, BER below the FEC limit of 2.8×10^{-3} for error free reception was achieved after 10 km SSMF. For 3D/4D-CAP signals at 4-L/D, a bit rate of 10.28 Gb/s and 10.66 Gb/s (including 7% FEC overhead) is obtained in the system. Spectral efficiencies of 2.44 bits/s/Hz and 1.33 bits/s/Hz are achieved for 3D-CAP and 4D-CAP respectively at 4-L/D. The added value of this demonstration is the coordinate transformed constant modulus algorithm (CT-CMA) channel estimation employed in this experiment. The CT-CMA improves the receiver sensitivity by 1 dB and suppresses inter-dimensional crosstalk of the CAP signals. Despite the fact that the spectral efficiencies are significantly lower when the dimension is increased, this modulation scheme has the potential of supporting multiple users with integrated services at higher bit rates with directly modulated 1310 nm VCSEL.

PAPER 3 presents a theoretical analysis and simulation performance evaluation of three codes; enhanced double weight (EDW), random diagonal (RD) and zero cross correlation (ZCC) for 10 Gb/s x 4 user, 20 km standard single mode fibre (SSMF) transmission link for OCDMA PON. The purpose of this study is to evaluate these new SAC codes that, to our knowledge, have never been compared before. These SAC codes have ideal in-phase cross-correlation properties to reduce multiple access interference (MAI) effects in OCDMA. The performance has been characterized through received optical power (ROP) sensitivity and dispersion tolerance assessments. The numerical results show that when considering ROP the ZCC code has a slightly better performance compared to the other two and similar behavior against the dispersion tolerance.

PAPER 4 presents the first known experimental demonstration 2x2D-ODMA configuration in a WDM access network. This new approach gives an alternative solution to overcome the problem of multiple domains coding being faced in the 2 dimensional optical code division multiple access

(2D-OCDMA). We believe this new concepts can be implemented in WDM networks in an elegant way by utilizing the orthogonal CAP filters designed in the digital domain. The flexibility of the 4D-CAP in dividing the dimensions indicates the prospects of combining the ODMA in WDM network for service and user allocation in next generation access network.

PAPER 5 reports the first demonstration of a smart grid communication system based on bi-directional fiber optical links using multi-dimensional CAP and employing DM-VCSELs operating around 1548.24 nm for downlink and 1548.96 nm for uplink. Off-line digital signal processing (DSP) algorithms of blind CMA channel estimation equalizer are implemented to compensate for inter symbol interference induced by 20 km single mode fiber (SMF) transmission impairments. Moreover, in this paper, 3D-CAP with 2-level/dimension (2-L/D) and 4-level/dimension (4-L/D) transmissions achieved the bit rates of 4.5 Gb/s and 7.2 Gb/s respectively.

2.2 MIMO Multiplexing Technique Implementation in Radio-over-Fiber System

PAPER 6 proposes and demonstrates the first experimental results of 2×2 MIMO-OFDM with wireless transmission for WDM-PON system using all-VCSELs optical sources. We report error free transmission after 20 km non zero dispersion shifted fiber (NZDSF) and 2 meter 2×2 wireless MIMO with 4-QAM-OFDM at 198.5Mb/s with 5.65 GHz RoF signaling transmission for WDM-PON system. We also investigate the effects of various wireless transmission path lengths and antenna separation distances to see the robustness of the MIMO-OFDM algorithm. No penalty was observed when varying the antenna separation of the sub-elements of the MIMO-OFDM signal with 1 m separation between remote antenna unit (RAU) and mobile station (MS). **PAPER 7** incorporates additional results in investigating the number of subcarriers in OFDM signals and 16-QAM OFDM-MIMO. The OFDM-MIMO training sequence algorithm which is applied to compensate the receiver's complexity is also described in **PAPER 7**. Additionally, this work is potentially an attractive candidate for future femto-cell networks especially for in-door office environments. **PAPER 6** was accepted in the 37^{th} European Conference on Optical Communication (ECOC'11) and **PAPER 7** is an extended work that has been published at the ECOC/Optics Express special issue.

PAPER 8 presents a 2×2 MIMO wireless over fiber transmission system by seamlessly translation of OFDM on dual polarization states at 795.5 Mbps net data rate using digital training-based channel estimation. A 1.25 GSa/s arbitrary waveform generator (AWG) is used to generate two baseband real-valued 4-QAM OFDM signals with 64 subcarriers by an upsampling factor of 4. The OFDM signals have a bandwidth of 625 MHz and they are arranged in frames of 10 symbols, out of which 3 are training symbols used for synchronization and channel estimation purpose. A cyclic prefix with 0.1 symbol length is added in each symbol. An external cavity laser (ECL) operating at 1550 nm is used as laser source. The signal is successfully transmitted over 22.8 km SMF with wireless link up to 3 m. The use of these technologies enables a net spectral efficiency of 2.55 bit/s/Hz. Furthermore, a training-based scheme is digitally developed to estimate the polarization multiplexed MIMO transmission channel.

PAPER 9 proposes a spectral efficient radio over wavelength division multiplexed passive optical network (WDM-PON) system by combining optical polarization division multiplexing (PDM) and wireless MIMO multiplexing techniques. In the experiment, a training-based zero forcing (ZF) channel estimation algorithm is employed to compensate the polarization rotation and wireless multipath fading. A 797 Mb/s net data rate QPSK-OFDM signal with error free ($< 1 \times 10^{-5}$) performance and a 1.59 Gb/s net data rate 16-QAM-OFDM signal with BER performance of 1.2×10^{-2} are achieved after transmission in 22.8 km single mode fiber followed by 3 m and 1 m air distances, respectively.

PAPER 10 demonstrates a PDM-RoF system with a 2×2 MIMO wireless link. By using both PDM and wireless MIMO, 5 Gbps QPSK signal at 5.4 GHz carrier radio frequency (RF) with spectral efficiency of 4 bits/s/Hz is achieved. The signals is successfully transmitted through a 10 km SMF plus up to 2 m wireless link by using 1550 nm DM-VCSELs. This is the highest wireless capacity reported at this carrier frequency to the best of our knowledge. An extended work of this system is presented in **PAPER 11**. The experimental setup is the same as the one in the previous work in **PAPER 10**, except for the laser source which is replaced with a distributed feedback (DFB)laser and the optical link is extended to 26 km of SMF. The CMA blind channel estimation is used in both papers and it adaptively equalize the 2×2 MIMO demodulated signal. Error free PDM-RoF signal over 26km fiber and 1m wireless transmission yields a required received power of -18 dBm and 2 dB power penalty is observed with respect to back to back (B2B) case. An up to 2 m wireless MIMO transmission performance is studied showing a required received optical power of -14 dBm. The results show an increased applicability of highly spectral efficient fiber-wireless systems.

Chapter 3

Conclusion

3.1 Conclusions

The research results presented in this thesis are pioneering in two main areas: firstly, 3D-CAP and 4D-CAP signals are successfully modulated and demodulated in optical fiber system using an offline digital signal processing. Secondly, 2×2 MIMO RoF with OFDM modulation have successfully been demonstrated in this Ph.D project. The achievements demonstrate that MIMO-OFDM can increase the bit rate and spectral efficiency while mitigating the multipath fading problem.

3.1.1 CAP Modulation Format

An important milestone in this Ph.D project is the first experimental demonstration of high dimensionality CAP in an optical link. Table 3.1 shows the main contribution of the CAP modulation results that have been achieved in **PAPER 1**, **PAPER 2**, **PAPER 4** and **PAPER 5**. The parameters such as modulation format (Mod. Format), bit rates (BR), spectral efficiency (SE), upsampling factor (UF) and VCSELs wavelength are listed in the Table 3.1.

High dimensionality CAP requires excess bandwidth due to the higher upsampling factor resulting in a decreased spectral efficiency. However the main advantage of high dimensionality CAP is the flexibility of CAP provided by an increase in the number of dimensions that can potentially be utilized to allocate different services to different users with single cabling infrastructure. This tradeoff between the flexibility and spectral efficiency needs to be considered in the system design.

Table 3.1: Summary results of CAP modulation for optical fiber systems.

	Mod. Format	BR	SE	UF	VCSELs
PAPER 1	3D-CAP 4-L/D	937.5 Mbps	2.68 bits/s/Hz	8	1550 nm
PAPER 2	3D-CAP 4-L/D	10.2 Gbps	2.44 bits/s/Hz	14	1310 nm
PAPER 4	2x2D-CAP 4-L/D	833.3 MHz	2.08 bits/s/Hz	12	1550 nm
PAPER 5	3D-CAP 4-L/D	7.2 Gbps	3.6 bits/s/Hz	10	1550 nm

By taking the idea and inspiration of optical code division multiple access (OCDMA) where the uniqueness of the codes addresses different users, the total of 4D-CAP have been divided into two WDM channels. The usability of CAP modulation dimensions for service and user allocation for WDM optical access is feasible with $2 \times$ 2D-ODMA configuration. Furthermore, the orthogonal FIR filters are designed in the digital domain which can be an alternative solution for higher dimensionality OCDMA which requires multiple domains coding. Finally, the bidirectional 3D-CAP transmission systems is successfully transmitted over 20 km of SMF for supporting high bit rate transmission, high spectral efficiency, multi-user application, and bi-directional communication.

In summary, high dimensionality CAP is attractive for supporting next generation network due to flexibility in increasing and dividing the number of dimensions. Furthermore by employing VCSELs the system design cost can be reduce due to the cost effective production and low modulation voltage [61].

3.1.2 MIMO Multiplexing Technique for Hybrid Wireless-Optical Link

Another achievement in this Ph.D project is the first experimental demonstration of 2×2 MIMO-OFDM for WDM PON networks. Table 3.2 shows

Table 3.2: Summary results of the main achievement for 2×2 MIMO RoF systems.

	Mod. Format	BR	SE	FL	WL
PAPER 6	4-QAM-OFDM	198.5 Mbps	0.64 bits/s/Hz	20 km	2 m
PAPER 7	16-QAM-OFDM	397 Mbps	1.27 bits/s/Hz	20 km	1 m
PAPER 8	4-QAM-OFDM	795.5 Mbps	2.55 bits/s/Hz	22.8 km	3 m
PAPER 9	16-QAM-OFDM	1.59 Gbps	2.52 bits/s/Hz	22.8 km	1 m
PAPER 10	QPSK	5 Gbps	4 bits/s/Hz	10 km	2 m
PAPER 11	QPSK	5 Gbps	4 bits/s/Hz	26 km	2 m

the main contribution of the 2×2 MIMO results that have been reported in **PAPER 6** through **PAPER 11**. The parameters such as modulation format (Mod. Format), bit rates (BR), spectral efficiency (SE), fiber link (FL) and wireless link (WL) are listed in the Table 3.2.

The use of MIMO multiplexing technique in RoF open new possibilities for increased coverage area and throughput in hybrid wired-wireless access links. Furthermore the combination of OFDM with MIMO technique provides an attractive solution because of the very simple implementation, and potentially high spectral efficiency. Wavelength division multiplexed passive optical network (WDM-PON) systems supporting higher bandwidth can transparently deliver radio frequency signaling required to support hybrid fixed and wireless access networking systems. WDM-PON technology can therefore further improve the throughput in the wireless service area covered by RoF-MIMO antennas. Furthermore the experimental demonstration have been proposed for femto-cell application with 2×2 MIMO wireless transmission for the first time.

In order to enhance the spectral efficiency, polarization division multiplexing (PDM) is an alternative solution to double the capacity. The zero forcing (ZF) algorithm has successfully been used to compensate the polarization rotation and wireless multipath fading. However, this channel estimation often needs a large number of overhead symbols to extract the channel response, resulting in a decrease of the net data rate in the system. Furthermore, to obtain the preamble or training symbols in the receiver, precise synchronization or timing recovery is essentially necessary since preamble-based approaches are all decision-directed. Considering that most synchronization algorithms cannot give a satisfying performance while spatial-correlation exists in the MIMO case, blind channel estimation without resorting to the preamble or training symbols can be very practically promising for MIMO signal demodulation in reality.

In summary, OFDM can successfully be applied in hybrid MIMO wireless optical links to deal with chromatic dispersion and polarization mode dispersion. Because the high data rate signal in OFDM is split into many lower data rate substreams, it demonstrates high robustness against different dispersion effects. Furthermore this approach is feasible for femto-cell applications due to reliability in using existing broadband internet connection and the improvement of the indoor coverage. In addition, sophisticated channel estimation in the receiver side is essential to compensate multipath fading in the wireless link.

3.2 Future Work

In this section I would like to provide a view of the future work that could be pursued for CAP modulation format and MIMO multplexing techniques using the optical technologies presented in this thesis.

3.2.1 Carrierless Amplitude-Phase Modulation for Photonic Technologies

Simulation work of 2D-CAP modulation format against QAM-optical OFDM (OOFDM), OOK, and pulse amplitude modulation (PAM) over single mode fibre (SMF), multimode fiber (MMF) and polymer optical fiber (POF) have been reported in the literature [62–64]. However the comparisons just focus on the link power budget and power dissipation. Further investigation parameters such as transmission distance, dispersion tolerance, and polarization mode dispersion (PMD) tolerance can be carried out for SMF trans-

mission. Different types of MMF such as OM1, OM2, OM3 and OM4 [65] can also be analyzed for in-home networks. The various types of MMF have different capabilities e.g maximum transmission distance and maximum bit rates. Furthermore, POF has emerged as a potentially lower cost alternative to glass-MMF in enabling high performance links an alternative solution for in-home networks due to easy-to-install and eye-satisfy solutions for these networks, with the potential of being future-proof [66–68]. Differential modal delay (DMD) evaluation can be observed in MMF and POF links. Additionally experimental investigations of different modulation formats against CAP should also been carried out to see the behavior in SMF, MMF and POF. Crosstalk is one of the major physical layer impairment that arises due to non-ideal nature of optical add-drop multiplexer and cross switches used in modern optical networks. The impact of in-band and out-band crosstalk on transmission performance by employing CAP modulation format in a transparent WDM system incorporating optical add drop multiplexers and space switches [69] can also be examined against other modulation formats.

Field-programmable gate array (FPGA) enables a variety of modulation formats and signal processing system algorithm to be loaded and evaluated. Previous work on real time transmission by employing the OFDM and DMT signals have been analyzed in [70, 71]. Real time CAP transmission is a promising field that can be realized by using the FPGA. For high dimensionality CAP as the dimensionality has been increased, the sampling rate of the digital to analog converters (DACs) and analog to digital converters (ADCs) also needs to be increased. Therefore, this would increase the cost of the system [34] and the receiver complexity. However, if the CAP filters could be designed in the analogue domain as in [32] the issue of high performance DAC/ADCs, could be avoided. CAP is an interesting modulation that could be applied via RoF system, having the potential of reducing the systems costs due to the simplicity of the transceiver design and the absence of the local oscillator (LO).

3.2.2 Towards Next Generation Wireless MIMO in RoF System

Although MIMO technology helps to significantly improve data access speeds of today's wireless systems, their performance (including the IEEE802.11n - the fastest WLAN standard) still falls well below 1 Gb/s. Further performance improvements require additional spectrum. Because of limited frequency spectra at low frequencies, millimeter wave frequencies including

up to 7 GHz license-free spectrum at the 60 GHz band is a promising path towards multi-Gb/s wireless access [72]. A 27.15 Gb/s using 16-QAM modulation is the highest bit rate reported so far in mm-waves by employing 2×2 MIMO technologies. However, the unregulated W-Band (75-110 GHz) is recently attracting increasing research interests due to less air absorption loss and larger available frequency window [73–75]. The latest achievement of 2×2 MIMO in this W-Band is presented in ECOC 2012 [76]. The total bit rates that has been achieved is 74.4 Gb/s by employing QPSK signals and PDM over 20 km SMF and 0.9 m wireless transmission. OFDM signals may be applied in mm-waves and W-band over WDM systems in order to further increase the bit rate and spectral efficiency.

MMF systems are widely used today for in-building baseband signal transport and it would be attractive to also use those fibers for RoF applications. It has been shown that multimode fiber can be used along with 850 nm VCSELs [27]. The advantages of employing the OFDM in MMF links are to extend transmission distance and to increase the aggregate data rate [77]. Exploration of MMF in MIMO technologies is very promising for short range femto-cell applications.

Besides that, the bidirectional WDM-PON with MIMO multiplexing technique is another step that needs to be accomplished. It's really interesting to observe the performance especially in the upstream direction because nowadays the end-users demands high application services such as online gaming, video on demands, online video conference and etc. The main challenge of these bidirectional systems is the high bandwidth required by all of these services. Furthermore the implementation of sophisticated receiver algorithms via combination of the linear techniques, such as zero forcing (ZF) and minimum mean square error (MMSE) equalization methods, with nonlinear techniques e.g. successive interference cancelation (SIC), could improve the system's performance as reported in [78].

Paper 1: Experimental Investigations Demonstration of 3D/4D-CAP Modulation with DM-VCSELs

M.B. Othman, X. Zhang, L. Deng, M. Wieckowski, J. Bevensee Jensen, and I. Tafur Monroy, "Experimental Investigations Demonstration of 3D/4D-CAP Modulation with DM-VCSELs," *Photonic Technology Letters*, accepted for publication, 2012.

Experimental Investigations of 3D/4D-CAP Modulation with DM-VCSELs

M.B. Othman[1,2], Xu Zhang[1], Lei Deng [1,3], M. Wieckowski [1,4], J. Bevensee Jensen [1] and I. Tafur Monroy [1]

***Abstract*—We report on experimental investigations of multi-dimensional multi-level carrierless amplitude-phase (CAP) modulation using directly-modulated VCSELs. The signals are transmitted over 20 km of standard single-mode fiber (SSMF). For multi-level 3D-CAP, bit rates of 468.75 Mb/s and 937.5 Mb/s are achieved at 2-levels/dimension and 4-levels/dimension respectively. For 4D-CAP, bit rates of 416.67 Mb/s and 833.3 Mb/s are achieved at 2-levels/dimension and 4-levels/dimension respectively. For all signals, a bit error rate (BER) below the FEC limit of 2.8×10^{-3} for error free reception is achieved after 20 km of SSMF transmission. Spectral efficiencies of 2.68 bits/s/Hz and 2.08 bits/s/Hz are reported for 3D-CAP and 4D-CAP respectively. We believe that multi-dimensional modulation formats represent an attractive solution for providing more flexibility for optical fiber systems.**

***Index Terms*—Carrierless Amplitude and Phase; Multi-level Multi-dimensional Modulation; VCSEL Optical Communication.**

I. Introduction

CARRIERLESS amplitude-phase (CAP) modulation is an advanced modulation format that has been proposed for copper wires as early as 1975 [1]. CAP is a multi-dimensional and multi-level signal format employing orthogonal waveforms; one for each dimension. These waveforms are obtained from frequency domain filters with orthogonal impulse responses. In its principle, it is akin to quadrature amplitude modulation (QAM) in the sense that both CAP and QAM supports multiple levels and modulation in more than one dimension. Contrary to QAM, however, CAP does not require the generation of sinusoidal carriers at the transmitter and the receiver. Additionally, CAP supports modulation in more than 2 dimensions, provided that orthogonal pulse shapes can be identified [2]. This possibility of multi-dimensional modulation makes CAP an attractive modulation format to support multiple services for next generation access networks and in-home networks [3].

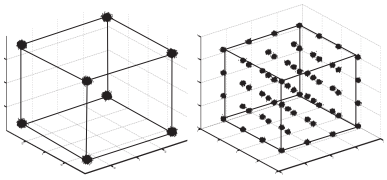

(a) 3D-CAP 2-L/D (b) 3D-CAP 4-L/D

Fig. 1: 3D-CAP with different L/D (a) 2-L/D and (b) 4-L/D

3D-CAP signal constellation with 2-levels/dimension (2-L/D) and 4-levels/dimension (4-L/D) are shown in Fig. 1. The relationship between L/D, bits/symbol and total number of levels are shown in Table I. For 3D-CAP, the 2-L/D corresponds to 3 bits/symbol and 4-L/D corresponds to 6 bits/symbol. For 4D-CAP, 2-L/D corresponds to 4 bits/symbol and 4-L/D corresponds to 8 bits/symbol. For 4D-CAP, there is no straight forward way to display the constellation in a single plot.

Recently, CAP modulation has received attention in the research of optical communication [4]–[6] due to the potentially high spectral efficiency and the possibility of generating the required orthogonal pulses by means of transversal filters. Two dimensional (2D)-CAP 8-levels per dimension (8-L/D) has been demonstrated over polymer optical fiber (POF) in [4], 2D-CAP 4-L/D employing directly modulated vertical cavity surface emitting lasers (DM-VCSELs) for wavelength division multiplexing (WDM) has been experimentally demonstrated in [5], and 40 Gbps 2D-CAP 4-L/D has been successfully generated with transversal filters [6]. Numerical simulations of higher order dimensionality CAP (3D, 4D, and 6D) have been presented in [2] for digital subscriber line (DSL) applications.

In this paper, we present what we believe is the first experimental demonstration of optical transmission of 3D-CAP and 4D-CAP signals using DM-VCSELs. The signals are successfully transmitted over 20 km of SSMF. For both 3D-CAP and 4D-CAP signals, BER

[1] Dep. of Photonics Eng., DTU, Ørsteds Plads 343, DK-2800 Kgs. Lyngby, Denmark. (e-mail: mabio@fotonik.dtu.dk; jebe@fotonik.dtu.dk; idtm@fotonik.dtu.dk).

[2] Dep. of Communication Engineering, FKEE, UTHM, 86400 Parit Raja, Johor, Malaysia.

[3] College of Optoelectronics Science and Engineering., HuaZhong Uni. of Science and Technology, Wuhan 430074, China.

[4] Fac. of Electronics and Information Technology, Institute of Telecommunication, Warsaw Uni. of Technology, Poland.

Manuscript received June XX, 2012; revised XXXX XX, 2012.

TABLE I:
RELATIONSHIP BETWEEN L/D, BITS/SYMBOL, TOTAL LEVELS, BIT RATES, SPECTRAL EFFICIENCY, UPSAMPLING FACTOR, BANDWIDTH AND SYMBOL RATE OF 3D/4D-CAP SIGNALS AT 2-L/D AND 4-L/D

Signal	3D 2-L/D	3D 4-L/D	4D 2-L/D	4D 4-L/D
Bits/symbol	3	6	4	8
Total levels	8	64	16	256
BR (Mb/s) including 7% FEC overhead	468.75	937.5	416.67	833.3
SE (bits/s/Hz)	1.33	2.68	1.04	2.08
Upsampling factor	8	8	12	12
Bandwidth (MHz)	350	350	400	400
Symbol rate (Mbaud)	156.25	156.25	104.16	104.16

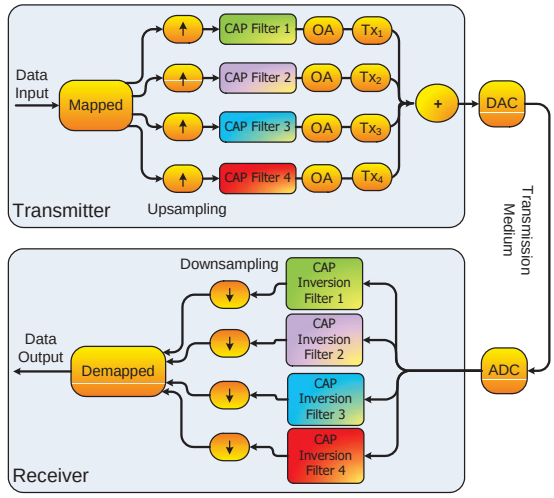

Fig. 2: CAP transmitter and receiver for 3D and 4D CAP system.

below the limit of 2.8×10^{-3} for error free reception was achieved after 20 km of SSMF. For 3D/4D-CAP signals at 4-L/D, a bit rate (BR) of 937.5 Mb/s and 833.3 Mb/s (including the 7% forward error correction (FEC) overhead) is obtained in the system, while spectral efficiencies (SE) of 2.68 bits/s/Hz and 2.08 bits/s/Hz are achieved for 3D-CAP and 4D-CAP respectively at 4-L/D. A total bandwidth of 350 MHz and 400 MHz are required for 3D-CAP and 4D-CAP signals. Symbol rates of 156.25 Mbaud and 104.16 Mbaud are achieved for 3D-CAP and 4D-CAP for both 2D and 4D L/D. The values of all parameters are listed in Table I. We believe that this modulation scheme has the potential to support multiple users with integrated services for optical fiber systems with directly modulated VCSELs.

II. HIGH DIMENSIONALITY CAP

The basic idea of the CAP system is to use different signals as signature waveforms to modulate different data streams. These waveforms are obtained from frequency domain filters with orthogonal impulse responses. Fig. 2 shows the 3D-CAP and 4D-CAP system. Data in the transmitter is mapped according to the given constellation by converting a number of raw data bits into a number of multi-level symbols. These symbols are upsampled and shaped by the CAP filters in order to achieve the desired waveforms. Eventhough CAP can increase the number of levels and dimensions simultaneously, it cannot be viewed as a straight forward way to increase the spectral efficiency. For higher dimensionality CAP, the required samples/symbol ratio is linearly proportional to the number of dimensions [2]. The upsampling factor therefore must be increased along with the increase in dimensionality. This means that the spectral efficiency has not been improved. The advantage of multi-dimensional CAP therefore lies in the possibility to flexibly allocate different services to different users rather than simply increase capacity [2]. From a network perspective, a broadcast-and-select architecture, where the receiver selects one of the data streams by choosing the corresponding filter, can be envisaged. Additionally, the matched filtering can be carried out in the digital domain. As the dimensionality has been increased, the sampling rate of the digital to analog converters (DACs) and analog to digital converters (ADCs) also needs to be increased. Therefore, this would increase the cost of the system [5] and the receiver complexity. However, if the CAP filters could be designed in the analogue domain as in [6] the issue of high performance DAC/ADCs, could be avoided.

The Hilbert pair which are sine and cosine waveforms used for 2D-CAP can not be used for 3D or 4D, so a new set of filters needs to be designed. The filters are added according to the dimensions that are required in the system. To avoid inter-dimensional crosstalk; it is vital that the transmitter-receiver filter combinations satisfy the orthogonality or perfect reconstruction (PR) criteria. In this experiment, the optimization algorithm (OA) described in [7] has been applied to extend the conventional 2D-CAP scheme to higher dimensionality and to assure the PR of the filters. The advantage of this formulation is that the frequency magnitude response of the transmitter and receiver filters will be identical. Additionally, it is a straight-forward method to extend the design to higher dimensionality CAP systems. In equation (1) the variables f_i and g_j represents the CAP transmitter and receiver finite impulse response (FIR) filters

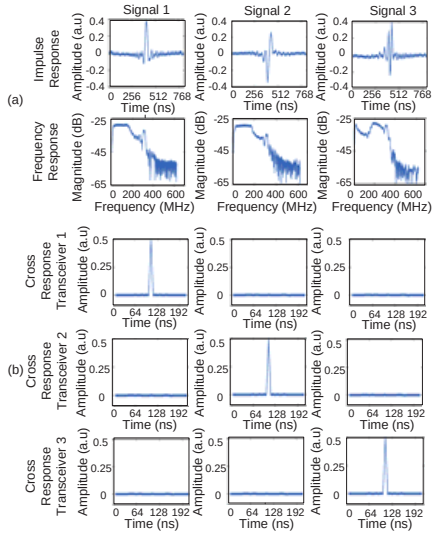

Fig. 3: 3D-CAP (a) impulse responses and frequency responses; b) cross responses of transceiver filters.

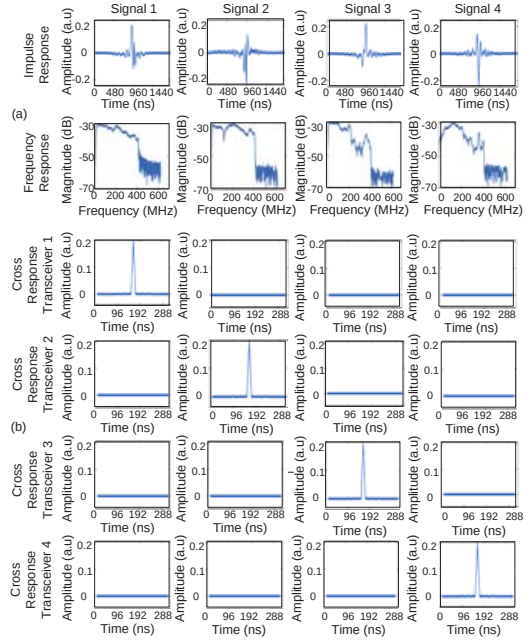

Fig. 4: 4D-CAP (a) impulse responses and frequency responses; b) cross responses of transceiver filters.

respectively.

$$P(f_i)g_j = \tilde{\delta}, \quad i \in \{1,2,3,4\}$$
$$P(f_i)g_j = \tilde{0}, \quad i,j \in \{1,2,3,4\} \text{ and } i \neq j \tag{1}$$

where $P(f_i)$ is a shift matrix that operates on vector f_i, $\tilde{\delta}$ is a vector with one unity element and $\tilde{0}$ is a vector of all zeros.

The optimization algorithm for high dimensionality CAP is described as follows

$$\min_{f_1,f_2,f_3,...f_N} \max\left(|F_{1,HP}|, |F_{2,HP}|, |F_{3,HP}|, ...|F_{N,HP}|\right) \tag{2}$$

subject to the PR condition in (1) and

$$g_i = \text{inverse}\left[F_i\right], i \in \{1,2,3,..N\} \tag{3}$$

where F_i is the discrete Fourier transform (DFT) of vector f_i. The $F_{i,HP}$ is the out-of-band portion of the transmitter response above the f_B. The boundary frequency f_B is to ensure the receivers frequency magnitude response will be exactly the same as the transmitters. This means that the out-of-band spectral content of the filters is zero. For 1D pulse amplitude modulation (PAM), Nyquist has proved that to avoid inter symbol interference (ISI), i.e., PR condition for one dimension, a minimum bandwidth of $\frac{1}{2T}$ is needed, where $\frac{1}{T}$ is the baud rate. Similarly, for the 3D-CAP system, there is a minimum bandwidth $(f_{B,min})$ value that will achieve the PR condition. It has been proven in [7], that f_B for the 3D-CAP system is at least equal to or greater than $\frac{3}{2T}$ to preserve the PR condition. In the experiments, the band limiting condition f_B is set to $\frac{2}{3}(2 \times f_s)$, where f_s is the sampling rate.

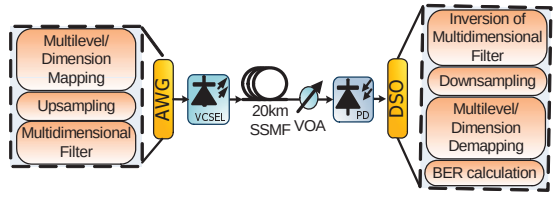

Fig. 5: Experimental setup for DM-VCSELs for 3D and 4D CAP signals over 20 km of SSMF.

Fig. 3 and 4 show the responses of the digital filters at the transmitter and receiver for 3D-CAP and 4D-CAP respectively. Fig. 3(a) and 4(a) show the impulse response and the frequency response for each of the signals. Fig. 3(b) and 4(b) shows the cross responses of the transmitter-receiver (transceiver) filters. We observe an impulse at the cross responses of corresponding filter, for example f_1 and g_1, f_2 and g_2, etc and zeros at the other transceivers, for example f_1 and g_2, f_1 and g_3, etc. This means that the filters have orthogonal impulse responses, and comply with equation (1).

III. Experimental Setup

Fig. 5 illustrates the experimental setup. An arbitrary waveform generator (AWG) with a sampling rate of 1.25 GSa/s is used to generate the 3D/4D-CAP at 2-L/D and 4-L/D signals. Data in the transmitter is mapped according to the given constellation by converting a

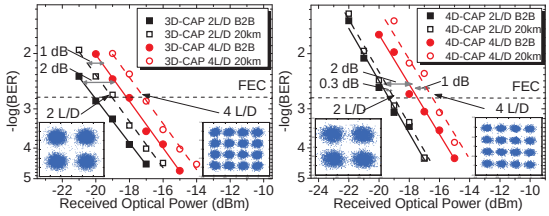

Fig. 6: BER vs. received optical power for (a) 3D-CAP at 2-L/D and 4-L/D and (b) 4D-CAP at 2-L/D and 4-L/D.

number of raw data bits into a number of multi-level symbols (i.e 2-L/D or 4-L/D). Those symbols are upsampled and later shaped (or filtered), according to the optimization algorithm. The transmitter signature filters are implemented as fixed FIR filters. A commercial Raycan VCSEL emitting at 1550 nm have been used. The VCSEL with 4.5 GHz bandwidth operating at 4 mA bias level are directly modulated with the CAP signals.

The signal is propagated through 20 km of SSMF with a total fiber loss of 6.5 dB. A variable optical attenuator (VOA) is placed after the fiber for bit error rate (BER) measurements. The signal is directly detected by a photodetector (PD) and stored in a digital storage oscilloscope (DSO) with a 40 GSa/s sampling rate for offline demodulation. At the receiver, the inversion of the transmission filter is implemented to retrieve the original sequence of symbols. The symbols are down sampled and demapped before the data can be recovered. Transmission quality was assessed using receiver sensitivity at a BER of 2.8×10^{-3}, since forward error correction (FEC) may be applied to obtain error free transmission when the 7% FEC overhead is taken into account.

IV. Results

Fig. 6(a) and (b) presents the BER results obtained for 3D-CAP and 4D-CAP signals. Both figures show the variation of BER in terms of received optical power for 3D-CAP and 4D-CAP. The solid symbols represent optical B2B and the hollow symbols represent 20 km of SSMF transmission. Additionally, the square symbols represent the 2-L/D and the round symbols represent the 4-L/D for 3D-CAP and 4D-CAP. Fig. 6(a) shows that for B2B, the receiver sensitivity at FEC limit is -19.8 dBm and -17.8 dBm for 2-L/D and 4-L/D respectively. After 20 km of SSMF transmission, the receiver sensitivity at the FEC limit is -18.8 dBm for 2-L/D, and -16.8 dBm for 4-L/D. A 1 dB power penalty is observed between B2B and 20 km of SSMF transmission. This low penalty shows that the orthogonality is preserved after 20 km of SSMF with a total chromatic dispersion of 340 ps/nm.km. The 3D-CAP signals are successfully demodulated below the FEC limit after 20 km of SSMF transmission. This can be clearly seen from the 2-L/D and 4-L/D constellation diagram in Fig. 6(a) with a BER of approximately 1×10^{-3} after 20 km of SSMF transmission.

Fig. 6(b) illustrates the BER results obtained for 4D-CAP. We observe a 0.3 dB (2-L/D) and 1 dB (4-L/D) power receiver sensitivity between B2B and 20 km of SSMF transmission. The insets show the received signal constellation with a BER of approximately 1×10^{-3} for 2-L/D and 4-L/D after 20 km of SSMF transmission. We attribute the 0.7 dB difference in penalty between 4D-CAP 2-L/D and 3D-CAP 2-L/D to measurement uncertainties mainly related to the performance of a free-running un-cooled VCSEL. The 4D-CAP has lower sensitivity compared to 3D-CAP since the additional dimension filters require additional bandwidth. A 2 dB difference in B2B receiver sensitivity is observed between the 2-L/D and 4-L/D for 3D-CAP and 4D-CAP. This is due to the dimensionality, greater receiver complexity and the increased receiver interference energy.

V. Conclusion

We have experimentally investigated and successfully demonstrated multi-dimensional multi-level 3D/4D-CAP transmission over 20 km of SSMF with DM-VCSELs. Spectral efficiencies of 2.68 bits/s/Hz and 2.08 bits/s/Hz for 4-levels per dimension are reported for 3D-CAP and 4D-CAP at bit rates of 937.5 Mb/s and 833.3 Mb/s respectively. The flexibility of CAP provided by an increase in the number of dimensions can potentially be utilized to allocate different services to different users. On the other hand, our results shows that the high dimensionality CAP requires excess bandwidth due to the higher upsampling factor. This results in a decreased spectral efficiency. This tradeoff between the flexibility and spectral efficiency needs to be considered in the system design. Future work of high dimensionality CAP at higher bit rates will be carried out to investigate the tradeoff of the CAP signals with DM-VCSELs.

References

[1] D.D. Falconer, “Carrierless AM/PM” in Bell Laboratories Technical Memorandum, 1975.
[2] A.F. Shalash, et.al, “Multidimensional carrierless AM/PM systems for digital subscriber loops” *IEEE Trans. on Comm.*, vol.47, no.11, pp.1655-1667, 1999.
[3] Antonio Caballero, et.al “Carrierless N-Dimensional Modulation Format for Multiple Service Differentiation in Optical In-home Networks”, in Proc. IPC, TuM4, 2011.
[4] M. Wieckowski, et.al, “300 Mbps transmission with 4.6 bit/s/Hz spectral efficiency over 50 m PMMA POF link using RC-LED and multi-level Carrierless amplitude phase modulation,” in Proc. OFC, NTuB8, 2011.
[5] Roberto Rodes, et.al,“Carrierless amplitude phase modulation of VCSEL with 4bit/s/Hz spectral efficiency for use in WDM-PON” *Optics Express*, vol.19, no.27, 2011.
[6] J. D. Ingham, et.al, “40 Gb/s Carrierless Amplitude and Phase Modulation for Low-Cost Optical Datacommunication Links” in Proc. OFC, OThZ3, 2011.
[7] Xiaosong Tang, et.al,“A new digital approach to design 3D CAP waveforms”,*IEEE Trans. on Comm.*, vol.51, no.1, pp. 12- 16,2003.

Paper 2: Experimental Demonstration of 3D/4D-CAP Modulation Employing CT-CMA Channel Estimation

M.B. Othman, X. Zhang, L. Deng, J. Bevensee Jensen, and I. Tafur Monroy, "Experimental Demonstration of 3D/4D-CAP Modulation Employing CT-CMA Channel Estimation," submitted to *Journal of Lightwave Technology*, 2012.

Experimental Demonstration of 3D/4D-CAP Modulation Employing CT-CMA Channel Estimation

Maisara Binti Othman,[1,2] *Student Member, IEEE,* Xu Zhang,[1] *Student Member, IEEE,*
Lei Deng,[1,3] *Student Member, IEEE,*
Jesper Bevensee Jensen,[1] *Member, IEEE,* and Idelfonso Tafur Monroy,[1] *Member, IEEE*

***Abstract*—The performance of multi-dimensional multi-level carrierless amplitude-phase (CAP) modulation using directly-modulated 1310 nm VCSELs is investigated and experimentally demonstrated. The signals are transmitted over 10 km standard single-mode fiber (SSMF). For multi-level 3D-CAP, bit rates of 6 Gb/s and 10.28 Gb/s are achieved at 2-levels/dimension (2-L/D) and 4-levels/dimension (4-L/D) respectively within a 4 GHz bandwidth. For 4D-CAP, bit rates of 6.85 Gb/s and 10.66 Gb/s are achieved at 2-L/D and 4-L/D respectively within a 8 GHz bandwidth. For all signals, bit error rate (BER) below the FEC limit of 2.8×10^{-3} for error free reception is achieved after 10 km SSMF transmission. Spectral efficiencies of 2.44 bits/s/Hz and 1.33 bits/s/Hz are reported for 3D-CAP and 4D-CAP respectively at 4-L/D. Furthermore an investigation of coordinate transformed constant modulus algorithm (CT-CMA) channel estimation to the CAP signals have been performed in this experiment.**

We believe high dimensionality CAP has potential for providing more flexibility for multiple services applications in future optical access.

***Index Terms*—Carrierless Amplitude-Phase; multi-level multi-dimensional modulation.**

I. Introduction

HISTORICALLY, optical communication systems were using a very simple modulation format, which is known as on-off keying (OOK) or amplitude shift keying (ASK). It is still the preferred modulation format for most links due its easy implementation [1]. However, as the transmission distances and the per channel bit rates increase, and the channel spacing decrease, more advanced modulation formats with higher dimensionality are suggested to mitigate nonlinear transmission impairments and to facilitate a per channel bit rate increase beyond the limits of binary systems

[1] DTU Fotonik, Department of Photonics Engineering, Technical University of Denmark, Ørsteds Plads 343, DK-2800 Kgs. Lyngby, Denmark. (e-mail: mabio@fotonik.dtu.dk; jebe@fotonik.dtu.dk; idtm@fotonik.dtu.dk).

[2] Department of Communication Engineering, Faculty of Electrical and Electronic Engineering, UTHM, 86400 Parit Raja, Johor, Malaysia.

[3] College of Optoelectronics Science and Engineering, Huazhong University of Science and Technology, Wuhan 430074, China.

Manuscript received June XX, 2012; revised XXXX XX, 2012.

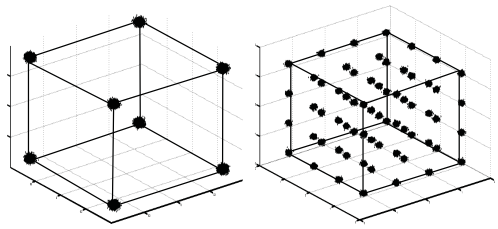

(a) 3D-CAP 2-L/D (b) 3D-CAP 4-L/D

Fig. 1: 3D-CAP with different L/D (a) 2-L/D and (b) 4-L/D

Higher order modulation formats so-called carrierless amplitude-phase (CAP) modulation has been proposed for copper wires as early as 1975 [2]. CAP is a multi-dimensional and multi-level signal format employing orthogonal waveforms; one for each dimension. These waveforms are obtained from frequency domain filters with orthogonal impulse responses. In its principle, it is akin to quadrature amplitude modulation (QAM) in the sense that both CAP and QAM supports multiple levels. Contrary to QAM, however, CAP does not require the generation of sinusoidal carriers at the transmitter and the receiver. CAP has been widely used for asymmetrical digital subscriber line (ADSL) and asynchronous transfer mode (ATM) local area networks (LANs) [3]. In both of these applications, CAP modulation has been adopted primarily because of its high bandwidth efficiency and low implementation costs. Additionally, CAP supports modulation in more than 2 dimensions, provided that orthogonal pulse shapes can be identified [4]. This possibility of multi-dimensional modulation makes CAP an attractive modulation format to support multiple services for next generation access and in-home networks [5]. 3D-CAP signal constellations with 2-levels per dimension (2-L/D) and 4-levels per dimension (4-L/D) are shown in Fig. 1. For 4D-CAP, there is no straight forward way to display the constellation in a single plot. The relationship between the number of levels

TABLE I:
RELATIONSHIP BETWEEN L/D, BITS/SYMBOL AND TOTAL LEVELS FOR 3D/4D-CAP SIGNALS

Signal	3D 2-L/D	3D 4-L/D	4D 2-L/D	4D 4-L/D
Bits/symbol	3	6	4	8
Total levels	8	64	16	256

per dimension (L/D), the number of bits/symbol and the total number of levels are listed in Table I. For 3D-CAP, 2-L/D yields 3 bits/symbol and 4-L/D yields 6 bits/symbol. Meanwhile for 4D-CAP, 2-L/D yields 4 bits/symbol and 4-L/D yields 8 bits/symbol.

Recently, CAP modulation has received attention in the research of optical communication [6]–[8] due to the potentially high spectral efficiency and the possibility of generating the required orthogonal pulses by means of transversal filters. In [6] 2D-CAP 8-L/D over 50 m polymer optical fiber (POF) has been demonstrated with resonant cavity light emitting diodes (RC-LEDs). Directly modulated vertical cavity surface emitting lasers (DM-VCSELs) for wavelength division multiplexing (WDM) application with 2D-CAP 4-L/D has been experimentally demonstrated in [7], reporting transmission of up to 1.25 Gbps over 26 km standard single mode fiber (SSMF). A spectral efficiency of 4 bit/s/Hz is reported. In [8] and [9], 10 Gb/s and 40 Gb/s 2D-CAP 4-L/D has been successfully generated with analogue transversal filters. The proposals of 3-dimensional (3D) CAP modulation have been presented in [4], [10] and [11]. Higher dimensionality such as 4-dimensional (4D) and 6-dimensional (6D) CAP have also been proposed in [4] for digital subsriber line (DSL) application. In [12] we reported on the first experimental investigations of 3D-CAP and 4D-CAP for optical fiber transmission at bit rates up to 937.5 Mb/s.

In this paper, we built on these results and increase bit rates to more than 10 Gb/s. Additionally we investigate coordinate transformed constant modulus algorithm (CT-CMA) for channel estimation. The optical transmission is realized using DM-VCSELs. The signals are successfully transmitted over 10 km SSMF.

For both 3D-CAP and 4D-CAP signals, BER below the forward error correction (FEC) limit of 2.8×10^{-3} for error free reception is achieved after 10 km SSMF. The bit rate (BR) and spectral efficiency (SE) of the 3D/4D-CAP signals are listed in Table II. For 3D/4D-CAP signals at 4-L/D, a bit rate of 10.28 Gb/s and 10.66 Gb/s (including 7% FEC overhead) is obtained in the system. Spectral efficiencies of 2.44 bits/s/Hz and 1.33 bits/s/Hz are achieved for 3D-CAP and 4D-CAP respectively at 4-L/D.

We believe that this modulation scheme has a potential to support multiple users with multiple services using a single directly modulated VCSEL.

TABLE II:
BIT RATES, SPECTRAL EFFICIENCY, UPSAMPLING FACTOR, BANDWIDTH AND SYMBOL RATE OF 3D/4D-CAP SIGNALS AT 2-L/D AND 4-L/D

Signal	3D 2-L/D	3D 4-L/D	4D 2-L/D	4D 4-L/D
BR (Gb/s) including 7% FEC overhead	6	10.28	6.85	10.66
SE (bits/s/Hz)	1.42	2.44	0.85	1.33
Upsampling factor	12	14	14	18
Bandwidth (GHz)	4.35	4	8	8
Symbol rate (Gbaud)	2	1.713	1.713	1.333

II. GENERATION OF CAP

A. Introduction of CAP modulation

The basic idea of the CAP system is to use different signature waveforms to modulate different data streams. At the transmitter, the signature waveforms are generated by orthogonal shaping filters. At the receiver, the individual data streams are reconstructed by matched filtering. The matched filter used in the receiver has an impulse response equal to the time domain inversion of the impulse response of the transmitter filter.

2D-CAP modulation traditionally employs the product of a square-root raised cosine (SRRC) filter (zero inter-symbol interference (ISI)) and sine or cosine waveforms (zero cross-correlation interference (CCI)). Perfect reconstruction (PR) at the receiver is secured through the orthogonality of the two filters (sine and cosine). The details of the 2D-CAP modulation generation can be found in [3] and [4]. Before the signals can be filtered digitally, the received symbols have to be upsampled. According to the Nyquists theorem, the minimum sampling rate has to be at least twice the highest frequency component of the signal. Moreover, the upsampling factor have to be high enough to prevent aliasing effects. The usual upsampling factors are 3 or 4, depending on the roll-off factor of the raised cosine filter used to design the shaping filter.

B. 3D-CAP and 4D-CAP

Similarly to other modulation formats, the throughput and spectral efficiency of the CAP system can be increased through multi-level encoding [13]. In addition, and contrary to e.g QAM, the data can be modulated in more than two dimensions.

For higher dimensionality CAP, the required sample/symbol ratio is linearly proportional to the number of dimensions [4]. The upsampling factor therefore

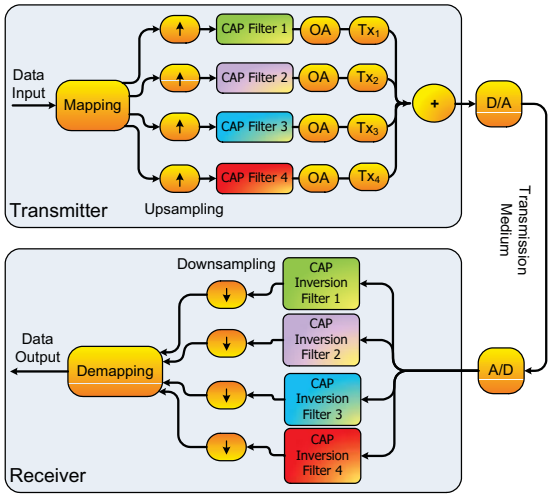

Fig. 2: CAP transmitter and receiver for 3D or 4D CAP system.

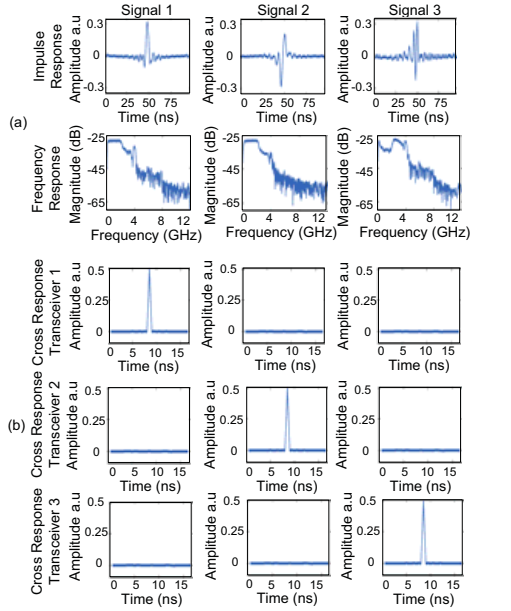

Fig. 3: 3D-CAP (a) impulse responses and frequency responses b) cross responses of transmitter-receiver filters.

must be increased in order to support the increased number of dimensions. This means that the spectral efficiency has not be improved. However, the additional dimensions can be used to support multiple access application.

Higher dimensionality CAP can be implemented by modulating the data streams using more than two signature waveforms. These signature waveforms need to be orthogonal to each other. The sine and cosine signals used in 2D-CAP can not be used for 3D or 4D, so a new set of filters needs to be designed. The 3D/4D CAP systems are shown in Fig. 2. The filters are added depending on the dimensions that are required in the system. A minimax optimization approach has been employed to extend the conventional 2D-CAP scheme to higher dimensionality such as 3D and 4D [4], [14]. In this experiment, the optimization algorithm (OA) in [14] has been used. The advantage of this formulation is that the frequency magnitude response of the transmitter and receiver filters will be exactly the same at both sides. Additionally, it is a straight-forward method to extend the design to higher dimensionality CAP systems. In equation (1) the variables f_i and g_j represents the CAP transmitter and receiver finite impulse response (FIR) filters respectively.

$$\begin{aligned} P(f_i)g_j &= \tilde{\delta}, \quad i,j \in \{1,2,3,4\} \\ P(f_i)g_j &= \tilde{0}, \quad i,j \in \{1,2,3,4\} \text{ and } i \neq j \end{aligned} \tag{1}$$

where $P(f_i)$ is a shift matrix that operates on vector f_i, $\tilde{\delta}$ is a vector with one unity element and $\tilde{0}$ is a vector of all zeros.

The optimization algorithm for high dimensionality CAP is described as follows

$$\min_{f_1,f_2,f_3,\ldots f_N} \max\left(|F_{1,HP}|, |F_{2,HP}|, |F_{3,HP}|, \ldots |F_{N,HP}|\right) \tag{2}$$

subject to the PR condition in (1) and

$$g_i = \text{inverse}\left[F_i\right], i \in \{1,2,3,..N\} \tag{3}$$

where F_i is the discrete Fourier transform (DFT) of vector f_i . The $F_{i,HP}$ is the out-of-band portion of the transmitter response above the f_B. The boundary frequency f_B is to ensure the receivers frequency magnitude response will be exactly the same as the transmitters. This means that the out-of-band spectral content of the filters is zero. For the one dimension (1D) pulse amplitude modulation (PAM) situation, Nyquist has proved that to achieve zero ISI, i.e., PR condition for one dimension, a minimum $\frac{1}{2T}$ bandwidth is needed, where $\frac{1}{T}$ is the baud rate. Similarly, for the 3D-CAP and 4D-CAP systems, there is minimum bandwidth $f_{B,min}$ value that will allow a PR condition. Any value smaller than $f_{B,min}$ will not result in a PR solution. It has been proven in [15], that f_B for 3D-CAP system is at least equal to or greater than $\frac{3}{2T}$ to preserve the PR condition. In the experiments, the band limiting condition f_B is set to $\frac{2}{3}(2 \times f_s)$, where f_s is the highest frequency component of the 3D/4D-CAP signals.

Fig. 3 and 4 shows the responses of the digital filters at the transmitter and receiver for 3D-CAP and 4D-CAP. The figures are divided into 2 sections (a) and

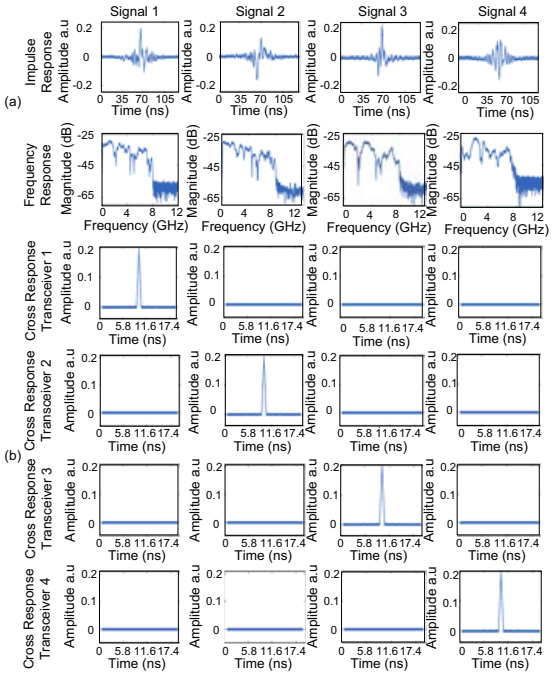

Fig. 4: 4D-CAP (a) impulse responses and frequency responses b) cross responses of transmitter-receiver filters.

(b). Section (a) shows the impulse response and the frequency response for each of the signal and section (b) shows the cross responses of the transmitter-receiver filters. The impulse only exists at the cross responses of f_1 and g_1, f_2 and g_2, f_3 and g_3, f_4 and g_4 (extra dimension for 4D-CAP), with zeros at the other transmitter-receiver pairs, for example f_1 and g_2, f_1 and g_3 and etc. The transmitter-receiver filter combinations are orthogonal and satisfy the perfect reconstruction criteria.

In order to make sure that the filters comply with equation (1) we have plotted their autocorrelation functions $(i = j)$ and their crosscorrelation functions $(i \neq j)$ as shown in Fig. 5 for the 3D-CAP and 4D-CAP. The autocorrelation and crosscorrelation functions satisfy the perfect reconstruction criteria.

Fig. 6 presents the added pulse shape in time domain and the combined spectrum of 3D-CAP and 4D-CAP for the CAP transmission respectively. For 3D-CAP, the upsampling factor is 12 and 14 for 2-L/D and 4-L/D respectively. For 4D-CAP the upsampling factor is 14 and 18 for 2-L/D and 4-L/D respectively. A total bandwidth of approximately 4 GHz and 8 GHz are required for the 3D-CAP and 4D-CAP signals respectively. A 2 Gbaud and 1.713 Gbaud symbol rate is achieved for 3D-CAP for 2-L/D and 4-L/D. For 4D-CAP symbol rates of 1.713 Gbaud and 1.33 Gbaud

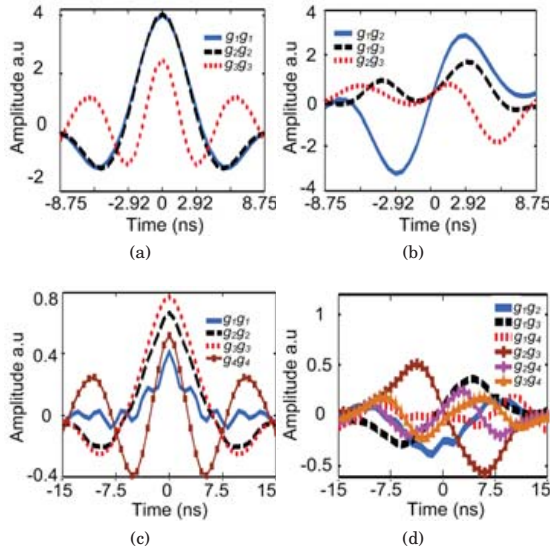

Fig. 5: (a) 3D-CAP auto correlation; (b) 3D-CAP cross correlation; (c) 4D-CAP auto correlation; and (d) 4D-CAP cross correlation.

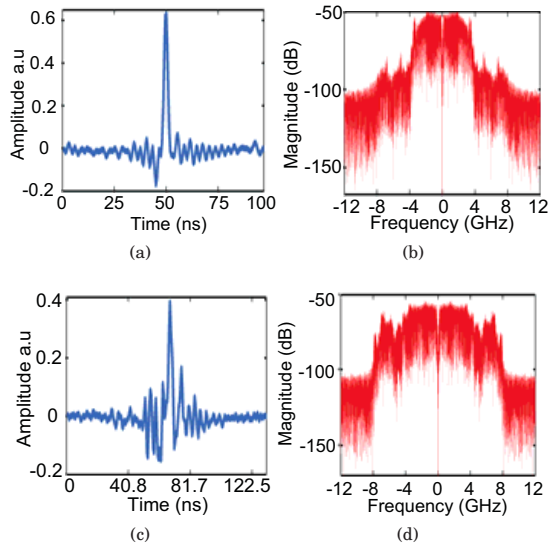

Fig. 6: (a) 3D-CAP added pulse response (b) 3D-CAP combined frequency spectrum (c) 4D-CAP added pulse response and (d) 4D-CAP combined frequency spectrum.

are obtained for 2-L/D and 4-L/D respectively. The summarized value of all the parameters are listed in Table II.

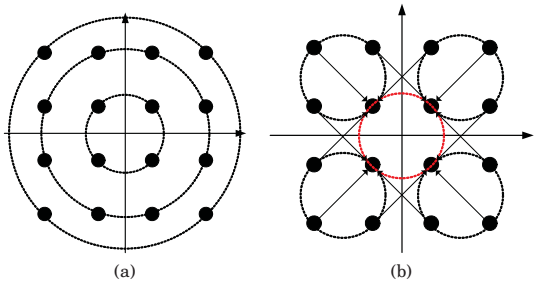

Fig. 7: Principle of blind CMA equalizer for 16-CAP (a) conventional circle classed CMA and (b) coordinate transformed CMA with highlighted unified circle in the middle.

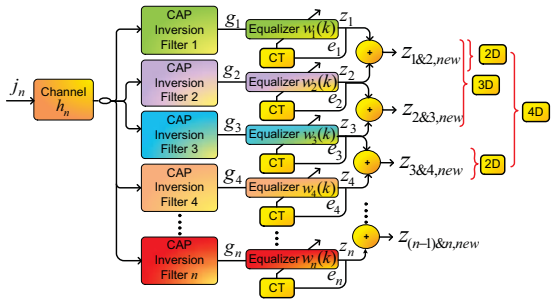

Fig. 8: Structure of n-dimensional CAP using coordinate transformed (CT) blind CMA equalizer channel estimation.

III. DSP Algorithms for CAP Transmission Channel Estimation

In optical multi-dimensional CAP transmission systems, inter symbol interference (ISI) induced by transmission impairments and multi-dimensional cross talk are the main factors that leads to system performance degradation. The potential of channel estimation by using constant modulus algorithm (CMA) to combat the ISI and inter-dimensional crosstalk in CAP signals is investigated in this experiment. The CMA equalizer is capable of tracking channel characteristic adaptively and compensating for transmission impairments effectively [16]. Moreover, blind CMA equalization is simple to implement and suitable to equalize constant envelope signal such as n-phase shift keying (PSK) signal. Standard CMA equalization, however, can not be used directly to multi dimensional CAP with higher modulation order signals 4-L/D. We therefore propose a coordinate transformed CMA equalizer for optical multi-dimensional CAP transmission systems.

A. Theoretical overview of blind CMA Equalizer

In general, two types of CMA equalizer; conventional circle class CMA and coordinate transformed CMA are used for n-QAM modulation format channel estimation. Fig. 7(a) shows the principle of conventional circle classed CMA and 7(b) coordinate transformed (CT) CMA for 4-L/D based on constellation diagram. In conventional circle classed CMA, signals of 4-L/D are divided into three categories with different radius. This means that three different structures of the CMA equalizer are required, one for each radius. For CT 4-L/D, the sixteen clusters of the 4-L/D constellation are transformed into a unified circle in the middle, and CMA can be performed in a manner similar to 2-L/D. This shows that coordinate transformed CMA is simple and feasible to employ as shown in Fig. 7(b). Fig. 8 presents the receiver structure of the n-dimensional CAP with coordinate transformed (CT) blind CMA equalizer [17]. The structure also shows how the CT-CMA is applied at the different dimensions of 3D and 4D CAP. j_n is the transmitted signal, h_n is the impulse response of the channel, g_n is the equalizer input signal from the inverse filter, $w_n(k)$ is the equalizer of N-taps weight, z_n is the equalizer output signal and e_n is the error function of the CMA.

The transformed signals $z_{n,new}$ after coordinate transformed CMA can be represented as

$$z_{n,new}(k) = \{z_{n,R}(k) - 2\text{sign}[z_{n,R}(k)]\} + i\{z_{n,I}(k) - 2\text{sign}[z_{n,I}(k)]\} \quad (4)$$

where sign$[\cdot]$ is the sign function. The $z_{n,R}(k)$ and $z_{n,I}(k)$ are the real (in-phase) and image (quadrature) parts of the two dimensional CAP signals after signal detection. The update function of the adaptive N-taps weight vector $w_n(k)$ using least mean square (LMS) algorithm is given as

$$w_n(k+1) = w_n(k) + \mu z_{n,new}(k)e(n)g_n^*(k) \quad (5)$$

where μ is the step size of the LMS algorithm and $e(n)$ is the error function, which is given by

$$e(n) = R^2 - |z_{n,new}(k)|^2 \quad (6)$$

where R is the radius of a unified circle. All of the steps are employed to each dimension of the signal.

IV. Experimental setup

Fig. 9 shows the setup implemented in the experiment. An arbitrary waveform generator (AWG) with a sampling rate of 24 GSa/s is used to generate the 3D/4D-CAP. Data in the transmitter is mapped according to the given constellation by converting a number of raw data bits into a number of multilevel symbols (i.e 2-L/D or 4-L/D). Those symbols are upsampled and later shaped by the filters designed by the optimization algorithm. The transmitter filters are implemented as fixed finite impulse response (FIR) filters. The 3D-CAP signals at bit rates of 6.28 Gb/s (2-L/D) and 10.28 Gb/s (4-L/D) with an upsampling factor of 12

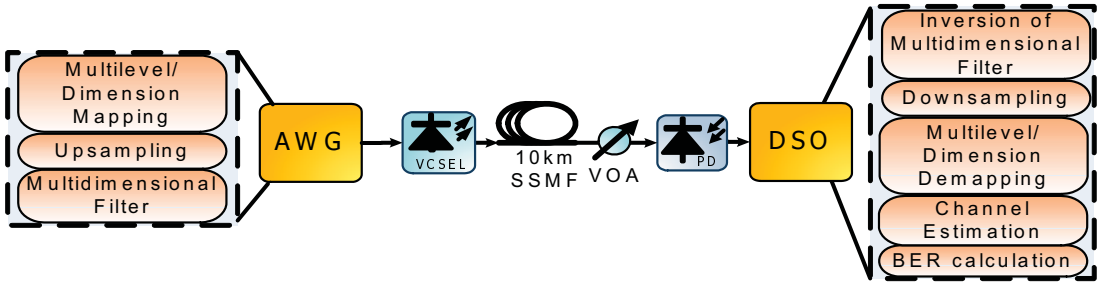

Fig. 9: Experimental setup for DM-VCSELs for 3D and 4D CAP signals over 10 km SSMF

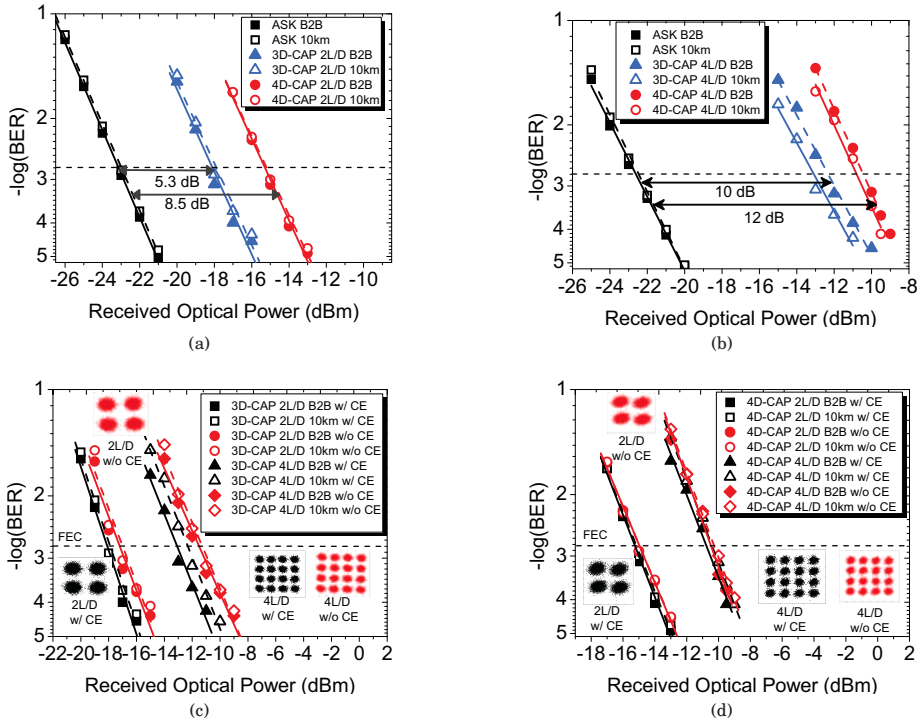

Fig. 10: Showing the BER vs ROP (a) comparing the ASK, 3D-CAP and 4D-CAP at 2-L/D at bit rate of 6 Gb/s; (b) comparing the ASK, 3D-CAP and 4D-CAP at 4-L/D at bit rate of 10 Gb/s; (c) 3D-CAP at 2-L/D and 4-L/D without channel estimation (w/o CE) and with channel estimation (w/ CE); and (d) 4D-CAP at 2-L/D and 4-L/D without channel estimation (w/o CE) and with channel estimation (w/ CE).

and 14 are generated by the AWG. For 4D-CAP, an upsampling factor of 14 and 18 are implied to produce the bit rate of 6.85 Gb/s (2-L/D) and 10.66 Gb/s (4-L/D). A 1310 nm VCSEL from Alight Technologies with 10 GHz bandwidth operating at 10 mA bias is directly modulated with the CAP signals.

The signal is propagated through 10 km SSMF with a total fiber loss of 3.5 dB. A variable optical attenuator (VOA) is placed after the fiber for bit error rate (BER) measurements. The signal is directly detected by a photodetector (PD) and stored in a digital storage scope (DSO) with 40 GSa/s sampling rate for offline demodulation.

At the receiver, the time inversions of the transmission filters are implemented to retrieve the original sequence of symbols. The symbols are down sampled and demapped before the data can be recovered. The CT CMA equalizer is employed to the received CAP signals. Transmission quality is assessed using receiver sensitivity at a BER of 2.8×10^{-3}, since forward

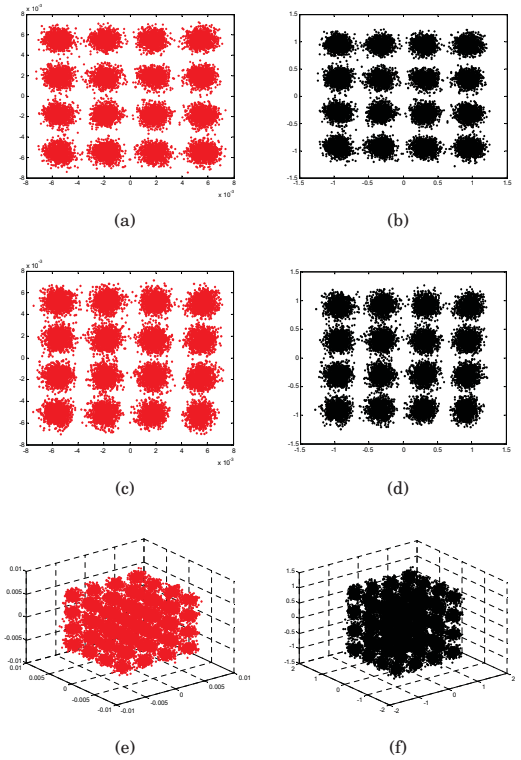

Fig. 11: 3D-CAP (a) receiver 1 and receiver 2 before coordinate transformed CMA (b) receiver 1 and 2 after coordinate transformed CMA (c) receiver 2 and receiver 3 before coordinate transformed CMA (d) receiver 2 and receiver 3 after coordinate transformed CMA (e) receivers in 3D before coordinate transformed CMA and (f) receivers in 3D after coordinate transformed CMA.

error correction (FEC) techniques may be applied to obtain error free transmission when the 7% of FEC overhead is taken into account.

V. Results

Fig. 10 (a) and (b) shows the BER of amplitude shift keying (ASK) signals compared to 3D-CAP and 4D-CAP bit rates of 6 Gb/s and 10 Gb/s respectively. From this comparison both results shows that ASK has a superior performance to 3D-CAP and 4D-CAP at 2-L/D and 4-L/D.

Fig. 10 (c) and (d) presents the BER results obtained for 3D-CAP and 4D-CAP signals. Both figures show the variation of BER in terms of received optical power (ROP) for 3D-CAP and 4D-CAP. The solid symbols represent optical B2B and the hollow symbols represent 10 km SSMF transmission. Additionally, the square symbols represent the 2-L/D and the round symbols represent the 4-L/D for 3D-CAP and 4D-CAP.

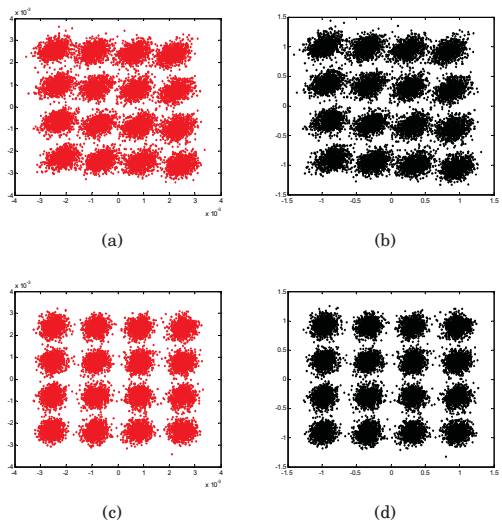

Fig. 12: 4D-CAP (a) receiver 1 and receiver 2 before coordinate transformed CMA (b) receiver 1 and 2 after coordinate transformed CMA (c) receiver 3 and receiver 4 before coordinate transformed CMA and (d) receiver 3 and receiver 4 after coordinate transformed CMA.

TABLE III:
ROP at BER of 2.8×10^{-3} for 3D-CAP and 4D-CAP at 2-L/D and 4-L/D for B2B and After 10 km SSMF Transmission without Channel Estimation and with Channel Estimation

Signal	B2B 2-L/D	10 km 2-L/D	B2B 4-L/D	10 km 4-L/D
3D-CAP w/o CE	-17.2 dBm	-17 dBm	-11.5 dBm	-11.3 dBm
3D-CAP w/ CE	-18.2 dBm	-18 dBm	-13.3 dBm	-12.3 dBm
4D-CAP w/o CE	-14.5 dBm	-14.5 dBm	-10.3 dBm	-10.3 dBm
4D-CAP w/ CE	-15 dBm	-15 dBm	-10.8 dBm	-10.3 dBm

For 3D-CAP B2B, the receiver sensitivity at the FEC limit is –17.2 dBm and –11.5 dBm for 2-L/D and 4-L/D respectively. After 10 km SSMF transmission, the receiver sensitivity at the FEC threshold is –17 dBm for 2-L/D, and –11.3 dBm for 4-L/D corresponding to a penalty of 0.2 dB. After employing the coordinate transformed (CT) blind CMA equalizer channel estimation (CE), the receiver sensitivity at the FEC limit is improved by 1 dB for B2B and after 10 km transmission at 2-L/D. At 4-L/D, an improvement of

1.8 dB for B2B and 1 dB after 10 km transmission is observed. This shows that the blind CMA equalizer helps to improve the performance and compensated the inter-dimensional crosstalk. The 3D-CAP signals are successfully demodulated below the FEC limit after 10 km SSMF transmission. This can be clearly seen from the constellation diagram of 2-L/D with ROP at –17 dBm and 4-L/D with ROP at –11 dBm before and after employeing the channel estimation with BER approximately 1×10^{-3} after 10 km SSMF transmission.

In Fig. 10(d) before employing the channel estimation, we observe no transmission penalty for 2-L/D and 4-L/D between B2B and after 10 km SSMF transmission. After employing the channel estimation there is a slight improvement of approximately 0.5 dB for both cases. The insets show the received signal constellation before and after channel estimation with BER of approximately 1×10^{-3}. Constellation of 2-L/D at ROP of –15 dBm and 4-L/D at ROP of –10 dBm after 10 km SSMF transmission are depicted in Fig. 10.

The power penalty between the B2B and after 10 km SSMF transmission are very small because of the low dispersion at 1310 nm. 4D-CAP has lower sensitivity compared to 3D-CAP since the additional dimension filter designs requires additional bandwidth. Different upsampling factor also effects the power penalty between the 2-L/D and 4-L/D. A 5.5 dB power penalty is observed between the 2-L/D and 4-L/D for 3D/4D-CAP. Of this, 3 dB is due to the decreased symbol spacing and 2.5 dB is attributed to the added of dimensionality as well as the increased complexity in the receiver and the increased receiver interference energy. The summarized results of the receiver sensitivity at BER of 2.8×10^{-3} are given in Table III for 3D-CAP and 4D-CAP at different L/D with out channel estimation (w/o CE) and with channel estimation (w/ CE).

Fig. 11 shows the 3D-CAP 4-L/D in combination of receiver 1 and 2, receiver 2 and 3 and three dimension (3D) of receiver 1, 2 and 3 before and after employing the coordinate transformed CMA channel estimation at ROP of –11 dBm. Fig 12 shows the 4D-CAP 4-L/D in combination of receiver 1 and 2 and receiver 3 and 4 before and after channel estimation at ROP of –10 dBm. The constellation diagrams shows that CAP signals are successfully demodulated at each of the dimensions after 10 km SSMF transmission.

VI. Conclusion

We have successfully demonstrated multi-dimensional multi-level 3D/4D-CAP over 10 km SSMF with a directly modulated 1310 nm VCSEL. Spectral efficiencies of 2.44 bits/s/Hz and 1.33 bits/s/Hz are reported for 4-L/D 3D-CAP and 4D-CAP at 10.28 Gb/s and 10.66 Gb/s. In this investigation, different upsampling factors are implemented at 2-L/D and 4-L/D for 3D/4D-CAP to maintain perfect reconstruction at each of the dimensions.

Although the spectral efficiency has not be improveded, the flexibility of the CAP in increasing the dimensions and levels in the optical fiber systems has been successfully demonstrated. Additionally, the coordinate transformed CMA improves the receiver sensitivity by 1 dB and suppressed inter-dimensional crosstalk.

We believe that in future the investigation of 10-GbE in real time systems using field-programmable gate arrays (FPGAs) can be a potentially attractive candidate for optical fiber system using multidimensional CAP. Moreover O-band VCSELs are attractive for 10-Gb Ethernet application because it has very low dispersion and low production cost.

References

[1] T. Tockle,M. Serbay, J.B. Jensen, W. Rosenkranz, and P. Jeppesen, "Advanced Modulation Formats for Transmission Systems",in Optical Fiber Communication/National Fiber Optic Engineers Conference (OFC),OMI1, 2008.

[2] D.D. Falconer, "Carrierless AM/PM" in Bell Laboratories Technical Memorandum, 1975.

[3] T. Collins, Carrierless Amplitude Phase Modulation, Handbook of Computer Networks: Key Concepts, Data Transmission, and Digital and Optical Networks, John Wiley and Sons, 2008.

[4] A.F. Shalash, K.K. Parhi, "Multidimensional carrierless AM/PM systems for digital subscriber loops" *IEEE Transactions on Communication*, vol.47, no.11, pp.1655-1667, Nov 1999.

[5] Antonio Caballero, Tien Thang Pham, Jesper B. Jensen, and Idelfonso Tafur Monroy "Carrierless N-Dimensional Modulation Format for Multiple Service Differentiation in Optical In-home Networks", in International Photonics Conference (IPC), TuM4, 2011.

[6] M. Wieckowski, J. B. Jensen, I. Tafur Monroy, J. Siuzdak, and J. P. Turkiewicz, "300 Mbps transmission with 4.6 bit/s/Hz spectral efficiency over 50 m PMMA POF link using RC-LED and multi-level Carrierless amplitude phase modulation," in Optical Fiber Communication/National Fiber Optic Engineers Conference (OFC),NTuB8, 2011.

[7] Roberto Rodes, Marcin Wieckowski, Tien-Thang Pham, Jesper Bevensee Jensen, and Idelfonso Tafur Monroy,"VCSEL-based DWDM PON with 4 bit/s/Hz Spectral Efficiency using Carrierless Amplitude Phase Modulation" in European Conference and Exposition on Optical Communications (ECOC),Mo.2.C.2, 2011.

[8] J. D. Ingham, R. Penty, I. White, and D. Cunningham, "40 Gb/s Carrierless Amplitude and Phase Modulation for Low-Cost Optical Datacommunication Links" in Optical Fiber Communication/National Fiber Optic Engineers Conference (OFC),OThZ3, 2011.

[9] J. D. Ingham, R. V. Penty, I. H. White and D. G. Cunningham, "Carrierless Amplitude and Phase Modulation for Low-Cost, High-Spectral-Efficiency Optical Datacommunication Links" CLEO ,CThC5, 2010.

[10] A. Shalash, K.K. Parhi, "Three-dimensional carrierless AM/PM line code for the unshielded twisted pair cables," *IEEE International Symposium on Circuits and Systems*, vol.3,pp.2136-2139, Jun 1997.

[11] I. Thng, Xinrong Li, Chi Chung Ko, "A new 3D CAP system" Proceedings of the IEEE Region 10 Conference (TENCON 99), vol. 1, pp. 309 - 312, 1999.

[12] M.B. Othman, et.al, "Experimental Investigations Demonstration of 3D/4D-CAP Modulation with DM-VCSELs" *IEEE Photonics Technology Letters*, accepted for publication.

[13] N.Mackintosh, F. Jorgensen, "An analysis of multi-level encoding," *IEEE Transactions on Magnetics*,vol.17, no.6, pp.3329-3331, Nov 1981.

[14] Xiaosong Tang, I.L.-J. Thng, Xinrong Li, "A new digital approach to design 3D CAP waveforms", *IEEE Transactions on Communications*, vol.51, no.1, pp. 12- 16, Jan 2003.

[15] Xiaosong Tang, I.L.-J. Thng, "An NS Frequency-Domain Approach for Continuous-Time Design of CAP/ICOM Waveform," *IEEE Transactions on Communications*, vol.52, no.12, pp. 2154-2164, Dec 2004.
[16] X.-L.Li and X.-D.Zhang, "A family of generalized constant modulus algorithms for blind equalization", *IEEE Transactions on Communications*, vol.54, no.11, pp. 1913- 1917, Nov 2006.
[17] Xue-qing Zhao, Ye-cai Guo and Wei Rao, "Blind Equalization Algorithms Based on Orthogonal Wavelet and Coordinate Transformation", Proceedings of the IEEE International Conference on Intelligent Human-Machine Systems and Cybernetics, vol. 1, pp. 284- 287, 2009.

ACKNOWLEDGMENT

This work was supported by Ministry of Higher Education Malaysia under Skim Latihan Akademik IPTA (SLAI) and Universiti Tun Hussein Onn Malaysia (UTHM). We would like to thank Alight Technologies for the VCSELs, Tektronix and Nortelco Electronics AS for allowing us to use the AWG7122B for the experiment.

Maisara Binti Othman received the Bachelor of Engineering in Computer System and Communication from the Universiti Putra Malaysia in 2001; a Master Science in Communication Network Engineering from the same university in 2005. She is currently pursuing a Ph.D. under Metro-access and Short Range System Group at DTU Fotonik, Technical University of Denmark. Her research interests include advanced modulation formats, photonic wireless integration and access and in-home network technologies.

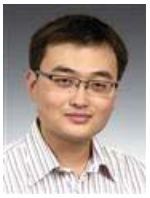

Xu Zhang received the Bachelor of Engineering in electronic technique department from the Jilin Universiti China, in 2006; a Master Science in Electronic and Computer Science department from University of Southampton UK in 2008. He is currently pursuing a Ph.D. under Metro-access and Short Range System Group at DTU Fotonik, Technical University of Denmark.

Lei Deng was born in Xiantao, Hubei, China, in 1985. He received the B.S. degree in Optoelectronic Science and Engineering from Huazhong university of science and technology, Wuhan, China, in 2006. And he received the M.S. degree in Optoelectronic Science and Engineering from Huazhong university of science and technology, Wuhan, China, in 2008. He is currently working toward the Ph.D. degree at the Department of Optoelectronic Science and Engineering, Huazhong University of Science and Technology and he is also the guest Ph.D student of the Department of Photonics Engineering, Technical University of Denmark. His current areas of interest are high-speed optical communications and Radio-over-fiber technology.

Jesper Bevensee Jensen is Assistant Professor in the Metro-access and Short Range Communications Group Department of Photonics Engineering at the Technical University of Denmark, from which he received his PhD in 2008. He has worked as a Postdoc on photonic wireless convergence in home and access networks within the European project ICT-Alpha. He is the coauthor of more than 70 journal and conference papers on optical communication technologies. His research interests include advanced modulation formats, access and in-home network technologies, multicore fiber transmission, advanced modulation of VCSELs, coherent detection using VCSELs, and photonic wireless integration.

Idelfonso Tafur Monroy received the M.Sc. degree in multichannel telecommunications from the Bonch-Bruevitch Institute of Communications, St. Petersburg, Russia, in 1992, the Technology Licentiate degree in telecommunications theory from the Royal Institute of Technology, Stockholm, Sweden, and the Ph.D. degree from the Electrical Engineering Department, Eindhoven University of Technology, The Netherlands, in 1999. He was an Assistant Professor until 2006 at the Eindhoven University of Technology. He is currently a Professor and head of the metro-access and short range systems group of the Department of Photonics Engineering, Technical University of Denmark. He has participated in several European research projects, including the ACTS, FP6, and FP7 frameworks (APEX, STOLAS, LSAGNE, MUFINS, ALPHA, BONE). At the moment, he is in involved the ICT European projects GiGaWaM, EURO-FOS and CHRON. His research interests are in hybrid optical-wireless communication systems, coherent detection technologies and digital signal processing receivers for baseband and radio-over-fiber links, optical switching, nanophotonic technologies, and systems for integrated metro and access networks, short range optical links, and communication theory.

Paper 3: Performance Evaluation of Spectral Amplitude Codes for OCDMA PON

M.B. Othman, J. Bevensee Jensen, X. Zhang, and I. Tafur Monroy, "Performance evaluation of spectral amplitude codes for OCDMA PON," in *(15th International Conference on Optical Network Design and Modeling (ONDM)*, 2011.

Performance Evaluation of Spectral Amplitude Codes for OCDMA PON

M.B. Othman[1,2], J.B. Jensen[1], Xu Zhang[1] and I. Tafur Monroy[1]
[1]DTU, Department of Photonics Engineering, Ørsteds Plads, DK 2800, Kgs. Lyngby, Denmark
[2]Department of Communication Engineering, FKEE, UTHM, 86400, Parit Raja, Batu Pahat, Johor, Malaysia.

***Abstract*- In this paper, we present a performance evaluation of three codes; enhanced double weight (EDW), random diagonal (RD) and zero cross correlation (ZCC) for 10 Gb/s x 4 user, 20 km standard SMF transmission link for OCDMA PON. These SAC codes have ideal in-phase cross-correlation properties to reduce the MAI effects in OCDMA. The performance has been characterized through received optical power (ROP) sensitivity and dispersion tolerance assessments. The numerical results show that the ZCC code has a slightly better performance compared to the other two codes for the ROP and similar behavior against the dispersion tolerence. In the analysis we also consider the character of the code properties and the flexibility as criteria for OCDMA PON network instead of the performance.**

***Index Terms*- optical code division multiple access (OCDMA), spectral amplitude coding (SAC), passive optical network (PON), multiple access interference (MAI)**

I. INTRODUCTION

Spread spectrum communication in the form of code division multiple access (CDMA) offered large advantages to the wireless communication industry in the 1970s [1] in terms of cellular telephony network, global positioning system (GPS), etc. The success of this technique has also motivated interest for applications in optical communication networks. There are six main categories of the coding schemes: pulse amplitude coding (PAC) based on incoherent processing (i.e., summing of optical intensity) with fiber optical delay lines and incoherent optical sources, pulse phase coding (PPC) which utilize the optical fields by using phase modulator within fiber optic delay lines for introducing 0^o or 180^o phase shift to pulses in a code sequence, spectral amplitude coding (SAC) and spectral phase coding (SPC), relies on the wavelength domain and the spectral coding is performed by passing spectral components of the pulse through a phase or amplitude mask, and the coded spectral components are finally recombined by another grating to form a code sequence, spatial coding (SC) require the use of multiple fibers or multicore fibers with two-dimensional (2D) optical codes in the time and space domain simultaneously and wavelength time coding (WTC) require 2D coding in the time and wavelength domains [2-3]. These coding schemes for optical code division multiple access (OCDMA) can grouped into two broad categories, which are coherent and incoherent OCDMA systems [2]. In a coherent OCDMA system, a given user's code is generally generated via phase modulation of the pulses in the encoding and decoding processes, whereas an incoherent OCDMA system typically relies on optical amplitude modulation and decoding is based on power summation rather than manipulation of field quantities. For coherent and incoherent OCDMA systems, bipolar and unipolar codes are respectively designed and applied in the network. Typically, incoherent OCDMA system architectures employ wideband incoherent sources, such as a broadband amplified spontaneous emission (ASE) source, while other incoherent architectures employ coherent laser sources as part of their implementation. Incoherent schemes use the simpler, more standard techniques of intensity modulation with direct detection (IM/DD) while coherent schemes are based on the modulation and detection of the optical phase [4]. Incoherent spectral amplitude coding SAC-OCDMA systems were chosen because it requires lower complexity (especially for synchronization) than the coherent system [5].

OCDMA is a promising approach for passive optical networks (PON) [6-7]. We consider the application of a SAC scheme in the PON environment; such systems offer an excellent ability to eliminate multiple access interference (MAI) [8]. Several codes for SAC have recently been proposed, including double weight (DW), modified double weight (MDW) [9] and enhanced double weight (EDW) [10]; mainly with the goal to overcome the limitations of non-orthogonality, reduced number of supported users and poor bit error rate (BER) performance [11]. The proposal of new SAC codes in [12-14] analyzed their performances in comparison with ordinary codes, for instance, to Hadamard [11] and modified frequency hopping (MFH) codes [15], which have high cross-correlation value and complexity in the code properties. However no comprehensive performance comparison has been made for the new arising codes in OCDMA PON.

Another primary goal that has to be considered in OCDMA systems is the data extraction by a user in the presence of other users in other words, the presence of multiple access interference (MAI). At the receiver, all the codewords from different users are correlated. If a correct codeword arrives, an autocorrelation function with a high peak results is archived. MAI was generated when the incorrect codewords arrives at the receiver. MAI can be reduced by using subtraction technique. The most common subtraction technique is the complementary subtraction or balanced detection technique [2,15]. The AND subtraction technique [16] were purpose to reduce the receiver complexity and at the same time to

improve the system performance. Currently, spectral direct detection (SDD) technique [12-14] were applied and shown successfully to eliminate MAI as only the desired spectral chips in the optical domain will be filtered. Subsequently, phase-induced intensity noise (PIIN) is suppressed at the receiver, and the system performance is improved.

In the following we describe the SAC-OCDMA passive optical networks (PON) architecture and the codes construction complexity in section II. In section III, we give an overview of the simulation setup. Section IV presents the performance comparison numerical results of EDW, RD and ZCC codes. Finally, section V gives some brief concluding remarks.

II. Spectral Amplitude Coding Ocdma Pon

A. *Principles of SAC-OCDMA PON*

Spectral amplitude coding (SAC) is one of the coding schemes that has been introduced in the early 1990's [2]. In the SAC scheme, an incoherent broadband optical signal source (BOSS), such as light emitting diode (LED) or amplified spontaneous emission (ASE) source is preferable, due to their cost effectiveness [2,12]. A typical application of OCDMA PON is presented in Fig. 1. The figure shows that in OCDMA systems, each user is assigned with a unique code that serves as its address. The encoder and decoder consists of fiber Bragg gratings (FBGs) that act as optical filters to define the spectral chips for a given code. In the OCDMA-PON network, data is encoded into optical codes by the encoder at the transmitter, and multiple users share the same medium by using the power combiner and splitter. At the receiver side, only the user with the correct matched filter will recognize the signals. The data is recovered by electrical thresholding.

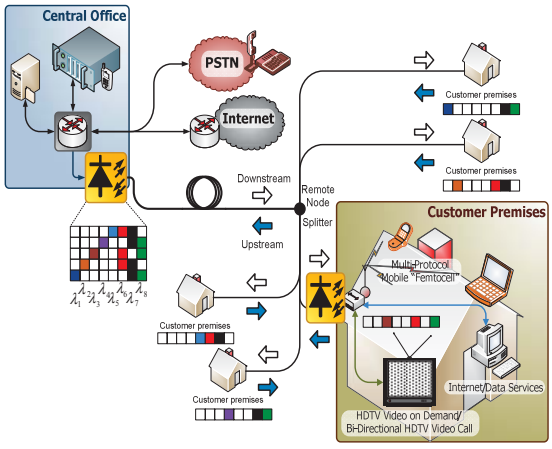

Fig. 1. Overview of OCDMA-PON system architecture

In general, OCDMA-PONs have several advantages such as easy scalability, fair division of bandwidths among users, differentiated service provision at the physical layer, the asynchronous access capability, etc [17-18] that have attracted attention of the researcher community. Asynchronous downstream OCDMA transmission does not require timing coordination because the signal and interference are received with random overlapping. The effect of random overlapping is taking care by most codes designs that keep the cross-correlation (λ_c) as minimum as possible. In contrast to synchronous transmission, proper timing coordination, to carefully avoid overlaps between signal and interference [19] is required, with the trade-off that it increases the transmission efficiency [20]. Due to possible different distances of the optical network units (ONUs) to the remote node, near-far attenuation difference issue arises [21-22]. To overcome the near-far problem, measures such as optical power leveling [21] and power control [23] was introduced in OCDMA.

B. *OCDMA codes complexity*

Recently, a number of conventional codes have been modified or developed for enhancing the performance of OCDMA [6-12]. An OCDMA code is represented in the form of (N, W, λ_c), where N is the code length, W is the weight of the code (the number of "1" inside the code sequence), and λ_c denotes the maximum cross-correlation value between any two code sequences (number of spectral overlapping in the sequence). Codes with ideal in-phase cross-correlation ($\lambda_c \leq 1$) are desirable in OCDMA systems [8] since these codes can reduce MAI. Another key factor is that increasing the weight necessarily increases the signal power of the users. This gives a better signal to noise ratio (SNR). But if the code length is too long, it is considered disadvantageous in implementation since either very wide band sources or very narrow filter bandwidths are required.

TABLE I
Comparison of Several Ocdma Codes for 30 Users

No	Codes	Number of user (K)	Weight (W)	Code Length (N)	Cross-correlation (λ_c)
1	OOC	30	4	364	≤ 1
2	Prime Code	30	31	961	≤ 2
3	MFH Code	30	7	42	$= 1$
4	Hadamard	30	16	32	≥ 1
5	MDW Code	30	4	90	$= 1$
6	EDW Code	30	3	60	$= 1$
7	RD Code	30	4 / 3	35/ 33	≥ 1
8	ZCC Code	30	4 / 3	120 / 90	$= 0$

Table I summarizes the three important elements in code properties for 30 users. From the table, the first four are the ordinary codes that already be mentioned before. There are

significant limitations associated with these ordinary codes, including high complexity because it's dependant on code weight (eg. Optical orthogonal code (OOC) and MFH code) [2,15]. The larger the code weight can increase the complexity and also lead to high power losses at encoder/decoder. For Hadamard and Prime codes [2, 11], the large cross-correlation value results in intensify the MAI effects, too long code lengths (eg. OOC and MFH) needs a broader spectrum, and fixed weight (eg. MDW and EDW) doesn't give a flexibility to the customers. Although these new SAC codes are not perfect but they do overcome some problems RD code for example, have shorter code length. RD and ZCC codes also have an advantage in flexibility to increase the weight. Therefore, for comparison purposes we will examine three codes: enhancement double weight (EDW) [10], zero cross-correlation (ZCC) [13], and a random diagonal (RD) code [14] because these new SAC codes never being compared before. The code structures for four users used in our simulations are shown in Table II – IV. The table also shows the code length for the three codes. The code length for EDW is 10, RD is 7 and ZCC is 12 respectively.

TABLE II
EDW CODE STRUCTURE FOR 4 USERS

Wave-length	λ1	λ2	λ3	λ4	λ5	λ6	λ7	λ8	λ9	λ10
User 1	0	0	0	0	0	0	1	1	0	1
User 2	0	0	0	0	0	1	0	0	1	1
User 3	0	0	0	0	1	1	0	1	0	0
User 4	1	1	0	1	0	0	0	0	0	0

TABLE III
RD CODE STRUCTURE FOR 4 USERS

Wave-length	λ1	λ2	λ3	λ4	λ5	λ6	λ7
User 1	0	0	0	1	1	1	0
User 2	0	0	1	0	0	1	1
User 3	0	1	0	0	1	0	1
User 4	1	0	0	0	1	1	0

TABLE IV
ZCC CODE STRUCTURE FOR 4 USERS

Wave-length	λ1	λ2	λ3	λ4	λ5	λ6	λ7	λ8	λ9	λ10	λ11	λ12
User 1	0	0	0	0	0	0	0	1	0	1	0	1
User 2	0	0	0	1	0	1	0	0	0	0	1	0
User 3	0	1	0	0	1	0	0	0	1	0	0	0
User 4	1	0	1	0	0	0	1	0	0	0	0	0

III. SIMULATION SETUP

The simulation was performed using the VPI 8.3 software tool. In our computer simulations we considered only four users to observe the code behavior in the network and reduce the required simulation time. As the number of users increase so does the effect of MAI, this factor is under current investigation. The code weights are fixed to three for all codes at 10 Gb/s bit rates. A simple schematic diagram of the simulation setup is illustrated in Fig. 2. The model is represented by three sections: transmitter section, link section and receiver section.

The transmitter section, which represents the central office consists of five components: pulse pattern generator (PPG), non-return-zero (NRZ) pulse generators, single broadband optical source: ASE, FBGs and external modulators. The pulse pattern generator (PPG) transmits a pseudo-random bit sequence of length 2^7-1 bits by using on-off keying (OOK) modulation. The time window is set to 256 μs and the sampling rate is 5120 GHz. The function of the FBG is to encode the source according to the specific code or wavelength that is intended to the user. One unique encoded spectrum represents one channel. The modulators are Mach-Zehnder modulators. The signals that coming from the transmitter will be combined and launched into a single fibre. At the fibre link section, we assessed a PON of length 20 km, implementing ITU-T G.652 standard single mode fibre (SMF). Fibre attenuation was set to 0.2 dB/km, a chromatic dispersion parameter 16 ps/nm-km was used, and nonlinear effects were activated in our simulation model. The polarization mode dispersion (PMD) coefficient is set to 0.1 ps/√km. In this network, the splitter splits the branches of PON to the receiver.

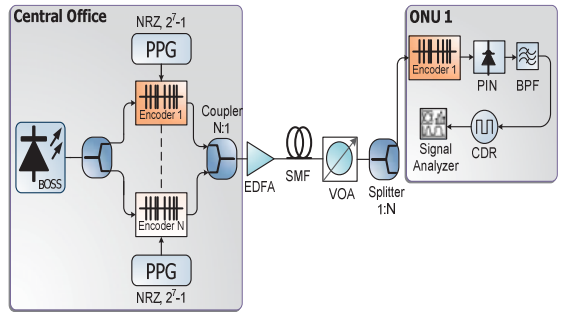

Fig. 2. Simulation setup for OCDMA-PON system architecture

At the receiver, Fig. 2 shows the equipment of the optical network unit (ONU) at the customer premises. The incoming signal is decoded by the FBG. The decoder has its own matched filtering frequency to recover the signal. The dark current value is set at 5nA and the thermal noise coefficient is 1.8×10^{-23} W/Hz for each of the photo-detectors. The clock data recovery (CDR) is used to recovered the intended signal. The

performance of the system was characterized by assessing the sensitivity of bit error rate (BER) at 10^{-9} against received optical power (ROP) and dispersion tolerance assessment with spectral direct detection (SDD) technique.

IV. Results

The BER back to back (B2B) and after 20 km transmission of EDW, RD and ZCC codes is plotted in Fig. 3. The sensitivity at BER of 10^{-9} for EDW, RD and ZCC for B2B are -23.2 dBm, -23.25 dBm and -24 dBm respectively. A 0.75 dB difference in B2B receiver sensitivity is observed between RD and ZCC. This improvement is attributed to the ZCC code structure, which the design properties does not have overlapping chips between the users which directly reduces MAI effects. In OCDMA system, PIIN is strongly related to MAI due to the overlapping spectra of different users. In this aspect ZCC code has an advantage because of the suppression of PIIN in non-overlapping code structures. After 20 km transmission using single mode fiber (SMF), a 0.2 dB transmission penalty was measured for ZCC code compared to 0.15 dB for RD and 0.1 dB for EDW codes. The result shows that the codes still give a good performance after 20 km transmission compared with B2B by using a single ASE source.

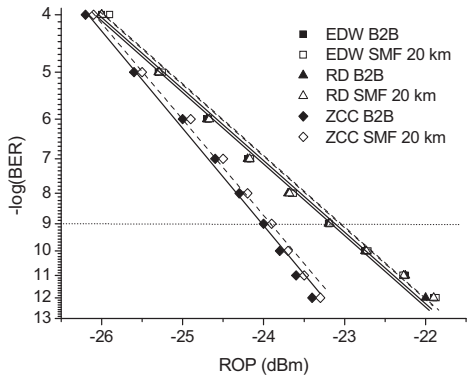

Fig. 3. BER plot for EDW, RD and ZCC codes against ROP

Receiver input power penalty at BER of 10^{-9} as a function of dispersion is depicted in Fig. 4. The 2 dB penalty dispersion limit was chosen for the three codes. The dispersion was applied in positive and negative form and nonlinear effects and attenuation was disregarded. All codes show similar behavior of positive and negative chromatic dispersions. For EDW code the dispersion limit is ±1750 ps/nm and ±1780 ps/nm for RD code. For ZCC code the dispersion limit is ±1690 ps/nm, i.e. slightly lower than the other two codes. From the reading in Fig. 4, the difference to each other is really small, meaning that the robustness of these codes to dispersion tolerance is quite similar.

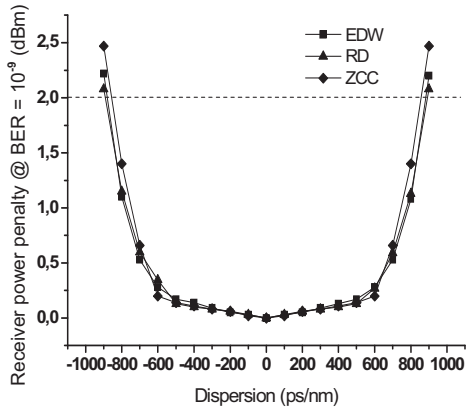

Fig. 4. Dispersion tolerance of 10 Gb/s EDW, RD and ZCC codes

V. Conclusion

The performance of EDW, RD and ZCC codes against the received optical power and the dispersion limits was evaluated in SAC-OCDMA PON. Codes with ideal in-phase cross-correlation ($\lambda_c \leq 1$) are desirable in OCDMA systems since these codes can reduce MAI and also suppressed the effect of PIIN. The numerical results show that ZCC have a slightly better performance compared to the other two codes for ROP but have a similar behavior for the dispersion tolerance. This is because only thermal noise and short noise has been considered, PIIN is neglected due to zero cross-correlation between users. ZCC code also has a flexibility to increase the weight. However in other aspects, when the number of users increases the code length will also become longer, thus demanding larger bandwidth. In order to avoid this problem we can narrow down the spacing between the chips but still maintaining the same spectral bandwidth. By the way, RD code gives a good performance in the results. The difference due to power penalty is not that big when compared with ZCC. RD code have an advantages because is just requires a shorter code length and variable weight systems. EDW also have the same performance with RD in ROP performance. However, the EDW code weight is always fixed to 3. So in order to find the suitable code we have to consider the flexibility for instance; freedom in adding new channel in the network, reduce the crosstalk inside the traffic, increase the security and other limitations factor rather than performance itself. From here what we can summarize that EDW, RD and ZCC codes has a potential to be applied in OCDMA PON.

REFERENCES

[1] Paul R. Prucnal, Mario A. Santoro, Ting Rui Fan, "Spread Spectrum Fiber-optic Local Area Network Using Optical Processing," Journal of Lightwave Technology, vol. 4, pp. 547-554, May 1986.

[2] Paul R. Prucnal, Optical Code Division Multiple Access: Fundamentals and Application, CRC Press, Boca Raton. Fl., 2006.

[3] I. Glesk, V. Baby, C.S.Brès, P.R. Prucnal, Wing C. Kwong, "Is optical CDMA viable technique for broadband networks? ", Proc. Of SPIE, vol. 6180, 2006.

[4] C.F. Lam, "To spread or not to spread: the myths of Optical CDMA", IEEE Annual LEOS Meeting, vol. 2, pp. 810-811, November 2000.

[5] Chih-Ta Yen, "Integrated dispersion slope equalizer of AWG-based optical CDMA for radio-over-fiber transmissions", Photonics Network Communications, vol.9, no. 3, pp. 311-319, 2010.

[6] Z.A. El-Sahn, B.J. Shastri, Ming Zeng, N. Kheder, D.V. Plant, L.A. Rusch, "Experimental Demonstration of a SAC-OCDMA PON With Burst-Mode Reception: Local Versus Centralized Sources", Journal of Lightwave Technology, vol. 26, no. 10, pp. 1192-1203, May 2008.

[7] N. Kataoka, G. Cincotti, N. Wada, K. Kitayama, "100km Transmission of Dispersion-Compensation-Free, Extended-Reach OCDMA-PON System with Passive Remote Node", 15th OptoElectronics and Communications Conference (OECC2010) Technical Digest, pp. 726-727, July 2010.

[8] Chao-Chin Yang, Jen Fa Huang, Teng-Chun Hsu, "Differentiated Service Provision in Optical CDMA Network Using Power Control," Photonic Tech. Letter, vol. 20, pp. 1664-1666, October 15, 2008.

[9] S. A. AlJunid, M.. Ismail, B. M. Ali, A. R. Ramli, M. K. Abdullah, "A New Family of Optical Code Sequences For Spectral-Amplitude-Coding Optical CDMA Systems", Photonics Technology Letters, vol. 16, no.10, 2383-2385, October 2004.

[10] Feras N. Hasoon, Sahbudin Shaari, S.A. Aljunid, M.K. Abdullah, "Improving the Bit Error Rate of Optical Spectrum CDMA Systems using Enhancement Double Weight Code," Proc. of SPIE, vol. 6021, 2005.

[11] C.F.Lam, T.K.Tong Dennis, M.C. Wu,"Experimental Demonstration of Bipolar Optical CDMA System Using A Balanced Transmitter and Complementary Spectral Encoding," IEEE Photonics Technology Letters, vol. 10, no. 10, pp. 1504-1506, October 1998.

[12] S. B. Ahmad Anas, M. K. Abdullah, M. Mokhtar, S.D. Walker, "Multiple access interference elimination with enhanced chromatic dispersion tolerance in SAC OCDMA," IEICE Electronics Express vol. 5, no. 16, pp. 617-623, 2008.

[13] M.S. Anuar, S.A.Aljunid, N.M. Saad, S.M. Hamzah, New design of spectral amplitude coding in OCDMA with zero cross correlation, Optics Communication, vol. 282, pp. 2659-2664, 2009

[14] Hilal Adnan Fadhil, S.A. Aljunid, R.B Ahmad, "Performance of Random Diagonal Codes for Spectral Amplitude Coding Optical CDMA Systems," World Academy of Science , Engineering and Technology 47, pp. 147-150, 2008.

[15] Zou Wei, H. Ghafouri-Shiraz, "Codes for Spectral-Amplitude-Coding Optical CDMA Systems," Journal of Ligthwave Technology, vol. 20, pp. 1284-1291, August 2002.

[16] S.A. Aljunid, Feras N. Hasson, M.D.A.Samad, M.K.Abdullah, M. Othman, S. Shaari, "Performance of OCDMA Systems Using AND Subtraction Technique," IEEE Proc. ICSE, pp. 464-467, 2006.

[17] Zhang Chong Fu, Qiu Kun, Xo Bo, "Passive optical networks based on optical CDMA: Design and system analysis," Chinese Sciece Bulletin, vol. 52, no. 1, pp. 118-126, 2007.

[18] Nobuyuki Kataoka, Naoya Wada, Gabriella Cincotti, and Ken-ichi Kitayama, "10 Gbps-Class, Bandwidth-Symmetric, OCDMA-PON System using Hybrid Multi-port and SSFBG En/Decoder, ONDM 2010, pp. 1-4, Feb. 2010.

[19] Xu Wang, Naoya Wada, Tetsuya Miyazaki, Gabriella Cincotti. Ken-ichi Kitayama, "Field Trial of 3-WDM x 10-OCDMA x 10.71- Gb/s Asynchronous WDM/DPSK-OCDMA Using Hybrid E/D Without FEC and Optical Thresholding" Journal of Ligthwave Technology, vol. 25, no.1, pp. 207-215, January 2007.

[20] Yen-Chun Liao, Chia-Chu Ho, Hen-Wai tsao, Jingshown Wu, "Design and Experimental Demonstration of a Synchronous OCDMA-Based 10 Gbit/s/1.25 Gbit/s EPON with a Novel Synchronization Scheme, J. Opt Communication, vol. 29, pp. 112-117, 2008.

[21] K. Ohara, V.J. Hernandez, Y. Du, Z. Ding, S.J.B. Yoo, Y. Horiuchi, "Resilency of OCDMA-PON against near-far problem", OFC/NFOEC 2007, pp. 1-3, March 2007.

[22] A.E.Willner, P. Saghari, V.R. Arbab, "Advanced Tehniques to Increase the Number of Users and Bit Rate in OCDMA Nwtworks", J. of Selected Topics in Quantum Electronics, vol 13, no. 5, pp. 1403- 1414, 2007.

[23] W.J.M. Al-galbi, M. Mokhtar, A.F. Abas, S.B.A. Anas and R.K.Z. Sahbudin, "Solving the Near-Far Problem in Dynamic Frequency Hopping-Optical Code Division Multiple Access using Power Control", J. of Computer Science 5, vol. 6, pp. 413 – 418, 2009.

Paper 4: Using CAP Dimensionality for Service and User Allocation for Optical Access Networks

M.B. Othman, X. Zhang, J. Bevensee Jensen, and I. Tafur Monroy, "Using CAP Dimensionality for Service and User Allocation for Optical Access Networks," in *Asia Communications and Photonics Conference (ACP)*, Guangzhou, China, accepted for publication, 2012.

Using CAP Dimensionality for Service and User Allocation for Optical Access Networks

M.B. Othman[1,2], **Xu Zhang**[1], **J. Bevensee Jensen** [1] **and I. Tafur Monroy** [1]

[1] *DTU Fotonik, Dep. of Photonics Engineering, DTU, Ørsteds Plads 343, DK-2800 Kgs. Lyngby, Denmark.*
[2] *Department of Communication Engineering, FKEE, UTHM, 86400 Parit Raja, Johor, Malaysia.*
mabio@fotonik.dtu.dk; jebe@fotonik.dtu.dk; idtm@fotonik.dtu.dk

Abstract: The usability of carrierless amplitude and phase (CAP) modulation dimensions for service and user allocation for WDM optical access is experimentally demonstrated in a 2X2D-ODMA configuration.

OCIS codes: 060.4080, 060.4230, 060.0060.

1. Introduction

Next generation access networks (NGAN) needs to supply multiple users with access to multiple services such as voice, data, images and video while sharing the same physical infrastructure in the fiber to the home (FTTH) network. All-optical 2 dimensional (2D) optical code division multiple access (OCDMA) has been proposed for NGAN for multimedia applications [1] and increased spectral efficiency in FTTH [2]. Due to the limited coding space, incoherent 1 dimensional (1D) optical coding technology (either in time or wavelength domain) is not feasible for future access networks which are required to support a large number of end users. Both 2D and 3 dimensional (3D) encoding techniques require multiple domains to realize optical codes. Therefore, it is difficult to smoothly upgrade the capacity of an access network where 2D or 3D encoders/decoders are employed [2]. In order to overcome this problem the encoder and decoder can be designed in the electrical domain. Orthogonal division multiple access (ODMA) exploring the multiple possible dimensions of carrierless amplitude and phase (CAP) modulation [3] has been proposed for multiple services application. Hybrid OCDMA and wavelength division multiple (WDM) network have been proposed and demonstrated in [4] to significantly improve the system flexibility and performance. Regarding light sources for optical access, directly modulated vertical cavity surface emitting lasers (DM-VCSELs) have emerged as an attractive solution due to the cost effective production and low modulation voltage.

In this paper, we propose what we believe is the first experimental demonstration 2x2D-ODMA configuration in WDM access network. We believe this new concepts can be implemented in WDM networks in an elegant way by utilizing the orthogonal CAP filters are designed in digital domain. Moreover the higher dimensionality ODMA is able to support multiple services without requiring additional domains in the optical link.

2. Principle of ODMA

Code division multiple access (CDMA) has been introduced in wireless communication. ODMA can be classified under the CDMA concept, with orthogonality imposed on the set of signals. The ODMA concepts have been proposed for higher dimensionality CAP in digital subscriber line (DSL) application [3]. CAP is a multi-dimensional multi-level signal employing orthogonal waveforms; one for each dimension. These waveforms are obtained from frequency domain filters with orthogonal impulse responses. The orthogonal waveforms are generated by using an optimization algorithm (OA) [5]. To avoid inter-dimensional crosstalk, it is vital that the transmitter-receiver (transceiver) filter combinations satisfy the orthogonality or perfect reconstruction (PR) criteria. Fig. 1(a) shows the cross responses of the four orthogonal transceiver filters for four dimensional (4D)-CAP. The transceiver filters combination satisfies the orthogonality or PR criteria. The transmitter is represented by f_N and the receiver is represented by g_N. The impulse only exists at the cross responses of f_1 and g_1, f_2 and g_2, f_3 and g_3, f_4 and g_4.

Fig.1(b) shows the scenario of the 2D-ODMA that has been demonstrated in a WDM architecture. There are 2 WDM channels; channel 1 (CH1) represented by filter 1D and 2D, and channel 2 (CH2) are represented by filter 3D and 4D in the central office (CO). From the concepts of OCDMA technique a unique code structure is designed to distinguish different users and services. In this demonstration, we divided the total 4D-CAP into 2 channels and successfully demodulated the signals in the optical network unit (ONU).

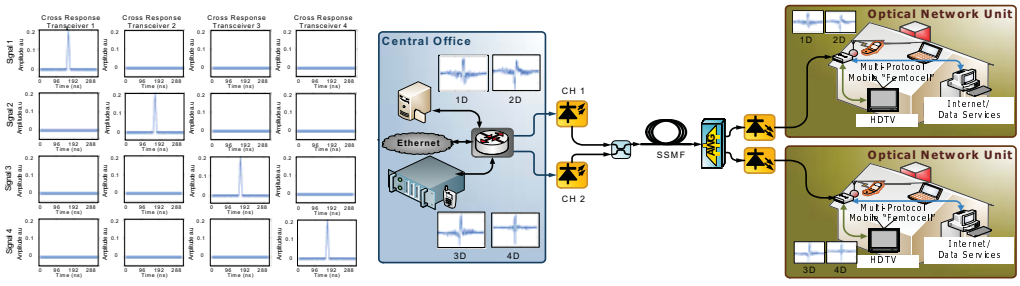

Fig. 1: 4D-CAP (a) cross responses of transceiver filter and (b) 2x2D-ODMA scenario for WDM system.

Table 1: Relationship of 2x2D-CAP at different L/D

Signal 2x2D-ODMA	Bits/symbol	Total levels	Upsampling Factor	Bit Rates (Mb/s)	Bandwidth (MHz)	Spectral Efficiency (b/s/Hz)	Sampling Rate (Mbaud)
2-L/D	4	16	12	416.67	400	1.04	104.16
4-L/D	8	256	12	833.3	400	2.08	104.16

3. Experimental Setup

Fig. 2 shows the setup implemented in the experiment. An arbitrary waveform generator (ArbWaveGen) with sampling rate of 1.25 GSa/s is used to generate the 2D-CAP signals. CH1 is represented by waveforms 1 and 2 and CH2 is represented by waveforms 3 and 4. Data in the transmitter is mapped according to the given constellation by converting a number of raw data bits into a number of multilevel symbols (i.e 2-L/D or 4-L/D). Those symbols are upsampled and later shaped (or filtered). The transmitter filters are implemented as fixed finite impulse response (FIR) filters. The 2 VCSELs at 1540.61 nm (CH1) and 1541.01 nm (CH2) with 4.5 GHz bandwidth operating at 4 mA bias level are directly modulated with the CAP signals. The two signals are combined using a 3 dB coupler as shown in Fig. 2(a). The signals are propagated through 20 km standard single mode fiber (SSMF) with a total fiber loss of 6.5 dB. A variable optical attenuator (VOA) is placed after the fiber for bit error rate (BER) measurements. At the receiver, the signals are been seperated into ONU1 and ONU2 by the arrayed waveguide grating (AWG). The signals is directly detected by a photodetector (PD) and stored in a digital storage scope (DSO) with 40 GSa/s sampling rate for offline demodulation. At the receiver, the inversion of the transmission filter is implemented to retrieve the original sequence of symbols. The symbols are down sampled and demapped before the data can be recovered. Transmission quality is assessed using receiver sensitivity at a BER of 2.8×10^{-3}, since forward error correction (FEC) techniques may be applied to obtain error free transmission when the 7% of FEC overhead are taken into account. The bits/symbol, total levels, upsampling factor, bit rates, bandwidth, spectral efficiency and sampling rate relationship of the total 2x2D-ODMA at different levels per dimension (L/D) are listed in Table 1.

4. Results

Fig. 3(a) and (b) shows the BER results obtained for 2D-ODMA signals at 2-L/D and 4-L/D at ONU1 and ONU2. The solid symbols represent optical back to back (B2B) and the hollow symbols represent 20 km SSMF transmission. For 2D-2L/D for B2B, the receiver sensitivity at the FEC threshold for ONU1 is –20.1 dBm and –19.9 dBm at ONU2. After 20 km SSMF transmission, the performance is similar for both RNs with the receiver sensitivity of –19.6 dBm. The signals are successfully demodulated below the FEC limit after 20 km SSMF transmission. This can be clearly seen from the constellation diagram of 2-L/D at ONU1 and ONU2 in the figure with BER approximately 1×10^{-3} after 20 km SSMF transmission. For 2D-4L/D, the power penalty is negligible between B2B and after 20 km SSMF transmission is observed. The insets show the received signal constellation with BER of approximately 1×10^{-3} at

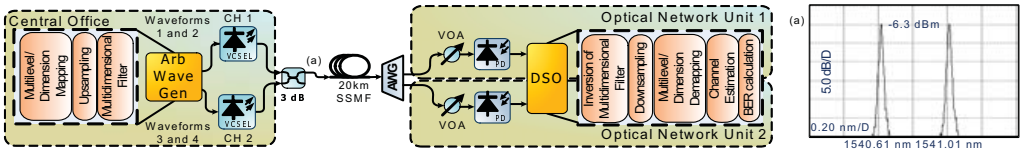

Fig. 2: Experimental setup for 2x2D-ODMA over 20 km SSMF with DM-VCSELs for WDM architecture.

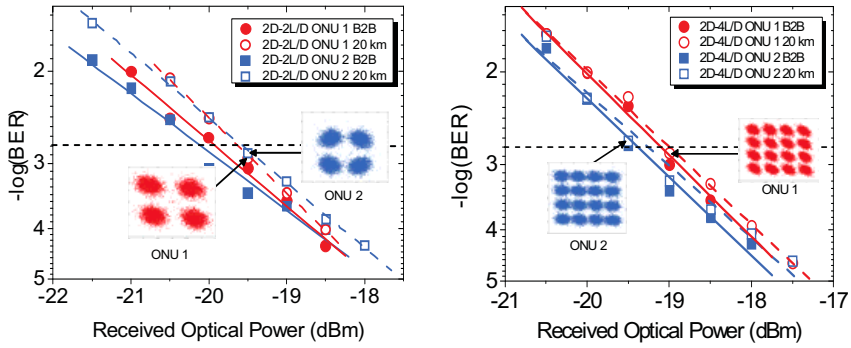

Fig. 3: Bit error rate (BER) vs received optical power (ROP) (a) 2D-ODMA 2-L/D and (b) 2D-ODMA 4-L/D

ROP of –19.5 dBm for ONU1 and ONU2 at ROP of –19 dBm after 20 km SSMF transmission. Similar performance is observed for 2L/D and 4L/D for 2D-ODMA.

5. Conclusions

We propose and experimentally demonstrate the 2x2D-ODMA/WDM network with DM-VCSEL over 20 km SSMF. Both signals are successfully demodulated below the FEC threshold. The spectral efficiency for 4-L/D is 2.08 bits/s/Hz with bit rate of 833.3 MHz is presented in this work. The flexibility of the 4D-CAP in dividing the dimensions in the optical fiber systems is successfully demonstrated. This result indicates the prospects of combining the ODMA in WDM network for service and user allocation in next generation access network. Furthermore, the orthogonal FIR filters are designed in digital domain which can be an alternative solution for higher dimensionality OCDMA which requires multiple domains coding.

References

1. Mikaël Morelle, et. al, "Quality of service differentiation in multimedia 2D optical networks", in *EU-SIPCO*,(2007).
2. FP7 Report, "Survey of next generation optical access system concepts", (2010).
3. A.F.Shalash, K.K. Parhi, "Multidimensional carrierless AM/PM systems for digital subscriber loops" IEEE Transactions on Communication, **47**, 11, 1655–1667, (1999).
4. Xu Wang et. al, "Flexible 10 Gbps, 8-User DPSK-OCDMA System with 16x16 Ports Encoder and 16-Level Phase-Shifted SSFBG Decoders" in *OFC/NFOEC*, (2008), paper OMR2.
5. Xiaosong Tang,et. al , "A new digital approach to design 3D CAP waveforms," IEEE Trans. on Comm., **51**, 1, 12–16,(2003).

Paper 5: Bi-directional Multi Dimension CAP Transmission for Smart Grid Communication Services

X. Zhang, M.B. Othman, X. Pang, J. Bevensee Jensen, and I. Tafur Monroy, "Bi-directional Multi Dimension CAP Transmission for Smart Grid Communication Services," *Asia Communications and Photonics Conference (ACP)*, Guangzhou, China, accepted for publication, 2012.

Bi-directional Multi Dimension CAP Transmission for Smart Grid Communication Services

Xu Zhang[1,2], Maisara B. Othman[2], Xiaodan Pang[2] , Jesper B. Jensen[2], Idelfonso T. Monroy[2]
1. State Grid Corporation of China, Tianjin Electric Power Corporation, Wujin Road 39, Hebei District, Tianjin, China
2. Technical University of Denmark, Department of Photonic Engineering, Building 343, Lyngby, 2800 kgs, Denmark
xuzhn@fotonik.dtu.dk

Abstract: We experimentally demonstrate bi-directional multi dimension carrierless amplitude and phase (CAP) transmission for smart grid communication services based on optical fiber networks. The proposed system is able to support multi-Gb/s transmission with high spectral efficiency.
OCIS codes: (000.2700) General science; (060.2330) Fiber optics communication.

1. Introduction

Recently, smart grid power infrastructure has emerged as the promising solution of future electric power distribution [1]. Main characteristics of smart grid include self-healing, flexible consumer participation, physical and cyber attack-resistance, and ability of providing more stable power with lower frequency and voltage fluctuations [2, 3]. The present power grid only allows one-way communication from the control systems to the downlink access points of distribution [4]. In such insufficient system, point of consumption could not play a role as the generator. However, the core fiber optical transmission networks for smart grid communication services have to fulfill several technical requirements which consist of high bit rate transmission, high spectral efficiency, multi-user supporting, and bi-directional communication.

In this paper, we have proposed the novel bi-directional multi dimension carrierless amplitude and phase (CAP) transmission systems for smart grid communication services. CAP is a multi dimensional and multi level signal modulation format employing orthogonal waveforms. These waveforms are generated by using FIR filters with orthogonal impulse responses in time domain, i.e. statistical expectation of correlation between different waveforms is zero [5, 6]. In principle, CAP modulation is similar to orthogonal frequency division multiplexing (OFDM) modulation, in the sense that both of CAP and OFDM support multiple levels modulation with more than one dimension or sub-carrier. Contrary to OFDM, generation of orthogonal sub-carriers in frequency domain is not required for CAP. Additionally, CAP supports modulation in more than two dimensions, provided that orthogonal pulse shapes can be identified [7]. To the best of author's knowledge, this is the first demonstration of the smart grid communication systems based on bi-directional fiber optical link using multi dimensional CAP and employing directly modulated (DM) vertical cavity surface emitting lasers (VCSELs) operating around 1550 nm wavelength (193.4145 THz) as transmitters. Moreover, in this paper, 3 dimension (3D) CAP with 2 level/dimension (2 L/D) and 4 level/dimension (4L/D) transmissions achieved bit rate of 4.5 Gb/s and 7.2 Gb/s separately.

2. Experiment Setup

Figure. 1 shows the setup implemented in the experiment. The arbitrary waveform generator (AWG) with 12 GSa/s is used to generate the 3D CAP with 2-L/D and 4-L/D signals. For example, 3D CAP constellations are shown in Fig. 2 (a) and Fig. 2 (b). As it can be noticed, denotation of 2-L/D can be considered as QPSK in two dimensions, as well the denotation of 4-L/D can be considered as 16 QAM in two dimensions.

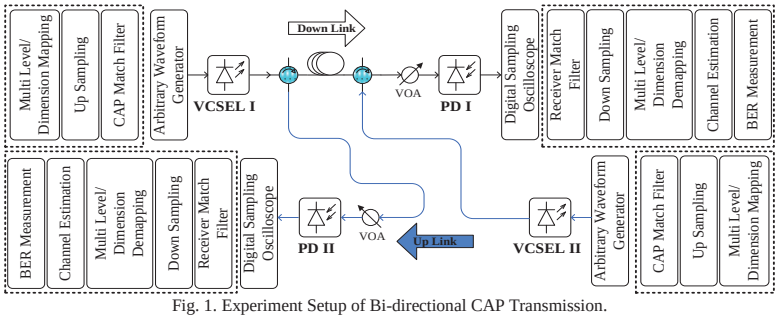

Fig. 1. Experiment Setup of Bi-directional CAP Transmission.

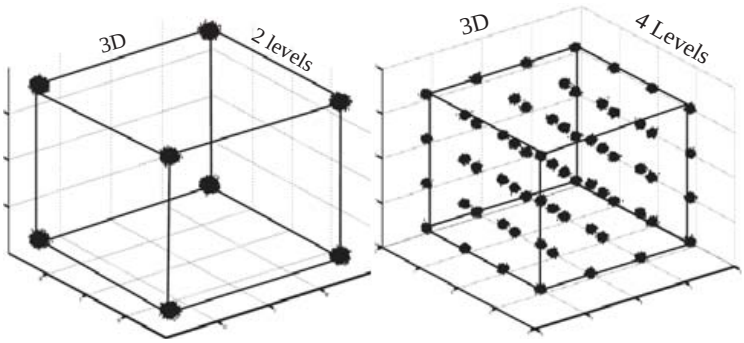

(a) (b)

Fig. 2. CAP Constellations of (a) 3D 2-L/D (b) 3D 4-L/D.

As it is shown in the experiment setup configuration, for down link, data in the transmitter side is firstly mapped according to the given modulation level, such as 2-L/D and 4-L/D. Those symbols are up sampled and later shaped (or filtered), according to the optimization algorithm. The transmitter signature filters are implemented as fixed FIR filters. The 3D CAP signals at bit rate of 4.5 Gb/s (2-L/D) with an up sampling factor of 8 and 7.2 Gb/s (4-L/D) with an up sampling factor of 10 are generated by the arbitrary waveform generator (AWG). Afterward, optical CAP signals are directly modulated with 1548.24 nm (193.63 THz) VCSEL with 4.5 GHz bandwidth operating at 4 mA bias level. Furthermore, table 1 shows the main parameters of CAP transmission experiment including bit rate with 7-% overhead forward error correction (FEC), spectral efficiency (SE), up sample factor, bandwidth and symbol rate. In the down link receiver side, a photodiode with 10 GHz bandwidth is used for direct detection. A 40 GSa/s digital sampling oscilloscope (DSO) is employed to sample the received analog signals. Several off-line digital signal processing (DSP) algorithms are implemented including receiver match filter, down sampling, signal demapping and DSP algorithms for transmission channel estimation. Finally the systems' bit error rate (BER) performance in terms of received optical power is obtained to measure the CAP system performance. Furthermore, the similar transmitter-receiver structure is used for the up link transmission. However the carrier frequency is assigned to be different from down link carrier. The optical CAP signals of down link are directly modulated with 1548.96 nm (193.54 THz) VCSEL. As it can be noticed, approximate 100 GHz channel spacing between up and down link is employed to mitigate cross talk interference. Moreover, off-line DSP algorithms of blind CMA channel estimation equalizer are implemented to compensate for inter symbol interference induced by 20 km single mode fiber (SMF) transmission impairments. Time domains cross correlation responses of match filters are shown in Fig. 3 (a). Moreover Fig. 3 (b) shows the optimized match filter impulse and frequency responses for 3D CAP.

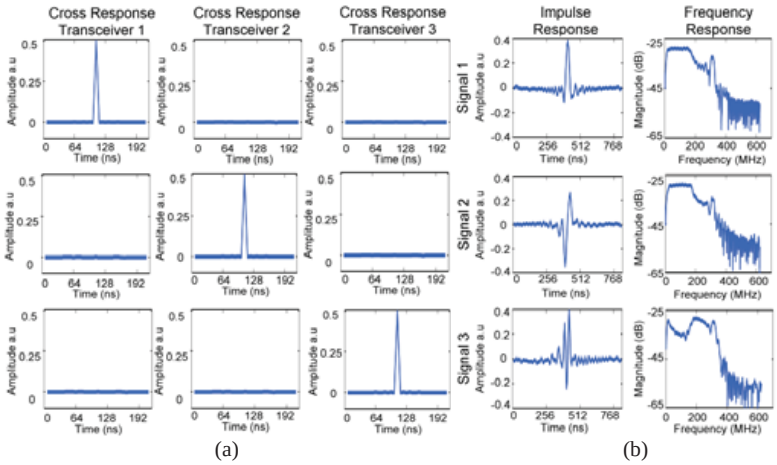

(a) (b)

Fig. 3. (a) 3D CAP cross-correlation of transmitter-receiver match filters; (b) 3D CAP optimal match filter impulse and frequency responses.

CAP Signals	Bit Rate (Gb/s)	SE (bits/s/Hz)	Up Sample Factor	Bandwidth (GHz)	Symbol Rate (Gbaud)
3D 2L/D	4.5	2.25	8	2	1.5
3D 4L/D	7.2	3.6	10	2	1.2

Table 1. 3D CAP up & down link: bit rate, spectral efficiency, up sampling factor, bandwidth and symbol rate with 2-L/D and 4-L/D.

4. Results

Results of BER performance in terms of received optical power are presented as below. Fig. 3 (a) and Fig. 3 (b) show the comparison between with and without offline channel estimation DSP algorithms for 3D 2-L/D CAP and 3D 4-L/D CAP in both of down and up transmission links. In short, BER performances are improved approximate 0.5 dB by using offline channel estimation DSP algorithms after 20 km SMF transmission for smart grid communication services.

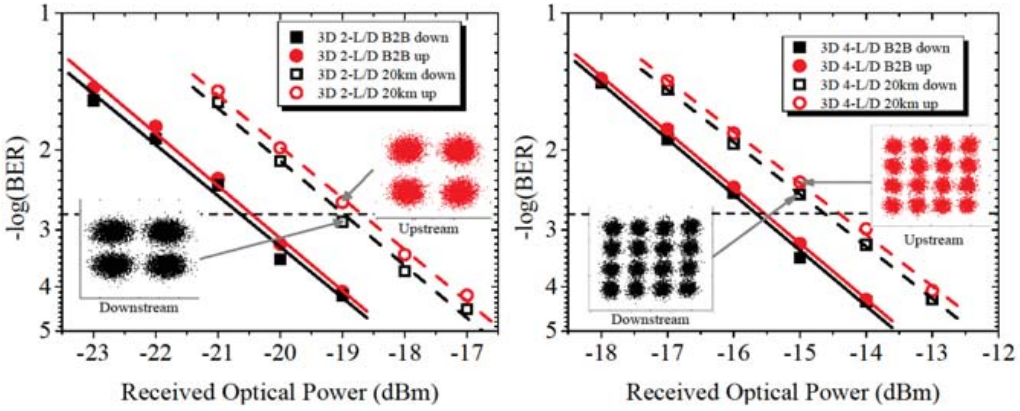

(a) (b)

Fig. 4 BER vs. Received Optical Power of (a) 3D CAP 2-L/D bidirectional transmission; (b) 3D CAP 4-L/D bidirectional transmission

5. Conclusion

A bi-directional optical transmission using 3D/4D CAP with 2-L/D and 4-L/D modulation is demonstrated. In order to achieve smart grid communication service of metro-access reach, blind coordinate transformed CMA equalizer to estimate transmission channel is implemented. This experiment demonstrated system provides potentially a cost effective solution for next generation smart grid power infrastructure access networks. The spectral efficiency achievements of 2.25 bits/s/Hz and 3.6 bits/s/Hz for 3D-CAP 2-level/dimension and 3D-CAP 4-level/dimension are presented in this paper. To the best of author's knowledge this is the first demonstration of a bi-directional optical link for smart grid networks using multi dimensional CAP and employing direct modulated VCSELs.

6. Reference

[1] Kathy kowalienko,"Smart Grid projects pick up speed", IEEE, The Institute, Standards, Article 06 Aug., 2009.

[2] A. Aggarwal, S. Kunta, and P.K. Verma, "A proposed communications infrastructure for the smart grid," Innovative Smart Grid Technologies (ISGT), 2010, 19-21 Jan. 2010.

[3] Francisco Lobo, Ana Cabello, Alberto Lopez, David Mora, and Rosa Mora, 2008, "Distribution Network as Communication system", Frankfurt: CIRED Seminar 2008: Smart Grids for distribution paper no 0022, June 2008.

[4] Roger N. Anderson, "The Distributed Storage-Generation 'Smart' Electric Grid of the Future," White paper, Columbia University.

[5] A. Shalash and K. Parhi. "Three-dimensional carrierless AM/PM line code for the unshielded twisted pair cables", in Circuits and Systems, ISCAS '97., Proceedings of 1997 IEEE International Symposium on, vol. 3, pp. 2136-2139 vol.3, jun 1997.

[6] A. Shalash and K. Parhi, "Multidimensional carrierless AM/PM systems for digital subscriber loops," Communications, IEEE Transactions on, vol. 47, no. 11, pp. 1655-1667, nov 1999.

[7] X. Tang, I.-J. Thng, and X. Li. "A new digital approach to design 3d cap waveforms," Communications, IEEE Transactions on, vol. 51, no. 1, pp. 12-16, jan 2003.

Paper 6: Directly modulated VCSELs for 2 × 2 MIMO-OFDM radio over fiber in WDM-PON

M. B. Othman, L. Deng, X. Pang, J. Caminos, W. Kozuch, K. Prince, J. B. Jensen, and I. T. Monroy, "Directly modulated VCSELs for 2 × 2 MIMO-OFDM radio over fiber in WDM-PON," in *37th European Conference and Exhibition on Optical Communication (ECOC)*, Geneva, Switzerland, paper We.10.P1.119, 2011.

Directly-Modulated VCSELs for 2x2 MIMO-OFDM Radio over Fiber in WDM-PON

M. B. Othman[1,2], Lei Deng[1], Xiaodan Pang[1], J. Caminos[1], W. Kozuch[1], K. Prince[1], J. Bevensee Jensen[1], I. Tafur Monroy[1]

[1]*DTUFotonik, Department of Photonics Engineering, Technical University of Denmark, Ørsteds Plads 343, DK-2800 Kgs. Lyngby, Denmark*
[2]*Department of Communication Engineering, Faculty of Electrical and Electronic Engineering, UTHM, 86400 Parit Raja, Johor, Malaysia.*
mabio@fotonik.dtu.dk, kpri@fotonik.dtu.dk, jebe@fotonik.dtu.dk, idtm@fotonik.dtu.dk

Abstract: We demonstrate directly- modulated VCSELs supporting 2x2 MIMO-OFDM 5.6-GHz radio over fiber signaling over 20-km WDM-PON. Error-free signal demodulation of 64-subcarrier 4-QAM signals modulated at 198.5-Mb/s is achieved after fiber and 2-m indoor wireless transmission.
OCIS codes: (060.0060) Fiber optics and optical communications; Radio frequency photonics (060.5625)

1. Introduction

Radio over fiber (RoF) technology is a promising solution for integrating wireless and fixed-line communication networks. Multiple input multiple output (MIMO) technology has improved transmission distances and increased the data rates supported by modern wireless networks without any additional power or bandwidth expenditure [1]. Such multiple antenna techniques however present a challenge for RoF systems, which have to ensure clean transmission of multiple signals between elements of the antenna array, and must mitigate signal path impairments which introduce crosstalk, attenuation and multipath fading [2]. Sophisticated receiver algorithms may be implemented to overcome these path-dependent effects. Orthogonal frequency division multiplexing (OFDM) has emerged as the leading modulation technique in the wireless domain. The combination of OFDM with MIMO technique provides an attractive solution because of the very simple implementation, and potentially high spectral efficiency [3]. Wavelength division multiplexed passive optical network (WDM-PON) systems supporting higher bandwidth can transparently deliver radio frequency signaling required to support hybrid fixed and wireless access networking systems. WDM-PON technology is therefore expected to further improve the throughput in the wireless service area covered by RoF-MIMO antennas [4]. Previously, distributed feedback (DFB) laser diodes have been suggested for use in WDM-PON but have failed to attract industry attention because of the high cost [5]. Directly modulated vertical-cavity surface-emitting lasers (VCSELs) have emerged as an attractive solution for WDM-PON due to the cost effective production, low power consumption [6], capability for chip integration with the low threshold and driving current operation [7].

Previous simulation work has been done towards integrating MIMO-OFDM technology with RoF [2], and integrating dense wavelength division multiplexing (DWDM) with MIMO-OFDM [8]. The experimental work in [9] demonstrates the MIMO RoF concepts, but that analysis implemented separate fibers for each remote access unit (RAU). This paper presents, to the best of our knowledge, the first experimental demonstration of a low cost all-VCSEL 2x2 MIMO OFDM over WDM-PON system. We have successfully demonstrated wireless MIMO transmission with 4-QAM OFDM over 2x2 MIMO array.

2. Experiment setup

The experimental setup of the system is illustrated in Fig.1. In the central office (CO), two different real valued 64-subcarrier 4-QAM OFDM baseband signals with 198.5 Mb/s net data rate and 312 MHz bandwidth are generated by an arbitrary waveform generator (ArbWaveGen). The OFDM symbols are arranged in frames of 10 symbols. The first 3 symbols implement the training sequence; and 10% cyclic prefix is added. A dual channel baseband MIMO-OFDM signal is generated in the ArbWaveGen, which is then up-converted to a 5.65 GHz radio frequency (RF) carrier; the signal in one arm is up-converted using the vector signal generator (VSG) and the other arm implements RF up-conversion using a mixer. Different training sequences are used for each sub-element of the MIMO-OFDM signal; this enables estimation of the MIMO wireless channel response. The electrical MIMO-OFDM signals directly modulate two VCSELs operating at different bias levels to generate different wavelengths of 1535.29 nm and 1536.09 nm. Both WDM optical signals are combined using 3 dB coupler; they propagate through 20 km non-

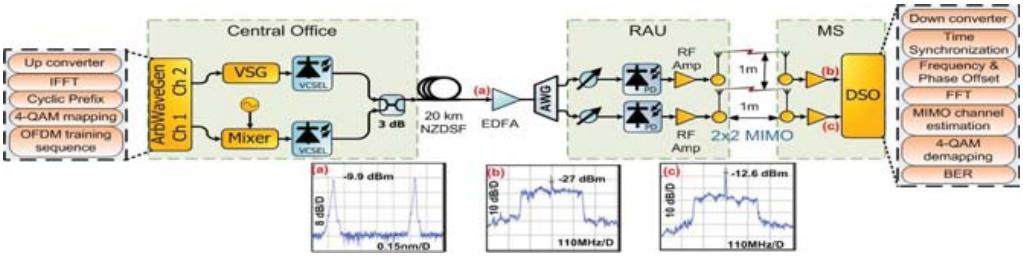

Fig. 1: Experiment setup for all-VCSELs for WDM-PON with 4-QAM OFDM signals over 20 km NZDSF and 2x2 wireless MIMO.

zero dispersion shifted fiber (NZDSF). The optical spectrum of the CO transmitter output is shown in Fig 1(a). After 20 km NZDSF transmission, the downstream WDM signals are divided using an arrayed waveguide grating (AWG). After the photodetector, RF amplifiers boost the signal with 20 dB gain, at the (RAU) antenna. The wireless signals propagate through 1 meter distance. Elements of the 2x2 antenna array implemented at both RAU and mobile station (MS) are vertically spaced by 1 meter; vertical polarization is implemented for the wireless link. At the MS receiver, the signals are captured by two antennas and amplified with 20 dB gain electrical amplifier. The RF OFDM signals are sampled by a digital sampling scope (DSO), with 20 Gs/s sampling rate. The electrical MIMO-OFDM spectrum is shown in Fig. 1 (b) for the VSG and (c) for the mixer. A digital signal processing (DSP) enabled receiver at the MS uses the different training sequences implemented on sub-elements of the MIMO-OFDM wireless transmission to identify the MIMO signals radiated from each antenna element, and demodulates the OFDM signals. Signal down-conversion, time synchronization, frequency and phase offset removal and fast Fourier transform (FFT) processing are implemented in DSP. Compensation for crosstalk and multipath fading is done using a minimum-mean-square-error MMSE algorithm. The bit error rate (BER) is calculated after symbol demapping. Transmission quality was assessed using BER sensitivity to received optical power metric. We consider a BER of 10^{-3}, since forward error correction (FEC) techniques may be applied to obtain error free transmission.

3. Results

Figure 2 presents BER results obtained as the MIMO signal propagates through the system; we distinguish between signal elements upconverted using mixer (solid symbols) and VSG (hollow symbols). Fig. 2(a) shows variation of BER with optical power for both signal paths, for optical back to back (B2B) (circle) and after fiber transmission (square). From these results, we observe that the mixer-generated signal requires 3 dB more optical power to achieve BER 10^{-3} than the VSG-generated signal. For B2B, the FEC threshold is achieved when PD input power is approximately -12.3 dBm and -15.2 dBm for VSG and mixer, respectively. After 20 km of fiber, the FEC limit at achieved with received optical power of approximately -11 dBm for VSG and -13.8 dBm for mixer. After fiber transmission, 1.5 dB power penalty is observed for both mixer and VSG-generated signal streams. Fig. 2(b) illustrates the BER results obtained with wireless transmission, for B2B (circle) and after fiber (square); corresponding post-PD electrical constellations are also shown in the inset. With wireless transmission, 2 dB additional power is required at the PD input was observed for both B2B and fiber transmission of both mixer and VSG-generated signals. Less than 2 dB power penalty is observed for both signal elements, for both B2B and after fiber. After fiber transmission, system performance is also affected by varying the separation between RAU and MS. Fig. 2(c) presents BER variation with received optical power (ROP) at different wireless distances between RAU and MS; results are assessed at 1 m (circle), 2 m (square) and 3 m (triangle). The insets show received constellation diagrams observed at the MS; clear 4-QAM OFDM constellations are obtained. Increasing power penalty is observed as wireless transmission distance is increased. For a fixed transmit power, increased wireless transmission distance also increases path attenuation. This reduced the received signal to noise ratio (SNR) and increased BER. This agrees well with experimental observations. Even though we are facing this problem as well as the interference effect and multipath fading, we could achieve error free transmission after 2 meters of wireless transmission. This can be clearly seen from the 4-QAM OFDM constellation diagram in Fig. 2(c). We observe that increasing the distance between RAU and MS reduces the performance difference observed between the two MIMO signals; this difference is within 0.5 dB after 3 m wireless transmission. After fiber transmission, the effect of antenna separation on performance is assessed by varying the spacing between the elements of the RAU and MS antenna arrays, while preserving 1 m transmission distance between RAU and MS. The results obtained with antenna spacing of 0.5 m (square), 1 m (circle) and 1.5 m (diamond) are presented in Fig. 2(d). We observe similar performance without any penalty for all separations for both channels in Fig. 2(d). This suggests that 0.5 m antenna separation is sufficient for

the system to implement MIMO transmissions. Furthermore, the MIMO-OFDM system demonstrates good tolerance to path-dependent effects for the demonstrated 2x2 MIMO array. 4-QAM constellation diagrams for 0.5 m antenna separation are shown for both channels in the Fig 2(d); these obtained at BER 10^{-3}.

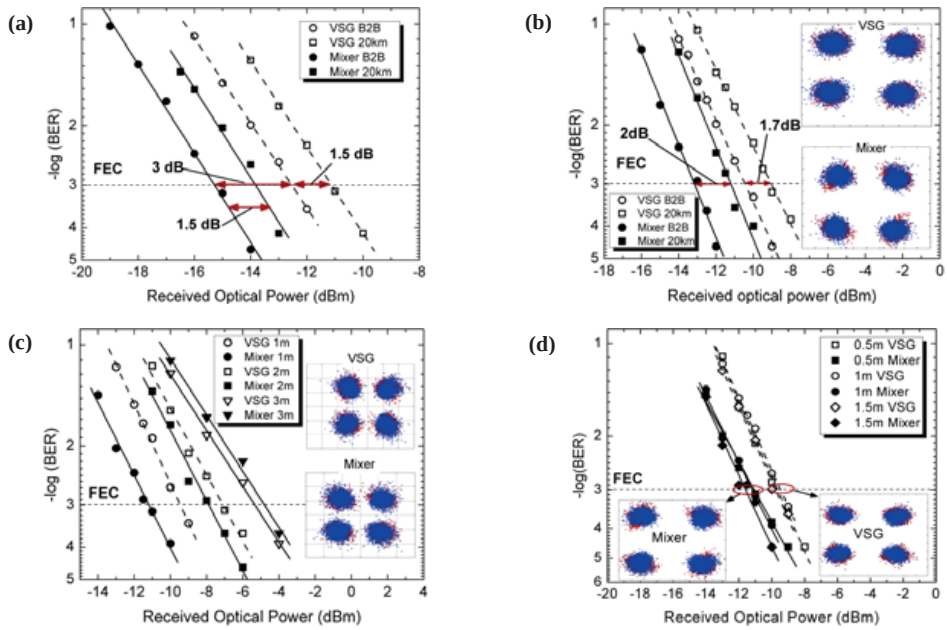

Figure 2: Showing variation of (a) BER with received optical power (ROP) for optical back-to-back (B2B) and after 20 km NZDSF: (b) BER with ROP for 2x2 MIMO wireless transmission at B2B and after optical fiber: (c) BER with ROP after fiber transmission, at various distances between RAU and MS: and (d) BER with ROP after fiber transmission, for different antenna separation, with fixed 1 meter distance between RAU and MS. MIMO signal elements which are upconverted using mixer (solid symbols) and VSG (hollow symbols) are identified. Insets show constellation obtained at FEC limit (BER = 10^{-3}).

4. Conclusions

We have presented the first known demonstration of MIMO-OFDM signal distribution in a WDM-PON system using all-VCSELs optical sources with wireless MIMO transmission; this provides potentially a cost effective solution for future access networks. MIMO-OFDM algorithms also effectively compensate for impairments in wireless link. We also investigate the effects of various wireless transmission path length and antenna separation to see the robustness of the MIMO-OFDM algorithm. We report error free transmission after 20 km NZDSF and 2 meter 2x2 wireless MIMO-OFDM at 198.5Mb/s with 5.65 GHz radio over fiber signaling transmission for WDM-PON system. No penalty was observed for varying antenna separation of the sub-elements of the MIMO-OFDM signal with 1 m separation between RAU and MS. We believe this work can be a potentially attractive candidate for last mile home network.

5. References

[1] M. Sauer, et. al, "Radio over fiber for picocellular network architectures" JLT, 25(11) (2007).
[2] I. Harjula et.al, "Practical issues in the combining of MIMO techniques and RoF in OFDM/A systems" Proc. of the 7th WSEAS, 244-248, (2008).
[3] W.Shieh at. al, *OFDM for Optical Communication*, Chapter 1 & 12, (Elsevier, 2010) .
[4] K.Tsukamoto, et.al, "Convergence of WDM Access and Ubiquitous Antenna Architecture for Broadband Wireless Services" PIERS Online, 6(4) (2010).
[5] Wen-Shing Tsai et. al, "Bidirectional dense wavelength-division multiplexing passive optical network based on injection-locked vertical cavity surface-emitting lasers and a data comparator" Optical Engineering, 45(9), (2006).
[6] E. Kapon et. al, "Long-wavelength VCSELs: Power-efficient answer" Nature Photonics 3, 27 - 29 (2009).
[7] R. Rodes et.al, "All-VCSEL based digital coherent detection link for multi Gbit/s WDM passive optical networks" Opt. Exp., 18(24) (2010).
[8] S. Nema, et.al, "Convergence Integrated DWDM and MIMO-OFDM System for 4G High Capacity Mobile Communication" Signal Processing an International Journal, 3(5),(2010).
[9] A. Kobyakov, et.al, "Effect of Optical Loss and Antenna Separation in 2x2 MIMO Fiber-Radio Systems" IEEE T. Ant & Prop, 58(1),(2010).

Paper 7: MIMO-OFDM WDM PON with DM-VCSEL for Femtocells Application

M. B. Othman, L. Deng, X. Pang, J. Caminos, W. Kozuch, K. Prince, X. Yu, J. B. Jensen, and I. T. Monroy, "MIMO-OFDM WDM PON with DM-VCSEL for femtocells application," *Optics Express* , vol. 19, no. 26, pp. B537—B542, 2011.

MIMO-OFDM WDM PON with DM-VCSEL for femtocells application

M. B. Othman,[1,2,*] Lei Deng,[1] Xiaodan Pang,[1] J. Caminos,[1] W. Kozuch,[1] K. Prince,[1] Xianbin Yu,[1] Jesper Bevensee Jensen,[1] and I. Tafur Monroy[1]

[1]*DTU Fotonik, Department of Photonics Engineering, Technical University of Denmark, DK-2800, Kgs. Lyngby, Denmark*

[2]*Department of Communication Engineering, Faculty of Electrical and Electronic Engineering, UTHM, 86400 Parit Raja, Batu Pahat, Johor, Malaysia*

**mabio@fotonik.dtu.dk*

Abstract: We report on experimental demonstration of 2x2 MIMO-OFDM 5.6-GHz radio over fiber signaling over 20 km WDM-PON with directly modulated (DM) VCSELs for femtocells application. MIMO-OFDM algorithms effectively compensate for impairments in the wireless link. Error-free signal demodulation of 64 subcarrier 4-QAM signals modulated at 198.5 Mb/s net data rate is achieved after fiber and 2 m indoor wireless transmission. We report BER of $7x10^{-3}$ at the receiver for 16-QAM signals modulated at 397 Mb/s after 1 m of wireless transmission. Performance dependence on different wireless transmission path lengths, antenna separation, and number of subcarriers have been investigated.

OCIS codes: (060.0060) Fiber optics and optical communications; (060.5625) Radio frequency photonics.

References and links

1. A. J. Cooper, "Fiber/Radio for the provision of cordless/mobile telephony services in the access network," Electron. Lett. **26**(24), 2054–2056 (1990).
2. M. Sauer, A. Kobyakov, and J. George, "Radio over fiber for picocellular network architectures," J. Lightwave Technol. **25**(11), 3301–3320 (2007).
3. I. Harjula, A. Ramirez, F. Martinez, D. Zorrilla, M. Katz, and V. Polo, "Practical issues in the combining of MIMO techniques and RoF in OFDM/A systems," Proc. of the 7th WSEAS, 244–248 (2008).
4. V. Tarokh, *New Directions in Wireless Communications Research*, Chap. 2 (Springer, 2009).
5. W. Shieh and I. Djordjevic, *OFDM for Optical Communication*, Chaps. 1, 4, 12 (Elsevier, 2010).
6. J. Zhang and G. de la Roche, *Femtocells: Technologies and Deployment*, Chaps. 2, 4, 9 (Wiley, 2010).
7. S. L. Jansen, I. Morita, T. C. Schenk, and H. Tanaka, "Long-haul transmission of 16x52.5 Gbits/s polarization-division multiplexed OFDM enabled by MIMO processing (Invited)," J. Opt. Netw. **7**(2), 173–182 (2008).
8. S. R. Saunders, S. Carlaw, A. Giustina, R. R. Bhat, V. S. Rao, and R. Siegberg, *Femtocells: Opportunities and Challenges for Business and Technology* (Wiley, 2009).
9. A. J. Paulraj, D. A. Gore, R. U. Nabar, and H. Bolcskei, "An overview of MIMO communications - a key to gigabit wireless," Proc. IEEE **92**(2), 198–218 (2004).
10. J. H. Winters, "Smart antennas for wireless systems," IEEE Personal Commun. **5**(1), 23–27 (1998).
11. K. Iwatsuki, T. Tashiro, K. Hara, T. Taniguchi, J.- Kani, N. Yoshimoto, K. Miyamoto, T. Nishiumi, T. Higashino, K. Tsukamoto, and S. Komaki, "Broadband Ubiquitous Femto-cell Network with DAS over WDM-PON (invited paper)," Proc. SPIE **7958**, 79580I (2011).
12. K. Tsukamoto, T. Nishiumi, T. Yamagami, T. Higashino, S. Komaki, R. Kubo, T. Taniguchi, J.-I. Kani, N. Yoshimoto, H. Kimura, and K. Iwatsuki, "Convergence of WDM Access and Ubiquitous Antenna Architecture for Broadband Wireless Services," PIERS Online **6**(4), 385–389 (2010).
13. W.-S. Tsai, H.-H. Lu, S.-J. Tzeng, T.-S. Chien, S.-H. Chen, and Y.-C. Chi, "Bidirectional dense wavelength-division multiplexing passive optical network based on injection-locked vertical cavity surface-emitting lasers and a data comparator," Opt. Eng. **45**(9), 095003 (2006).
14. E. Kapon and A. Sirbu, "Long-wavelength VCSELs: Power-efficient answer," Nat. Photonics **3**(1), 27–29 (2009).
15. R. Rodes, J. B. Jensen, D. Zibar, C. Neumeyr, E. Roenneberg, J. Rosskopf, M. Ortsiefer, and I. T. Monroy, "All-VCSEL based digital coherent detection link for multi Gbit/s WDM passive optical networks," Opt. Express **18**(24), 24969–24974 (2010).
16. S. Nema, A. Goel, and R. P. Singh, "Integrated DWDM and MIMO-OFDM System for 4G High Capacity Mobile Communication," Signal Process. Int. J. **3**(5), 132–143 (2010).
17. A. Kobyakov, M. Sauer, A. Ng'oma, and J. H. Winters, "Effect of Optical Loss and Antenna Separation in 2x2 MIMO Fiber-Radio Systems," IEEE Trans. Antenn. Propag. **58**(1), 187–194 (2010).

#155874 - $15.00 USD Received 3 Oct 2011; revised 17 Nov 2011; accepted 18 Nov 2011; published 30 Nov 2011

18. M. B. Othman, L. Deng, X. Pang, J. Caminos, W. Kozuch, K. Prince, J. B. Jensen, and I. T. Monroy, "Directly-modulated VCSELs for 2×2 MIMO-OFDM radio over fiber in WDM-PON," ECOC (2011).
19. Y. S. Cho, J. Kim, W. Y. Yang, and C.-G. Kang, *MIMO-OFDM Wireless Communication with MATLAB*, Chap. 6 (Wiley, 2010).
20. X. Liu and F. Buchali, "A novel channel estimation method for PDM-OFDM enabling improved tolerance to WDM nonlinearity," OFC/NFOEC (2009).
21. M. Beltran, J. B. Jensen, R. Llorente, and I. Tafur Monroy, "Experimental Analysis of 60-GHz VCSEL and ECL Photonic Generation and Transmission of Impulse-Radio Ultra-Wideband Signals," IEEE Photon. Technol. Lett. **23**(15), 1055–1057 (2011).

1. Introduction

Wireless networks based on radio over fiber (RoF) technologies have been proposed as a promising cost effective solution to meet ever increasing user demands for high data rate and mobility. Since it was first demonstrated for cordless and mobile telephone services in 1990 [1], extensive research has been carried out to investigate its limitation and develop new high performance RoF technologies. Multiple input multiple output (MIMO) is widely used to increase wireless bit rates [2] and improve larger area coverage than traditional single input single output (SISO) antennas. Such multiple antenna techniques, however, present a challenge for RoF systems, which have to ensure clean transmission of multiple signals between elements of the antenna array, and must mitigate signal path impairments which introduce crosstalk, attenuation and multipath fading [3]. Sophisticated receiver algorithms have to be implemented and receiver components synchronization needs to be very accurate to overcome these path-dependent effects [4].

Orthogonal frequency division multiplexing (OFDM) has emerged as one of the leading modulation techniques in the wireless domain. The combination of OFDM with MIMO provides an attractive solution because OFDM potentially offers high spectral efficiency and resilience to multipath fading. Specifically, MIMO-OFDM signals can be processed using relatively straightforward matrix algebra, and seems to be a promising candidate for RoF system because of the simultaneous compensation of multipath fading in wireless channels and dispersion effects in optical fiber links [5]. Furthermore, OFDM is a future candidate for femtocell application [6] because the interference can be reduced by using more frequency resources. In addition, for multi-carrier systems like OFDM, a large computational complexity will be introduced by using the classical MIMO channel estimation method based on the butterfly structure because an adaptive filter needs to be assigned for each OFDM subcarrier. Consequently, a training-based channel estimation method has the relatively low computational complexity at the receiver [7] and draws more interest in analyzing multi-carrier systems.

The goal of femtocells is to provide reliable communication using existing broadband internet connection and improve the indoor coverage [8]. Femtocells provide many benefits in terms of cost, power, capacity and scalability [6]. However, there are many challenges in the deployment of femtocell such as network architecture, allocation of spectrum resources and the avoidance of electromagnetic interference. One of the main impairments of wireless channels is frequency selective fading. It is especially so in intense multipath environments where the behaviour of the channel differs between different frequencies. This is particularly true in indoor and urban environments. The combination of the throughput enhancement [9] and path diversity [10] offered by MIMO technologies with the robustness of OFDM against frequency selective fading is regarded a very promising basis for femtocell multi-user wireless transmission applications [6]. A small sized femtocell access point (FAP) is usually located in a home or office where it also linked to a broadband internet connection as shown in Fig. 1. The recent explosive growth of the internet has triggered the introduction of a broadband access network based on fiber to-the-office (FTTO) and fiber-to-the-home (FTTH). Therefore, the increasing of wireless demands makes RoF as an enabling technology to support femtocell in the WDM network [11] for FTTH and FTTO network.

Wavelength division multiplexed passive optical network (WDM-PON) systems can transparently deliver radio frequency signaling required to support hybrid fixed and wireless access networking systems. WDM-PON technology is therefore expected to further improve

#155874 - $15.00 USD Received 3 Oct 2011; revised 17 Nov 2011; accepted 18 Nov 2011; published 30 Nov 2011

the throughput in the wireless service area covered by RoF-MIMO antennas [12]. Previously, distributed feedback (DFB) laser diodes have been suggested for use in WDM-PON but have only gained limited industry attention because of the high cost [13]. Directly modulated

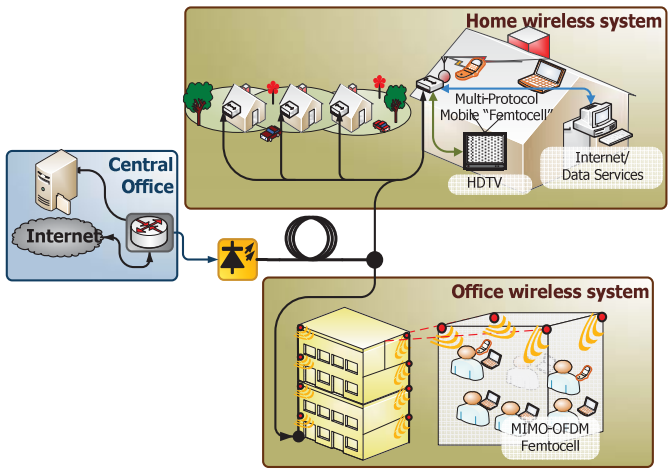

Fig. 1. Femtocell in home and office environment for radio over fiber network.

vertical-cavity surface-emitting lasers (VCSELs) have emerged as an attractive solution for WDM-PON due to the cost effective production, low power consumption [14], and low threshold and driving current operation [15]. Simulation work regarding integration of MIMO-OFDM technology with RoF has been presented in [3], and regarding integration of dense wavelength division multiplexing (DWDM) with MIMO-OFDM in [16]. The experimental work in [17] demonstrates the MIMO RoF concepts, but implemented separate fibers for each remote access unit (RAU).

Previously in [18], we have successfully demonstrated DM-VCSEL 2 x 2 MIMO OFDM over WDM-PON. The OFDM-MIMO training sequence algorithm are applied to compensate the receiver complexity will be further described in this paper. We give an overview of the experimental setup and present the performance evaluation and discussion. Additionally we add investigations of the influence on performance by the number of subcarriers in the OFDM signals, and we present initial experimental results of 16-QAM OFDM-MIMO at 397 Mb/s.

2. OFDM-MIMO training sequence algorithm

Multiple transmit-and-receive antennas in OFDM systems can improve communication quality and capacity. For the OFDM systems with multiple transmitter antennas, each tone at each receiver antenna is associated with multiple channel parameters, which makes channel estimation difficult. Fortunately, channel parameters for different tones of each channel are correlated and the channel estimators are based on this correlation. Several channel estimation schemes have been proposed for the OFDM systems with multiple transmit-and-receive antennas for space diversity, or (MIMO) systems for wireless data access [19]. Channel estimation is important for signal demodulation in MIMO systems, in particular when a large number of subcarriers and advanced multiplexing technique are employed. The training-based channel estimation method is computationally efficient because of its simple expression [20]. However, their transmission efficiencies are reduced due to required overhead of training symbols such as preamble or pilot tones that are transmitted in addition to data symbol. In our work we allocated three training symbols in each of the frame. We implemented different

#155874 - $15.00 USD Received 3 Oct 2011; revised 17 Nov 2011; accepted 18 Nov 2011; published 30 Nov 2011

training symbols for each sub-element of the MIMO-OFDM signal. This enables estimation on the receiver side of the MIMO wireless channel response using this MIMO-OFDM algorithm.

3. Experimental setup

Experimental setup of the system is illustrated in Fig. 2. In the central office (CO), two different real valued 64-subcarrier 4-QAM OFDM baseband signals with 198.5 Mb/s net data rate (excluding the training symbols) and 312 MHz of bandwidth are generated by an arbitrary waveform generator (ArbWaveGen). The OFDM symbols are arranged in frames of 10 symbols. The first 3 symbols implement the training sequence, and 10% cyclic prefix is added. A dual channel baseband MIMO-OFDM signal is generated in the ArbWaveGen, which is then up- converted to a 5.65 GHz radio frequency (RF) carrier; the signal in one arm is up-converted using a mixer and the other arm implements RF up-conversion using the vector signal generator (VSG).

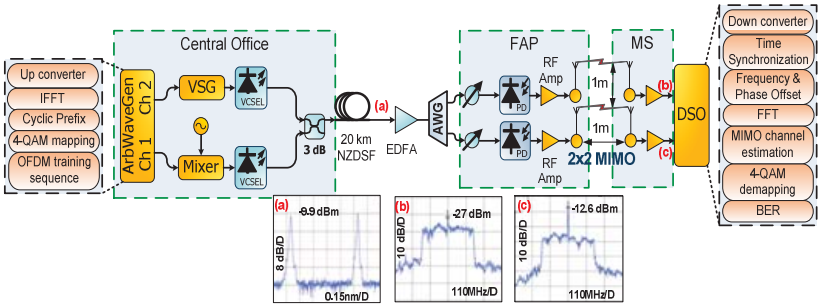

Fig. 2. Experiment setup for all-VCSELs for WDM-PON with 4-QAM OFDM signals over 20 km NZDSF and 2x2 wireless MIMO. RF carrier frequency of 5.65 GHz was used for both branches of the MIMO channel.

Different training sequences are used for each sub-element of the MIMO-OFDM signal; this enables estimation of the MIMO wireless channel response. The electrical MIMO-OFDM signals directly modulate two VCSELs operating at different bias levels to generate different wavelengths of 1535.29 nm and 1536.09 nm. The two optical signals are combined using a 3 dB coupler; they propagate through 20 km non- zero dispersion shifted fiber (NZDSF). The NZDSF is employed due to improved dispersion performance in the PON system [21]. The optical spectrum of the CO transmitter output is shown in Fig. 2(a). After 20 km NZDSF transmission, the downstream WDM signals are divided using an arrayed waveguide grating (AWG). After the photodetector, RF amplifiers boost the signal with 20 dB gain, at the FAP antenna. The wireless signals propagate through 1 meter distance. Elements of the 2x2 antenna array implemented at both femtocell access point (FAP) and mobile station (MS) are vertically spaced by 1 meter; vertical polarization is implemented for the wireless link for femtocell network. At the MS receiver, the signals are captured by two antennas and amplified with a 20 dB gain electrical amplifier. The RF OFDM signals are sampled by a digital sampling scope (DSO), with 20 Gs/s sampling rate. The electrical MIMO-OFDM spectrum is shown in Fig. 2(b) for the VSG and Fig. 2(c) for the mixer.

A digital signal processing (DSP) enabled receiver at the MS uses the different training sequences implemented on sub-elements of the MIMO-OFDM wireless transmission to identify the MIMO signals radiated from each antenna element, and demodulates the OFDM signals. Signal down-conversion, time synchronization, frequency and phase offset removal and fast Fourier transform (FFT) processing are implemented in DSP. Compensation for crosstalk and multipath fading is done using a minimum-mean-square-error (MMSE) algorithm. The bit error rate (BER) is calculated after symbol demapping. Transmission quality was assessed using BER sensitivity to received optical power metric. We consider a

#155874 - $15.00 USD Received 3 Oct 2011; revised 17 Nov 2011; accepted 18 Nov 2011; published 30 Nov 2011

BER of $2x10^{-3}$, since forward error correction (FEC) techniques may be applied to obtain error free transmission when the 7% of FEC overhead are taken into account.

4. Results and discussion

Figure 3 presents BER results obtained as the MIMO signal propagates through the system: we distinguish between signal elements upconverted using mixer (solid symbols) and VSG (hollow symbols). Figure 3(a) presents BER variation with received optical power (ROP) at different wireless distances between FAP and MS; results are assessed at 1 m (circle), 2 m (square) and 3 m (triangle). We fixed the separation spacing between the elements of the FAP and MS antenna arrays at 1 meter. The insets show received constellation diagrams observed at the MS; clear 4-QAM OFDM constellations are obtained. The increasing of power penalty is observed as wireless transmission distance increases. With a fixed transmit power, the increased path loss associated with longer wireless transmission lengths results in reduced receiver signal to noise ratio (SNR), leading to increased BER. This agrees well with experimental observations. The MIMO-OFDM signal could be received error free after 2 meters of wireless transmission. This can be clearly seen from the 4-QAM OFDM constellation diagram in Fig. 3(a). After 3 meters wireless transmission, the signals could still be demodulated with a BER below FEC limit of $2x10^{-3}$. We observe that the increase of the distance between FAP and MS reduces the performance.

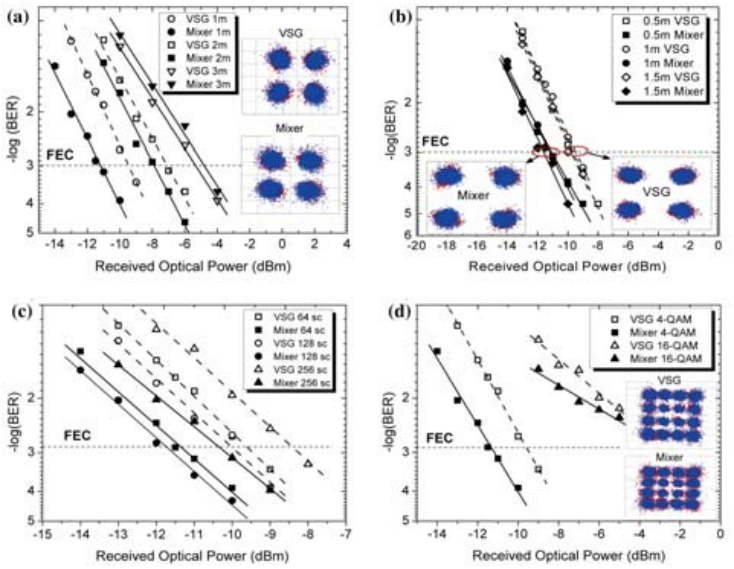

Fig. 3. Showing variation of (a) BER with ROP after fiber transmission, at various distances between RAU and MS: and (b) BER with ROP after fiber transmission, for different antenna separation, with fixed 1 meter distance between RAU and MS. (c) BER with ROP with 4-QAM modulation using different subcarriers: (d) BER with ROP for 4-QAM and 16-QAM modulation scheme with 64 subcarriers and fixed 1 meter distance between RAU and MS. MIMO signal elements which are upconverted using mixer (solid symbols) and VSG (hollow symbols) are identified. Insets show constellation obtained at FEC limit (BER = $2x10^{-3}$).

After fiber transmission, the effect of antenna separation on performance is assessed by varying the spacing between the elements of the FAP and MS antenna arrays, while preserving 1 m transmission distance between FAP and MS. The results obtained with antenna spacing of 0.5 m (square), 1 m (circle) and 1.5 m (diamond) are presented in Fig. 3(b). We observed similar performance without any penalty for all separations for both

#155874 - $15.00 USD Received 3 Oct 2011; revised 17 Nov 2011; accepted 18 Nov 2011; published 30 Nov 2011

channels in Fig. 3(b). This is shows that the good transmission was obtained at different antenna separation higher than 0.5m. 4-QAM constellation diagrams for 0.5 m antenna separation are shown for both channels in the Fig. 3(b); these obtained at BER $2x10^{-3}$.

Figure 3(c) shows the different number of subcarriers transmitted in the system over wireless transmission with 4-QAM modulation scheme. The 64 subcarriers represent by (square), 128 subcarriers (circle) and 256 subcarriers (triangle). Theoretically increasing the number of subcarriers should be able to give better performance in a sense that we will be able to handle larger delay spreads. This statement can be supported by looking at the Fig. 3(c) when the number of subcarriers increased from 64 to 128 the ROP performance become better. But several typical implementation problems arise with a large number of subcarriers. When we have large numbers of subcarriers, we have to assign the subcarrier frequencies very close to each other with same amount of bandwidth. We know that the receiver needs to synchronize itself to the carrier frequency very well, otherwise a comparatively small carrier frequency offset may cause a large frequency mismatch between neighboring subcarriers. When the subcarrier spacing is very small, the receiver synchronization components need to be very accurate, which is still not possible with low-cost RF hardware [4]. We observe that at 256 subcarriers, the performance is degraded. We attribute this degradation to a combination of RoF nonlinearities and receiver synchronization to the narrowly spaced subcarriers. Thus, a reasonable trade-off between the subcarrier spacing and the number of subcarriers must be achieved.

A performance comparison between different modulation scheme also been done in this experiment. Figure 3(d) shows the performance evaluation of 4-QAM (square) and 16-QAM (triangle). The insets show received constellation diagrams observed at the MS; 16-QAM OFDM constellations are obtained at BER of 7x10-3 with 397Mb/s net data rate. At higher amplitudes, the constellation symbols are dispersed widely compared with the one at the center because the nonlinearity of the VCSELs. The BER curves for 16-QAM also do not reach the standard FEC limit because the higher the modulation format requires higher power to increase the signal to noise ratio (SNR).

5. Conclusions

We have presented the MIMO-OFDM signal distribution in a WDM-PON system using DM-VCSELs optical sources with wireless MIMO transmission. This provides potentially a cost effective solution for future femtocells access networks. MIMO-OFDM algorithms effectively compensate for impairments in the wireless link. We also investigate the effects of various wireless transmission path lengths, antenna separation, various number of subcarriers in OFDM and different modulation schemes to see the ability of the MIMO-OFDM algorithm to estimate the MIMO wireless channel response. We report error free transmission after 20 km NZDSF and 2 meter 2x2 wireless MIMO-OFDM. The 4-QAM signals modulated at 198.5Mb/s net data rate with 5.65 GHz radio over fiber signaling transmission for WDM-PON system. For 16-QAM, after 1m wireless transmission a BER of $7x10^{-3}$ is reported at the receiver. MIMO-OFDM has a good potential to be implemented for indoor systems because the complexity at the receiver side can be reduced with training sequence algorithm. The maximum number of subcarriers that are allowed in this system is 128 because of the tradeoff between the subcarrier spacing and the number of subcarriers must be achieved. However, for higher modulation technique, powerful receiver algorithm is required to synchronize the signals and higher power to drive the transmission signal. Future work needs to be done for the upstream to demonstrate the bidirectional WDM PON with MIMO in femtocell application. We believe this work can be a potentially attractive candidate for future femtocells network especially for indoor office environment.

#155874 - $15.00 USD Received 3 Oct 2011; revised 17 Nov 2011; accepted 18 Nov 2011; published 30 Nov 2011

Paper 8: Seamless Translation of Optical Fiber PolMux-OFDM into a 2×2 MIMO Wireless Transmission Enabled by Digital Training-Based Fiber-Wireless Channel Estimation

X. Pang, L. Deng, Y. Zhao, M. B. Othman, X. Yu, J. Bevensee Jensen, D. Zibar, and I. Tafur Monroy, "Seamless Translation of Optical Fiber PolMux-OFDM into a 2×2 MIMO Wireless Transmission Enabled by Digital Training-Based Fiber-Wireless Channel Estimation," in *Asia Communications and Photonics Conference and Exhibition*, Proceedings of SPIE, 2011.

Seamless Translation of Optical Fiber PolMux-OFDM into a 2×2 MIMO Wireless Transmission Enabled by Digital Training-Based Fiber-Wireless Channel Estimation

Xiaodan Pang*[a], Ying Zhao[b], Lei Deng[c], M. B. Othman[a], Xianbin Yu[a], J. B. Jensen[a], D. Zibar[a] and I.T. Monroy[a]

[a]DTU Fotonik, Technical University of Denmark, DK-2800, Kgs. Lyngby, Denmark
[b]Department of Electronic Engineering, Tsinghua University, 10084, Beijing, China
[c]School of Optoelectronics Science and Engineering, HuaZhong University of Science and Technology, Wuhan, China

ABSTRACT

We propose and demonstrate a 2 × 2 multiple-input multiple-output (MIMO) wireless over fiber transmission system. Seamless translation of two orthogonal frequency division multiplexing (OFDM) signals on dual optical polarization states into wireless MIMO transmission at 795.5 Mbit/s net data rate is enabled by using digital training-based channel estimation. A net spectral efficiency of 2.55 bit/s/Hz is achieved.

Keywords: radio frequency photonics, wireless communication, polarization multiplexing, MIMO, OFDM

1. INTRODUCTION

Hybrid optical fiber-wireless transmission systems will play an important part in the next generation user-centered access networking. This truly user-centered network will be powered by free access to services and applications enabled by seamless broadband fiber-wireless connections to various devices nearby. To realize the seamless integration of wireless and fiber-optic networks, the wireless links needs to be developed to preserve transparency to bit-rates and modulation formats.[1]

Orthogonal frequency division multiplexing (OFDM) is a promising candidate signal format for future hybrid optical fiber-wireless access systems. This is because of the inherent high chromatic dispersion tolerance of OFDM signals in optical fibers and its robustness against frequency selective fading or narrowband interference in wireless channels.[2,3] More interestingly, the spectral efficiency in fiber links can be further increased by polarization multiplexing (PolMux).[4] Research on baseband PolMux OFDM transmission has been reported.[5,6] In wireless channels, multiple-input multiple-output (MIMO) technique provides an attractive solution to increase capacity for bandwidth limited systems.[7] Meanwhile, the well-known radio-over-fiber (RoF) technology, which combines optical fiber and wireless techniques, provides a good solution to increase the coverage while maintaining the mobility of the broadband services in the local area networking scenarios. Based on these reasons, a RoF system combining optical PolMux, wireless MIMO and OFDM data format is able to fulfill the requirements of robustness, high flexibility and high spectral efficiency for providing broadband services in local networks. So far, in reported work focusing on PolMux wireless MIMO systems, only simple modulation format like on-off keying (OOK) is used.[7]

In addition, for multi-carrier systems like OFDM, a large computational complexity will be introduced by using the classical MIMO channel estimation method based on the butterfly structure because an adaptive filter needs to be assigned for each OFDM subcarrier. Consequently, a training-based channel estimation method has the relatively low computational complexity at the receiver[5] and draws more interests in analyzing multi-carrier systems.

* Send correspondence to Xiaodan Pang: E-mail: xipa@fotonik.dtu.dk, Telephone: +45 4525 7375

In this paper, we experimentally demonstrate a proof-of-concept hybrid fiber wireless system. A PolMux 4-quadrature amplitude modulation (4-QAM) OFDM RoF signal is seamlessly translated into a 2×2 MIMO wireless transmission. By using training sequence-based OFDM-MIMO channel estimation, transmitted wireless signal in both branches are successfully demodulated and a net spectral efficiency of 2.55 bit/s/Hz is achieved.

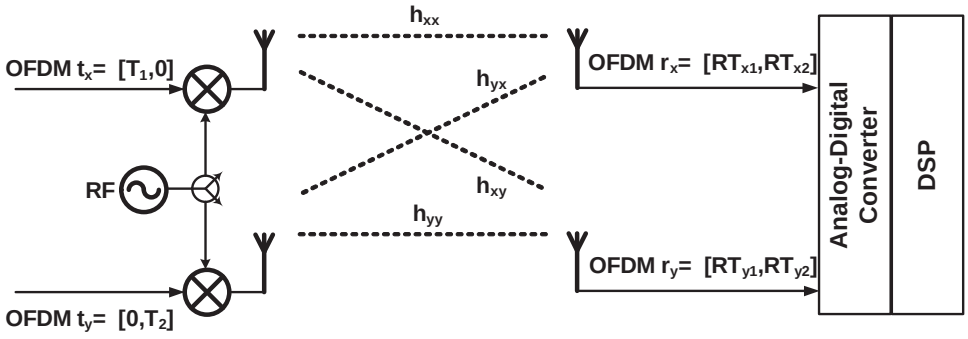

Figure 1. Block diagram of a wireless MIMO Channel

2. TRAINING-BASED CHANNEL ESTIMATION FOR OFDM-MIMO

In optical fiber-wireless MIMO systems, accurate channel estimation is important for signal demodulation. This is because it is the prerequisite for designing the channel equalizer in the digital domain at the receiver. In particular, when a large number of sub-carriers and advanced multiplexing technique are employed, more accurate channel estimation is required. Figure 1 shows the block diagram of a wireless MIMO OFDM channel.

In our proposed PolMux-MIMO system, the total fiber-wireless channel response for a MIMO-OFDM signal can be described as:

$$\begin{bmatrix} r_x \\ r_y \end{bmatrix} = \begin{bmatrix} h_{xx} & h_{yx} \\ h_{xy} & h_{yy} \end{bmatrix} \times \begin{bmatrix} t_x \\ t_y \end{bmatrix} \tag{1}$$

where t_x and t_x respectively stands for the transmitted signal in X and Y branch, and t_y and r_y are the received X and Y branch signal at the receiver. The 2×2 matrix in the equation describes the response of the fiber-wireless MIMO channel, including both the polarization mixing in the fiber and the crosstalk during wireless transmission. To obtain the parameters in the channel transfer matrix is the purpose of the channel estimation.

In order to derive this channel transfer matrix parameters, we transmit a pair of time-interleaved training sequences $T_X = [T_1, 0]^T$, $T_Y = [0, T_2]^T$ in the OFDM signal of the two tributaries, respectively. By precisely controlling the synchronization between the two branches' signals during the fiber-wireless transmission, assuming there is no difference in the arrival time of the two transmitted signals to the receivers in the two branches, the received training sequences in two consecutive training durations can be described as

$$\begin{bmatrix} RT_{x1} & RT_{x2} \\ RT_{y1} & RT_{y2} \end{bmatrix} = \begin{bmatrix} h_{xx} & h_{yx} \\ h_{xy} & h_{yy} \end{bmatrix} \times \begin{bmatrix} T_1 & 0 \\ 0 & T_2 \end{bmatrix} \tag{2}$$

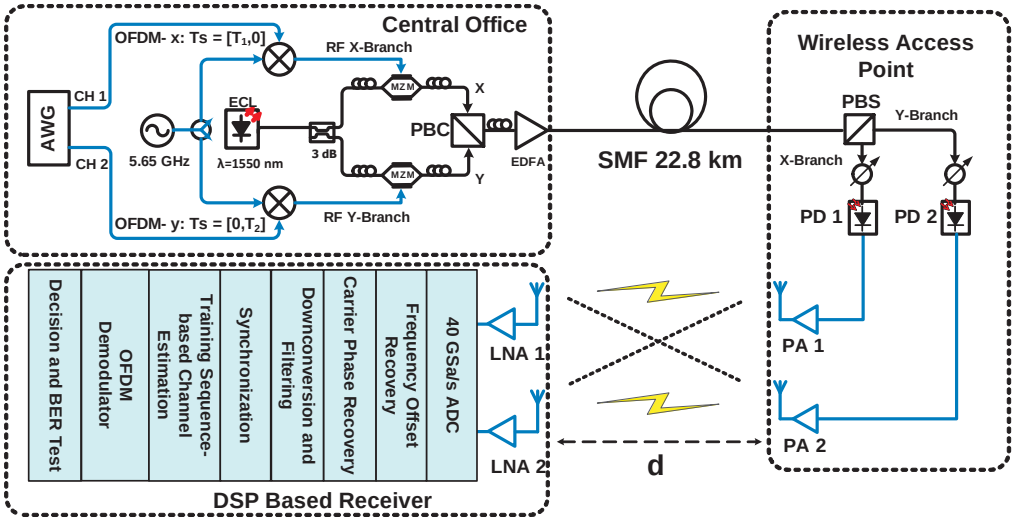

Figure 2. Experimental set-up (AWG: Arbitrary waveform generator; ECL: External cavity laser; MZM: Mach-Zehnder modulator; PBC/PBS: Polarization beam combiner/splitter; PA: Power amplifier; LNA: Low-noise amplifier)

in which RT_{x1} and RT_{x2} stands for the received training symbol from X branch at the first and second training durations respectively. So are the RT_{y1} and RT_{y2} for the Y branch. As these received training symbols can be directly obtained at the receiver side after transmission, the channel transfer matrix then can be easily calculated as

$$\begin{bmatrix} h_{xx} & h_{yx} \\ h_{xy} & h_{yy} \end{bmatrix} = \begin{bmatrix} RT_{x1}/T_1 & RT_{x2}/T_2 \\ RT_{y1}/T_1 & RT_{y2}/T_2 \end{bmatrix} \tag{3}$$

This training-based channel estimation method is computationally efficient because of its simple expression.[8] On the other hand, when implementing this channel estimation method into practice, especially in the wireless MIMO systems, strict synchronization between the two channels is required. By using this method, the MIMO-OFDM signals demodulation algorithm can be implemented digitally.

3. EXPERIMENTAL SETUP

The experimental setup for the PolMux RoF plus wireless 2×2 MIMO system is shown in figure 2. At the RoF signal transmitter, a 1.25 GSa/s arbitrary waveform generator (AWG) is used to generate two baseband real-valued 4-QAM OFDM signals with 64 sub-carriers by an up-sampling factor of 4. The OFDM signals have bandwidth of 625 MHz, corresponding to a gross data rate of 625 Mbit/s in each branch. The signals are arranged in frames of 10 symbols, out of which 3 are training symbols used for synchronization and channel estimation purpose. An cyclic prefix with 0.1 symbol length is added in each symbol. Therefore the signal in each X branch and Y branch has a net data rate of 397.7 Mbit/s. These two OFDM signals with time-interleaved training sequences are then separately up-converted to 5.65 GHz.

A narrow line width external cavity laser (ECL) with central wavelength at 1550 nm is used as the lightwave source. The output optical signal is equally divided into two optical tributaries at a 3 dB coupler. By using

two Mach-Zehnder modulators (MZM) which are biased at their linear points, the two RoF OFDM signals are modulated onto the optical carriers at each of the two branches. After that, by using two polarization controllers to align the polarization states of the signals at the two branches to the X and Y inputs of a polarization beam combiner (PBC), which are designed orthogonal with each other, the two signals are polarization multiplexed at the output of the PBC. A polarization controller placing after the PBC is used for roughly controlling the polarization state of the signal. The output signal then has a net data rate of 795.5 Mbit/s and thus a net spectral efficiency of 2.55 bit/s/Hz is achieved. In fact, the spectral efficiency of this system is expected to be further increased if an AWG with a higher sample rate is employed and higher level modulation formats are to be used.

After being amplified by a booster erbium-doped fiber amplifier (EDFA), the PolMux RoF OFDM signal transmits through a 22.8 km standard signal mode fiber (SSMF). At the wireless access point, the optical signal is divided back to X and Y polarizations by a polarization beam splitter (PBS). After electrical amplification, the optical signals of these two tributaries are converted into the RF domain by two photodiodes (PD), separately, and then fed to two transmitter antennas. At the user side, two receiver antennas, placed with the same separation as the transmitter antennas, form a 2×2 wireless MIMO system. The received signals are then delivered to a 40 GS/s analog-digital convertor (ADC), where the analog signals are converted into the digital domain. A digital signal processing (DSP) based receiver, consisting of frequency and phase recovery, frequency down-conversion, training based MIMO-OFDM channel estimation and OFDM demodulation modules, is used to demodulate the received signals and evaluate bit error rate (BER).

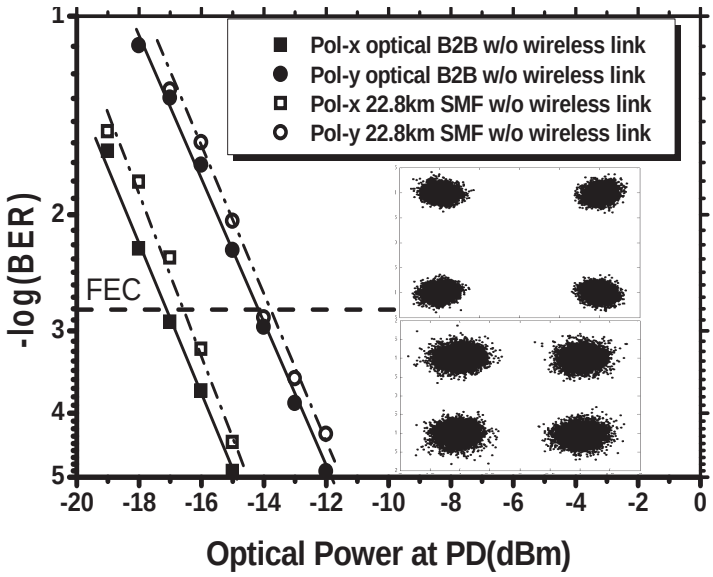

Figure 3. BER as a function of optical power at PD without wireless links (upper constellation: X polarization branch after 22.8 km SMF; lower constellation: Y polarization branch)

4. RESULTS

Figure 3 shows the tested bit-error-rate (BER) curves for the two channels' RoF signals in both optical back-to-back and after 22.8 km single mode fiber transmission without any wireless through the air. Considering the

FEC limit at a BER of 2×10^{-3}, from the figure it can be seen that there is around 3 dB difference between X and Y polarization signals. This difference is attributed to the fact that the performances of the components used during the experiment, particularly the responsivity of the two photodiodes used in the two branches are different. Apart from the difference in the performance of components, we can see that the penalty between back-to-back and fiber transmission in both branches are less than 1 dB at the FEC limit. The reason for such small penalty is that at low bit rate the dispersion effect in the fiber is almost negligible. Moreover, it can also be seen from the inserts of figure 3 that the received constellations of optical signals after fiber transmission in X branch (upper) and Y branch (below) are both clear.

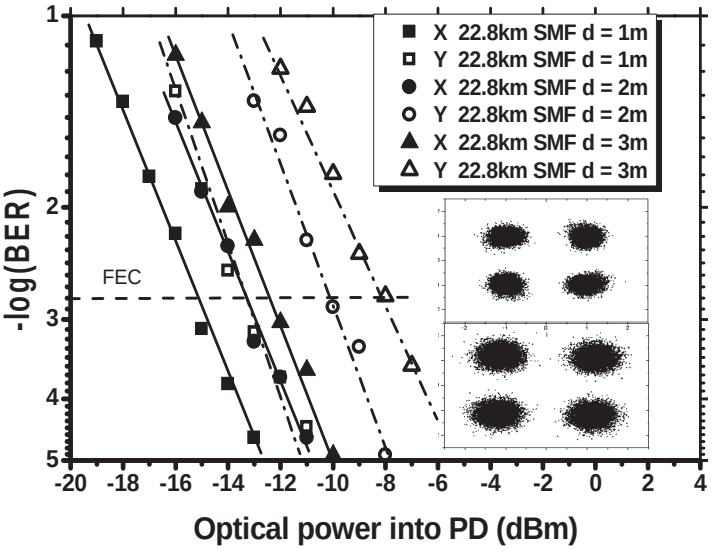

Figure 4. BER as a function of optical power at PD for different wireless distances (upper constellation: X branch at 1 m; lower constellation: Y branch at 1 m)

The BER curves as a function of the received optical power at the photodiode after 22.8 km fiber for different wireless transmission distances are shown in figure 4. From the figure we can see that both X and Y channels achieve up to 3 m wireless transmission with BER well below the FEC limit. Moreover, the power differences between the BER curves achieving FEC limit at 1 meter wireless and 2 meters wireless are smaller than the differences between 2 meters and 3 meters wireless, for both X and Y branches. We attribute this phenomena to the more accurate channel estimation when the crosstalk angle from reference angle becomes smaller, which exceeds the influence of the decreased received RF power. The constellations of received signals after 1 m wireless transmission for X and Y branches are also shown in the insert of figure 4. It can be seen that the clusters in the constellations are still clearly separated.

5. CONCLUSION

We propose an hybrid fiber-wireless system which seamlessly translate the optical PolMux OFDM signal into a wireless MIMO channel. The combination of the PolMux and MIMO technologies enables data transmission with a net spectral efficiency of 2.55 bit/s/Hz. Furthermore, a training-based scheme is digitally developed to estimate the polarization multiplexed MIMO transmission channel. A net data rate of 795.5 Mbps OFDM

signal transmission over 22.8 km SMF plus 3 m wireless distance is successfully demodulated at the receiver for demonstration purpose. This experimental result is believed to be the first step in our ultrahigh capacity fiber-wireless system research. Therefore, higher bit rate with larger bandwidth at higher frequency band together with more advanced modulation formats can be expected in our future works.

REFERENCES

[1] J. Wells, "Faster than fiber: the future of multi-Gb/s wireless," IEEE Microw. Mag, vol. 10, no. 3, pp. 104-112, 2009.

[2] Chow, C.W.; Yeh, C.H.; Wang, C.H.; Wu, C.L.; Chi, S.; Chinlon Lin; , "Studies of OFDM signal for broadband optical access networks," Selected Areas in Communications, IEEE Journal on , vol.28, no.6, pp.800-807, Aug. 2010

[3] Kumar, G.J.R.; Shaji, K.S.; , "Low complexity algorithm for channel estimation of UWB MIMO-OFDM wireless fading channels," Emerging Trends in Robotics and Communication Technologies (INTERACT), 2010 International Conference on , vol., no., pp.125-128, 3-5 Dec. 2010

[4] Alfiad, M.S.; Kuschnerov, M.; Jansen, S.L.; Wuth, T.; van den Borne, D.; de Waardt, H.; , "Transmission of 11 × 224-Gb/s POLMUX-RZ-16QAM over 1500 km of LongLine and pure-silica SMF," Optical Communication (ECOC), 2010 36th European Conference and Exhibition on , vol., no., pp.1-3, 19-23 Sept. 2010

[5] S.L. Jansen; I. Morita; T.C. Schenk; H. Tanaka, "Long-haul transmission of 16×52.5 Gbits/s polarization-division multiplexed OFDM enabled by MIMO processing", J. Opt. Netw., vol. 7, pp. 173-182, 2008.

[6] Cvijetic, N.; Prasad, N.; Dayou Qian; Ting Wang; , "Block-Diagonal MIMO Equalization for Polarization-Multiplexed OFDM Transmission With Direct Detection," Photonics Technology Letters, IEEE , vol.23, no.12, pp.792-794, June15, 2011

[7] Shu-Hao Fan; Hung-Chang Chien; Chowdhury, A.; Cheng Liu; Wei Jian; Yu-Ting Hsueh; Gee-Kung Chang; , "A novel radio-over-fiber system using the xy-MIMO wireless technique for enhanced radio spectral efficiency," Optical Communication (ECOC), 2010 36th European Conference and Exhibition on , vol., no., pp.1-3, 19-23 Sept. 2010

[8] Xiang Liu; F. Buchali, "A novel channel estimation method for PDM-OFDM enabling improved tolerance to WDM nonlinearity" *paper OWW5*, OFC/NFOEC'2009.

Paper 9: 2×2 MIMO-OFDM Gigabit Fiber-Wireless Access System Based on Polarization Division Multiplexed WDM-PON

L. Deng, X. Pang, Y. Zhao, M. B. Othman, J. Bevensee Jensen, D. Zibar, X. Yu, D. Liu, and I. Tafur Monroy, "2×2 MIMO-OFDM Gigabit fiber-wireless access system based on polarization division multiplexed WDM-PON," *Optics Express*. vol. 20, no. 4, pp. 4369-4375, 2012.

2x2 MIMO-OFDM Gigabit fiber-wireless access system based on polarization division multiplexed WDM-PON

Lei Deng,[1,2] Xiaodan Pang,[2] Ying Zhao,[3] M. B. Othman,[2] Jesper Bevensee Jensen,[2] Darko Zibar,[2] Xianbin Yu,[2,4] Deming Liu,[1,*] and Idelfonso Tafur Monroy[2,5]

[1]*College of Optoelectronics Science and Engineering, HuaZhong University of Science and Technology, Wuhan 430074, China*

[2]*DTU Fotonik, Department of Photonics Engineering, Technical University of Denmark, Kgs. Lyngby DK-2800, Denmark*

[3]*Department of Electronic Engineering, Tsinghua University, 10084, Beijing, China*

[4]*xiyu@fotonik.dtu.dk*

[5]*idtm@fotonik.dtu.dk*

[*]*dmliu@mail.hust.edu.cn*

Abstract: We propose a spectral efficient radio over wavelength division multiplexed passive optical network (WDM-PON) system by combining optical polarization division multiplexing (PDM) and wireless multiple input multiple output (MIMO) spatial multiplexing techniques. In our experiment, a training-based zero forcing (ZF) channel estimation algorithm is designed to compensate the polarization rotation and wireless multipath fading. A 797 Mb/s net data rate QPSK-OFDM signal with error free ($<1 \times 10^{-5}$) performance and a 1.59 Gb/s net data rate 16QAM-OFDM signal with BER performance of 1.2×10^{-2} are achieved after transmission of 22.8 km single mode fiber followed by 3 m and 1 m air distances, respectively.

OCIS codes: (060.0060) Fiber optics and optical communications; (060.2360) Fiber optics links and subsystems; (060.5625) Radio frequency photonics.

References and links

1. J. Zhang and G. de la Roche, *Femtocells: Technologies and Deployment* (Wiley, 2010), Chaps. 2, 4, 9.
2. M. Sauer, A. Kobyakov, and J. George, "Radio over fiber for picocellular network architectures," J. Lightwave Technol. **25**(11), 3301–3320 (2007).
3. K. Tsukamoto, T. Nishiumi, T. Yamagami, T. Higashino, S. Komaki, R. Kubo, T. Taniguchi, J.-I. Kani, N. Yoshimoto, H. Kimura, and K. Iwatsuki, "Convergence of WDM access and ubiquitous antenna architecture for broadband wireless services," PIERS Online **6**(4), 385–389 (2010).
4. S. Chen, Q. Yang, Y. Ma, and W. Shieh, "Real-time multi-gigabit receiver for coherent optical MIMO-OFDM signals," J. Lightwave Technol. **27**(16), 3699–3704 (2009).
5. A. Agmon, B. Schrenk, J. Prat, and M. Nazarathy, "Polarization beamforming PON doubling bidirectional throughput," J. Lightwave Technol. **28**(17), 2579–2585 (2010).
6. G. L. Stuber, J. R. Barry, S. W. Mclaughlin, Y. Li, M. A. Ingram, and T. G. Pratt, "Broadband MIMO-OFDM wireless communications," Proc. IEEE **92**(2), 271–294 (2004).
7. W. Shieh and I. Djordjevic, *OFDM for Optical Communications* (Springer, 2009), Chap. 2.
8. S. L. Jansen, I. Morita, T. C. Schenk, and H. Tanaka, "Long-haul transmission of 16x52.5 Gbits/s polarization-division multiplexed OFDM enabled by MIMO processing (Invited)," J. Opt. Netw. **7**(2), 173–182 (2008).
9. A. Kobyakov, M. Sauer, A. Ng'oma, and J. H. Winters, "Effect of optical loss and antenna separation in 2x2 MIMO fiber-radio systems," IEEE Trans. Antenn. Propag. **58**(1), 187–194 (2010).
10. M. B. Othman, L. Deng, X. Pang, J. Caminos, W. Kozuch, K. Prince, J. B. Jensen, and I. T. Monroy, "Directly-modulated VCSELs for 2x2 MIMO-OFDM radio over fiber in WDM-PON," in *37th European Conference and Exhibition on Optical Communication (ECOC)*, 2011 (2011), Paper We.10.P1.119.
11. M. B. Othman, L. Deng, X. Pang, J. Caminos, W. Kozuch, K. Prince, X. Yu, J. B. Jensen, and I. T. Monroy, "MIMO-OFDM WDM PON with DM-VCSEL for femtocells application," Opt. Express **19**(26), B537–B542 (2011).
12. S.-H. Fan, H.-C. Chien, A. Chowdhury, C. Liu, W. Jian, Y.-T. Hsueh, and G.-K. Chang, "A novel radio-over-fiber system using the xy-MIMO wireless technique for enhanced radio spectral efficiency," in *36th European Conference and Exhibition on Optical Communication (ECOC)*, 2010 (2010), Paper Th.9.B.1.

#160864 - $15.00 USD Received 4 Jan 2012; revised 30 Jan 2012; accepted 30 Jan 2012; published 7 Feb 2012

13. X. Liu and F. Buchali, "Intra-symbol frequency-domain averaging based channel estimation for coherent optical OFDM," Opt. Express **16**(26), 21944–21957 (2008).
14. X. Liu, S. Chandrasekhar, B. Zhu, P. J. Winzer, A. H. Gnauck, and D. W. Peckham, "448-Gb/s reduced-guard-interval CO-OFDM transmission over 2000km of ultra-large-area fiber and five 80-GHz-Grid ROADMs," J. Lightwave Technol. **29**(4), 483–490 (2011).

1. Introduction

Recently, known as 'home base station', femtocell network has been attracting more and more attentions due to its improved indoor coverage, increased capacity and reliable communication compared to macrocell network [1]. Radio-over-fiber (RoF) is considered as a promising candidate technology for femtocell networks because it allows for centralization of signal processing and network management, resulting in simple remote antenna unit (RAU) design and therefore low-cost implementation [2]. However, to meet the ever growing demand for high capacity wireless services like video-on-demand and video conferencing, it is highly desirable to develop new technologies for in-building femtocell networks. Wavelength division multiplexed passive optical network (WDM-PON) technology is therefore widely adopted to increase the capacity of RoF networks and the number of base stations serviced by a single central station [3], and the schematic scenario of in-home and in-building femtocell network is shown in Fig. 1. Moreover, to further increase the capacity per-wavelength of the femtocell network system, high spectral efficiency modulation and transmission technologies are highly desired. For instance, optical polarization division multiplexing (PDM) technology [4, 5] is regarded as an appealing solution by transmitting data in two orthogonal polarization modes within the same spectral range. Likewise, wireless multiple-input multiple-output (MIMO) technology is also a promising technology to exploit the spatial dimension by applying multiple antennas at both the transmitter and receiver sides [6].

Due to the inherent high chromatic dispersion tolerance in optical fibers and robustness against frequency selective fading or narrowband interference in wireless channels, orthogonal frequency division multiplexing (OFDM) has been widely used in current RoF systems [7]. Therefore, a RoF system combining OFDM with PDM and MIMO techniques can fulfill requirements of robustness, high flexibility and high spectral efficiency for providing broadband services in femtocell network. In addition, for multi-carrier systems like OFDM, a large computational complexity will be introduced by using the classical MIMO channel estimation method. In contrast, training-based channel estimation has the relatively low computational complexity at the receiver and draws more interests [8].

To date, some work has presented the concept of MIMO RoF system, but implemented separate fibers for each RAU [9]. A 397 Mb/s 16-quadrature amplitude modulation (QAM) OFDM-MIMO signal over WDM-PON system has been demonstrated in [10, 11] using different wavelengths instead of PDM technique for two transmitter antennas. 5 Gb/s PDM wireless MIMO transmission over 60 GHz wireless link has also been reported in [12], however, employing on-off keying (OOK) modulation. Moreover, some high speed PDM-OFDM transmission systems have been realized in [13, 14] without wireless transmission.

In this paper, we demonstrate a 2x2 MIMO-OFDM radio over WDM-PON system based on polarization division multiplexing and wireless MIMO techniques. The MIMO-OFDM training-based zero forcing (ZF) channel estimation algorithm is designed to compensate the optical polarization rotation and the wireless multipath fading. Furthermore, up to 1.59 Gb/s 16-QAM MIMO-OFDM fiber-wireless transmission over 1 m air distance and 22.8 km single mode fiber (SMF) are achieved for broadband wireless services around Gb/s. We also demonstrate the scalability of the proposed system under different signal to noise ratio (SNR), cross channel interference and wireless coverage by changing the wireless distance in our experiment.

#160864 - $15.00 USD Received 4 Jan 2012; revised 30 Jan 2012; accepted 30 Jan 2012; published 7 Feb 2012

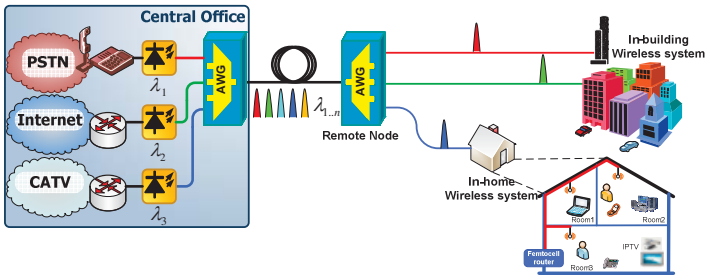

Fig. 1. The schematic scenario of in-home and in-building femtocell network system.

2. Training-based PDM-MIMO-OFDM composite channel estimation

Channel estimation is important for signal demodulation in MIMO system, in particular when a large number of subcarriers and advanced multiplexing technique are employed. In our PDM MIMO-OFDM system, the two orthogonal polarization modes which carry independent OFDM signal will experience a slow polarization rotation, which can be described as:

$$\begin{bmatrix} r_x \\ r_y \end{bmatrix} = H_F \begin{bmatrix} \cos\theta & \sin\theta \\ -\sin\theta & \cos\theta \end{bmatrix} \begin{bmatrix} t_x \\ t_y \end{bmatrix}, \tag{1}$$

where t_x and r_x are respectively transmitted and received X branch optical signals, so as t_y and r_y for Y branch signals. The symbol θ is the rotational angle. H_F represents the combined effect of fiber chromatic dispersion and polarization dependent loss. In our transmitter, after two photodetectors, two antennas are used to radiate two radio signals, respectively. The wireless channel response could be represented by a matrix H_{MIMO}. Notice that, the polarization rotation in fiber does not change so fast compared to the wireless channel, so it is not difficult to estimate the channel. The hybrid optical and wireless response for our MIMO-OFDM signal can be represented as Eq. (2), where n_x and n_y are the random noises, and h_{xx}, h_{xy}, h_{yx} and h_{yy} represent the elements in the combined channel response matrix.

$$\begin{bmatrix} r_x \\ r_y \end{bmatrix} = H_{MIMO} H_F \begin{bmatrix} \cos\theta & \sin\theta \\ -\sin\theta & \cos\theta \end{bmatrix} \begin{bmatrix} t_x \\ t_y \end{bmatrix} + \begin{bmatrix} n_x \\ n_y \end{bmatrix} = \begin{bmatrix} h_{xx} & h_{xy} \\ h_{yx} & h_{yy} \end{bmatrix} \begin{bmatrix} t_x \\ t_y \end{bmatrix} + \begin{bmatrix} n_x \\ n_y \end{bmatrix}. \tag{2}$$

In order to estimate this composite channel transfer matrix at the receiver, we transmit a pair of time-interleaved training sequences $T_X = [T_1, 0]^T$, $T_Y = [0, T_2]^T$ in the two tributaries. The received training sequences in two consecutive training durations can be expressed as:

$$\begin{bmatrix} RT_{x1} & RT_{x2} \\ RT_{y1} & RT_{y2} \end{bmatrix} = \begin{bmatrix} h_{xx} & h_{xy} \\ h_{yx} & h_{yy} \end{bmatrix} \begin{bmatrix} T_1 & 0 \\ 0 & T_2 \end{bmatrix} + \begin{bmatrix} n_{x1} & n_{x2} \\ n_{y1} & n_{y2} \end{bmatrix}, \tag{3}$$

where RT_{x1} and RT_{x2} stand for the received training symbol from X branch at the first and second training duration, respectively, so do RT_{y1} and RT_{y2} for the Y branch. And n_{x1}, n_{x2}, n_{y1} and n_{y2} are the random noises. The estimated channel transfer matrix then can be easily calculated as Eq. (4). From Eq. (4) we see that even with perfect channel estimation an error term will occur due to the random noises. More advanced algorithm such as minimum mean-squared-error (MMSE) algorithm could be used to improve the performance. However, in our experiment, zero forcing (ZF) instead of MMSE algorithm is used for channel estimation due to its lower computational complexity [4].

#160864 - $15.00 USD Received 4 Jan 2012; revised 30 Jan 2012; accepted 30 Jan 2012; published 7 Feb 2012

$$\begin{bmatrix} \tilde{h}_{xx} & \tilde{h}_{xy} \\ \tilde{h}_{yx} & \tilde{h}_{yy} \end{bmatrix} = \begin{bmatrix} RT_{x1}/T_1 & RT_{x2}/T_2 \\ RT_{y1}/T_1 & RT_{y2}/T_2 \end{bmatrix} = \begin{bmatrix} h_{xx} & h_{xy} \\ h_{yx} & h_{yy} \end{bmatrix} + \begin{bmatrix} n_{x1}/T_1 & n_{x2}/T_2 \\ n_{y1}/T_1 & n_{y2}/T_2 \end{bmatrix}. \quad (4)$$

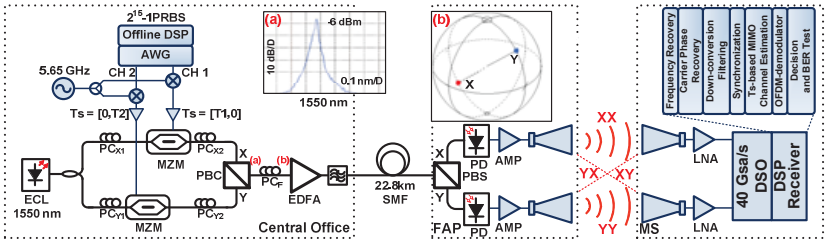

Fig. 2. Experimental setup for the proposed PDM MIMO-OFDM system.

3. Experimental setup

The experimental setup for a single wavelength channel of our proposed MIMO-OFDM signal over PDM WDM-PON system is shown in Fig. 2, for a demonstration purpose. At the central office (CO), a 1.25 GSa/s arbitrary waveform generator (AWG) is performed to generate two-channel baseband real-valued OFDM signals. For each channel, a data stream with a pseudo-random bit sequence (PRBS) length of 2^{15}-1 is mapped onto 129 subcarriers, of which 64 subcarriers carry real QPSK/16-QAM data and one is unfilled DC subcarrier. The remaining 64 subcarriers are the complex conjugate of the aforementioned 64 subcarriers to enforce Hermitian symmetry in the input facet of 256-point inverse fast Fourier transform (IFFT). The cyclic prefix is 1/10 of the IFFT length resulting in an OFDM symbol size of 281. To facilitate time synchronization and MIMO channel estimation, 3 training symbols are inserted at the beginning of each OFDM frame that contains 7 data symbols. Each channel has a net data rate of 398.5 Mb/s (1.25 GSa/s × 2 × 64/281 × 7/10) for QPSK case and 797.1 Mb/s for 16QAM case with a bandwidth of 629.8 MHz (1.25 GSa/s × 129/256). For simplicity, one frame delay is applied in one channel to decorrelate the two channel signals in the AWG. These two-channel OFDM signals are then separately up-converted to 5.65 GHz. The two RF OFDM signals are used to modulate a 100 kHz-linewidth continuous-wave (CW) external cavity laser (ECL, λ_1 = 1550 nm) at two Mach-Zehnder modulators (MZMs), respectively. A pair of polarization controllers (PCs), namely PC_{X1} and PC_{Y1} are used to optimize the response of the MZMs. PC_{X2} and PC_{Y2} are inserted at the MZMs outputs to align the optical OFDM signal in each channel to the X and Y axis of the following polarization beam combiner (PBC), which then combines the two orthogonal polarizations. Subsquently PC_F is introduced to roughly adjust the polarization of optical signal in the trunk fiber and set the variable power splitting ratio for equal SNR at each transmitter antenna. An erbium-doped fiber amplifer (EDFA) and an optical filter with 0.8 nm bandwidth are used to boost the optical OFDM signal and filter out the outband noise. The optical spectrum and the poincaré sphere of the combined optical signal are shown in the insets of Fig. 2. After excluding the overhead from cyclic prefix and training sequences, the output signal from the PBC is at a net data rate of 797 Mb/s with a spectral efficiency of 1.26 bits/s/Hz for QPSK case and 1.59 Gb/s with a spectral efficiency of 2.52 bits/s/Hz for 16-QAM case.

After 22.8 km of standard single mode fiber (SSMF) propagation, the optical OFDM signal is divided back to X and Y polarizations by a polarization beam splitter (PBS) at the femtocell access point (FAP). By using two 10 GHz bandwidth photodiode (PD), these two tributaries are converted into the RF signals, which are then fed into the FAP antennas after two RF amplifiers with 20 dB gain. After air transmission, these two wireless signals are detected by two receiver antennas and amplified by two 20 dB gain low-noise amplifiers

#160864 - $15.00 USD Received 4 Jan 2012; revised 30 Jan 2012; accepted 30 Jan 2012; published 7 Feb 2012

(LNAs) at the mobile station (MS) receiver. Subsequently, a 40 GSa/s digital sampling oscilloscope (DSO) with 13 GHz analog bandwidth is used to capture these two RF signals. Offline signal demodulation is then performed by a digital signal processing (DSP)-based receiver consisting of frequency and phase recovery, frequency down-conversion, training-based PDM MIMO-OFDM channel estimation, OFDM demodulation modules, data mapping and bit error rate (BER) tester. In our experiment, 80896 bits are calculated for BER test.

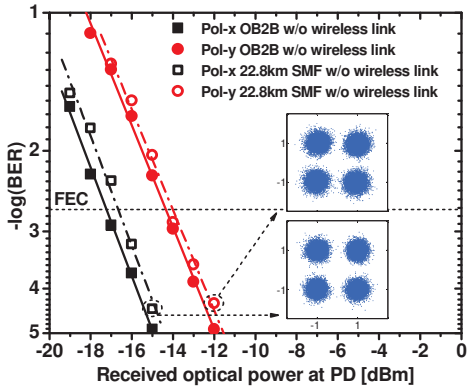

Fig. 3. Measured BER performance of Pol-x and Pol-y singal in optical B2B case and 22.8 km SMF fiber transmission case.

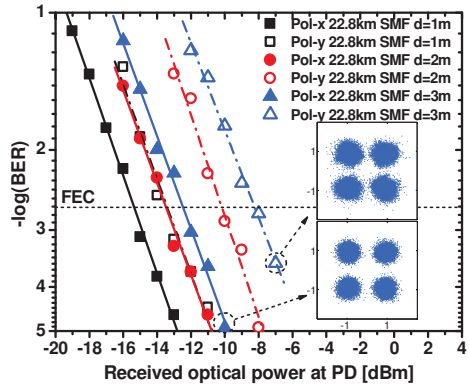

Fig. 4. Measured BER performance of PDM MIMO-OFDM signal wireless transmission with 22.8 km SMF fiber transmission.

4. Experimental results and discussions

Figure 3 shows the measured BER in terms of the receiver optical power into the PD in both optical back to back (OB2B) and 22.8 km SMF transmission cases without wireless link. In optical B2B case, we can observe that the receiver sensitivity at the forward-error correction (FEC) limit (BER of 2×10^{-3}) is achieved at −17.2 dBm and −14.3 dBm for the X polarization OFDM signal (Pol-x) and Y polarization OFDM signal (Pol-y), respectively. This 2.9 dB power penalty between Pol-x and Pol-y could be attributed to the different performances of optical and electrical components, particularly the responsivity of the two

#160864 - $15.00 USD Received 4 Jan 2012; revised 30 Jan 2012; accepted 30 Jan 2012; published 7 Feb 2012

photodiodes used in these two branches. Negligible power penalty (around 0.5 dB) is induced after 22.8 km SMF transmission by using training-based MIMO OFDM channel estimation algorithm. The received constellations of Pol-x and Pol-y signal after 22.8 km SMF transmission are shown in the insets of Fig. 3 as well.

Figure 4 presents the wireless transmission BER performance of QPSK-OFDM PDM-MIMO signal after 22.8 km SMF transmission. The separation spacing between the elements of the FAP and MS antenna arrays is fixed at 1 m in the experiment. The received sensitivity at the FEC limit is obtained at −15.2 dBm, −13.4 dBm and −12.5 dBm for the Pol-x signal over air transmission of 1 m, 2 m and 3 m, respectively. The higher required optical power at the FEC limit as air distance increases can be attributed to the increasing cross interference, severer multipath effect and lower SNR. We can also note that larger power penalty is induced between Pol-x and Pol-y for longer air distance. This could be explained by the misalignment between the transmitter and receiver antennas. The received constellations of Pol-x and Pol-y with 3 m air distance and 22.8 km SMF transmission are indicated in the insets of Fig. 4.

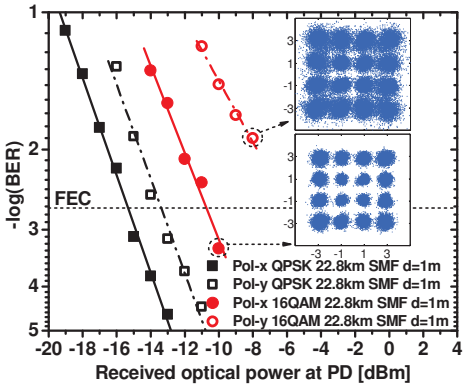

Fig. 5. Measured BER performance of 797 Mb/s QPSK MIMO-OFDM and 1.59 Gb/s 16-QAM MIMO-OFDM signal over 1 m air distance and 22.8 km SMF transmission.

We also test the performance of 1.59 Gb/s 16-QAM MIMO-OFDM signal over 1 m air distance and 22.8 km SMF transmission, as depicted in Fig. 5. We can see that the receiver sensitivity of 16-QAM MIMO-OFDM Pol-x signal to reach the FEC limit is −10.7 dBm. 4.5 dB power penalty compared to QPSK MIMO-OFDM Pol-x wireless transmission can be explained that the constellations states of higher-level modulation format are closer than QPSK, resulting in higher SNR requirement for the same performance. The received constellations of 16-QAM MIMO-OFDM signal are shown in the insets of Fig. 5. The constellation symbols at the higher amplitude are dispersed widely compared to the center ones. This is expected, since OFDM signal is sensitive to the nonlinearity of fiber and wireless transmission due to its high peak-to-average-power-ratio (PAPR). However, we can get BER of 5.01×10^{-4} and 1.28×10^{-2} for 16-QAM MIMO-OFDM Pol-x and Pol-y signal after 1 m air distance and 22.8 km SMF transmission, respectively.

5. Conclusion

We have presented a spectral efficient and WDM-PON compatible MIMO-OFDM access system by combining optical polarization division multiplexing (PDM) and wireless multiple input multiple output (MIMO) spatial multiplexing techniques. Moreover, a training-based zero forcing (ZF) scheme is digitally developed to estimate the polarization multiplexed MIMO transmission channel. A 797 Mb/s net data rate QPSK-OFDM signal and a 1.59 Gb/s

#160864 - $15.00 USD Received 4 Jan 2012; revised 30 Jan 2012; accepted 30 Jan 2012; published 7 Feb 2012

net data rate 16 QAM-OFDM signal at 5.65 GHz RF carrier frequency are transmitted over 3 m and 1 m air distance with 22.8 km single mode fiber, respectively. This system has potential application in future in-door femtocell network supporting Gb/s broadband wireless service.

Acknowledgments

We would like to acknowledge the support of the Chinese Scholarship Council (CSC), National "863" Program of China (No. 2009AA01A347) and National Science and Technology Major Project of the Ministry of Science and Technology of China (No. 2010ZX03007-002-02).

#160864 - $15.00 USD Received 4 Jan 2012; revised 30 Jan 2012; accepted 30 Jan 2012; published 7 Feb 2012

Paper 10: A Spectral Efficient PoIMux-QPSK-RoF System with CMA-Based Blind Estimation of a 2×2 MIMO Wireless Channel

X. Pang, Y. Zhao, L. Deng, M. B. Othman, X. Yu, J. Bevensee Jensen, and I. Tafur Monroy, "A Spectral Efficient PoIMux-QPSK-RoF System with CMA-Based Blind Estimation of a 2×2 MIMO Wireless Channel," in *IEEE Photonics Conference, (IPO)*, paper TuM2, pp. 296–297, 2011.

TuM2 (Contributed Oral)
11:15 AM – 11:30 AM

A Spectral Efficient PolMux-QPSK-RoF System with CMA-Based Blind Estimation of a 2×2 MIMO Wireless Channel

Xiaodan Pang*, Ying Zhao†, Lei Deng‡, , M. B. Othman*, Xianbin Yu*, Jesper B. Jensen*, I. T. Monroy*
*Department of Photonics Engineering, Technical University of Denmark, DK-2800, Kgs.Lyngby, Denmark
Email: xipa@fotonik.dtu.dk
†Department of Electronic Engineering, Tsinghua University, 10084, Beijing, China
‡School of Optoelectronics Science and Engineering, HuaZhong University of Science and Technology, Wuhan, China

***Abstract*—We experimentally demonstrated a polarization multiplexed (PolMux) RoF system with a 2×2 MIMO wireless link using constant modulus algorithm (CMA) channel estimation. 4 bit/s/Hz spectral efficiency and CMA-enabled 2 dB receiver sensitivity improvement were achieved.**

I. Introduction

Radio-over-fiber (RoF) technology provides a good solution to increase the coverage while maintaining the mobility of the broadband services in the local area network scenario. However, there are challenges when turning this technology into practice, including spectral efficiency, wavelength reuse, wireless channel capacity and components cost [1]. Polarization multiplexing (PolMux) is a promising technique to double the spectral efficiency by transmitting data in two orthogonal polarization modes within the same spectral range. [2]. Furthermore, wireless multiple-input multiple-output (MIMO) technique provides the possibility for bandwidth-limited systems to increase their channel capacity through spatial multiplexing [3]. For the wireless MIMO systems, channel estimation is essential for signal demodulation. Work has been done either using fixed antenna distances [4] or using training-based channel estimation [5]. However, strict synchronizations are required in these methods. In contrast, constant modulus algorithm (CMA) based equalizer is able to make blind estimation when transmitting constant envelope signals, e.g. QPSK [6]. Meanwhile, CMA could also treat the polarization rotation in the fiber together with the wireless crosstalk when combining the PolMux RoF system with MIMO technique.

In this paper we experimentally demonstrate a PolMux-RoF system with a 2×2 MIMO wireless link. By using both PolMux and wireless MIMO, 5 Gbps QPSK signal at 5.4 GHz carrier radio frequency (RF) with spectral efficiency of 4 bit/s/Hz is successfully transmitted through a 10 km SMF plus up to 2 m wireless link. This is the highest wireless capacity reported at this carrier frequency to the best of our knowledge.

II. Experimental Setup

The experimental setup for our PolMux-MIMO system is shown in Fig. 1. Two 1.25 Gbps pseudorandom bit sequences (PRBS) with a bit length of $2^{15} - 1$ are generated from a pattern generator. These two data sequences are combined and modulated as in-phase and quadrature components at a vector signal generator (VSG) to generate a 2.5 Gbps electrical QPSK signal with 5.4 GHz carrier frequency. The signal is directly modulated on to the lightwave by using a vertical-cavity surface-emitting laser (VCSEL) at central wavelength 1550 nm. After a 3 dB power divider and by adding a delay in one branch, the signals at the two branches become uncorrelated, representing two independent RoF QPSK signals. The two signals are polarization multiplexed at a polarization beam combiner (PBC). The combined PolMux QPSK RoF signal with data rate of 5 Gbps is amplified by a booster Erbium-doped fiber amplifier (EDFA)and transmitted over a 10 km single mode fiber (SMF).

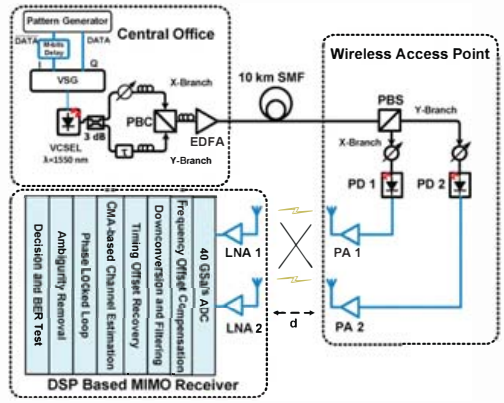

Fig. 1. Experimental set-up (VSG: Vector signal generator; PBC/PBS: Polarization beam combiner/splitter; PA: Power amplifier; LNA: Low-noise amplifier)

At the wireless access point (WAP), the received signal is aligned to a polarization beam splitter (PBS), which divides the PolMux signal back to X and Y polarization. The RF signals are then recovered by two photodiodes (PD) and fed to two transmitter antennas. The two pairs of transmitter and receiver antennas formed a 2×2 wireless MIMO system. The

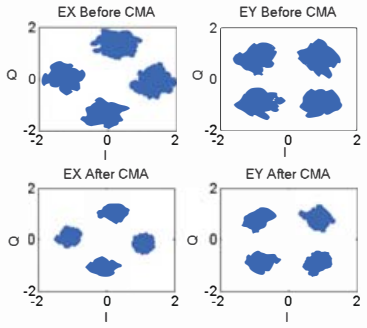

Fig. 2. Received signals' constellations of X and Y branches before (upper) and after (lower) CMA equalization)

separation between the two transmitter antennas is set to 1 meter, so as the separation between the receiver antennas. The two signals received by the receiver antennas are sampled by a 40 GSa/s digital anology converter (ADC) and demodulated by a digital signal processing (DSP) based MIMO receiver.

III. Results

CMA equalizer, which has two input signals with crosstalk from each other, can lock each one component of the equalizer outputs on to each input. Therefore after equalization the crosstalk can be reduced or eliminated. The performance improvement is studied by comparing the received signal quality before and after the CMA processing. As shown in Fig. 2, after back-to-back (B2B) optical PolMux plus 1 m wireless MIMO transmission, the received signals' constellations disseminated due to polarization rotation in optical links and the wireless crosstalk from neighboring transmitter antennas. In contrast, after the optimized CMA equalization, the constellations became much smoother and more compact.

Fig. 3 (a) shows the bit-error rate (BER) as a function of received optical power by the PDs in optical B2B and after 10 km SMF, both with 1 m wireless distance between the transmitting and receiving antennas. Due to the slightly different responsivity of two PDs, the performances have around 0.5 dB penalty between the X and Y branches. Meanwhile, we can observe that there are around 2 dB penalties between 10 km SMF transmission and optical B2B. BER curves for different wireless distances (1 m, 2 m and 3 m) after fiber transmission are shown in Fig. 3 (b). In this figure the BER are calculated for the total 5 Gbps QPSK signals transmitted in both channels. It indicates that there is only 1 dB penalty between 1 m and 1.5 m wireless transmission, while 3 dB when the distance goes up to 2 m, This is because as the attenuation in the air becomes larger, the SNR at the receiver goes lower, so that the system turn to noise-limited,where CMA has limited equalization capability. Considering the FEC limit at a BER of 2×10^{-3}, it is clearly shown that in all measured distances we are able to achieve transmissions with BER well below this limit.

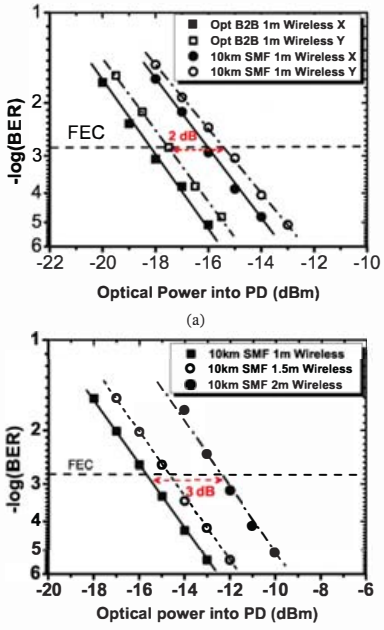

Fig. 3. (a) BER as a function of optical power into PD for optical B2B and 10 km SMF transmission, both with 1 m wireless MIMO; (b) BER curves for different wireless distances after 10 km SMF transmission

IV. Conclusion

We experimentally demonstrated a VCSEL-based RoF system by combining PolMux and wireless MIMO techniques to increase the spectral efficiency. A CMA-based digital equalizer was proposed to implement blind estimation of a wireless MIMO channel. In the experiment, a 2 m wireless and 10 km SMF transmission of 5.4 GHz QPSK with data rate up to 5 Gbps, and hence 4 bit/s/Hz spectral efficiency was successfully achieved. The performance improvement by the CMA equalizer in its supportable wireless distance makes our spectral efficient MIMO system an attractive solution for providing short range wireless services.

References

[1] L. Christina et al., *paper OWP5*, OFC/NFOEC'2009.
[2] A. Sano et al., "Ultra-High Capacity WDM Transmission Using Spectrally-Efficient PDM 16-QAM Modulation and C- and Extended L-Band Wideband Optical Amplification", J. of Lightw. Tech., vol. 29, no.4, pp.578-586, Feb.15, 2011.
[3] M. A. Jensen; J.W. Wallace, "A review of antennas and propagation for MIMO wireless communications", IEEE Trans. on Antennas and Propagation, vol.52, no.11, pp.2810- 2824, Nov. 2004.
[4] Shu-Hao Fan et al., *paper Th.9.B.1*, ECOC 2010.
[5] T.H. Chang; Wei-Cheng Chiang; Y.-W.P. Hong; Chong-Yung Chi, "Training Sequence Design for Discriminatory Channel Estimation in Wireless MIMO Systems", IEEE Transactions on Signal Processing , vol.58, no.12, pp.6223-6237, Dec. 2010.
[6] P. Johannisson et al., *paper Th.9.A.3* ECOC 2010

Paper 11: Experimental Demonstration of 5-Gb/s Polarization-Multiplexed Fiber-Wireless MIMO Systems

Y. Zhao, X. Pang, L. Deng, M. B. Othman, X. Yu, X. Zheng, H. Zhang and I. Tafur Monroy, "Experimental Demonstration of 5-Gb/s Polarization-Multiplexed Fiber-Wireless MIMO Systems," in *International Topical Meeting on & Microwave Photonics Conference (MWP/APMP)*, pp. 13–16, 2011.

Experimental Demonstration of 5-Gb/s Polarization-Multiplexed Fiber-Wireless MIMO Systems

Ying Zhao [†1, 2], Xiaodan Pang [2], Lei Deng [2, 3], Maisara B. Othman [2], Xianbin Yu [‡2], Xiaoping Zheng [††1], Hanyi Zhang [1] and Idelfonso T. Monroy [2]

[1]Department of Electronic Engineering, Tsinghua National Laboratory for Information Science and Technology, Tsinghua University, 100084 Beijing, China. E-mail: [†]yinzh@fotonik.dtu.dk, [††]xpzheng@mail.tsinghua.edu.cn.

[2]DTU Fotonik, Technical University of Denmark, DK-2800, Kgs. Lyngby, Denmark. E-mail: [‡]xiyu@fotonik.dtu.dk.

[3]School of Optoelectronics Science & Engineering, HuaZhong University of Science & Technology, Wuhan, China.

***Abstract*—We experimentally demonstrate a 5-Gb/s fiber-wireless transmission system combining optical polarization-division-multiplexing (PDM) and wireless multiple-input, multiple-output (MIMO) spatial multiplexing technologies. The optical-wireless channel throughput is enhanced by achieving a 4b/s/Hz spectral efficiency. Based on the implementation of constant modulus algorithm (CMA), the 2×2 MIMO wireless channel is characterized and adaptively equalized for signal demodulation. The performance of the CMA-based channel adaptation is studied and it is revealed that the algorithm is particularly advantageous to the MIMO wireless system due to the inter-channel delay insensitivity. The hybrid transmission performance of 26km fiber and up to 2m wireless MIMO is investigated.**

Keywords—constant modulus algorithm (CMA); fiber-wireless access; multiple input multiple output (MIMO); polarization-division-multiplexing (PDM).

I. INTRODUCTION

Scaling wireless channel capacity is important to accommodate the continuing increase in multi-services demand of wireless access systems, and is currently an area of intense research. Multiple-input multiple-output (MIMO) systems have been actively investigated [1] and successfully deployed for current broadband wireless applications such as mobile WiMAX [2]. On the other hand, Radio-over-Fiber (RoF) technology provides elegant solutions for even higher bandwidth requirements beyond ~Gb/s thanks to the ultra-wide bandwidth and agility characteristics of photonic devices [3]. To further increase transmission capacity per-wavelength of a fiber-wireless system, polarization-division-multiplexing (PDM) is a promising technique since it offers higher spectral efficiency and transmitter uniformity. Therefore the convergence of multiple antenna and PDM-RoF technologies can be greatly advantageous to emerging high speed telecommunication systems with advantages of high spectral efficiency, flexible transmitter/receiver reconfigurability and efficient wireless channel adaptability [4].

In a PDM-MIMO transmission system, two independent radio signals are carried by two orthogonal polarizations and then sent to an N×N antenna array. The wireless channel capacity can be increased by the factor of N without additional transmitting power or spectral resources. The key issue for a MIMO system is to adaptively demodulate the received spatial-correlated radio signals in the case of various resolvable and irresolvable wireless paths interfering each other. In general, the synthesized channel can be estimated by using preamble or training symbols known to both transmitter and receiver [5,6], which develops many numerical techniques to perform channel estimation. However, it often needs a large number of overhead symbols to extract the channel response, resulting in the decrease of the net data rate in the system. Furthermore, to obtain preamble or training symbols in the receiver, precise synchronization or timing recovery is essentially necessary [7,8] since preamble-based approaches are all decision-directed. Considering most of synchronization algorithms cannot give a satisfying performance while spatial-correlation exists in the MIMO case [9], blind channel estimation without resorting to the preamble or training symbols can be very practically promising for MIMO signal demodulation in reality.

The research on hybrid RoF and MIMO systems is still at an early stage with so far limited work on system implementation. Recently, training symbol based MIMO channel estimation with on-off keying (OOK) modulation is reported [10] and a multi-services PDM-RoF system is also demonstrated [4]. The potential of integrating PDM-RoF and MIMO on the system level, in terms of modulation formats, radio frequency (RF) efficiency and algorithm adaptability of channel estimation, remains unexplored.

In this paper, we present and experimentally demonstrate a PDM-RoF system with 1.25Gbaud/s QPSK sequence on each polarization state and followed by a 2×2 MIMO wireless link. At the receiver end, to demodulate the spatial-correlated signals, blind lattice filter adaptation based on constant modulus algorithm (CMA) is implemented in the digital domain. The performance of CMA-based channel estimation is studied and it is validated that MIMO signal demodulation is beneficial from the blind estimation algorithm by avoiding strict channel delay calibration and digital timing recovery. The bit-error-rate (BER) performances of the optical and wireless links are evaluated for the 5-Gb/s QPSK signal at 5.4GHz RF carrier over a 26km single mode fiber (SMF) plus 2m wireless link transmission. The net spectral efficiency of the system is 4b/s/Hz, which is the highest wireless capacity reported at this carrier frequency, to the best of our knowledge.

978-1-61284-718-4/11/$26.00 ©2011 IEEE

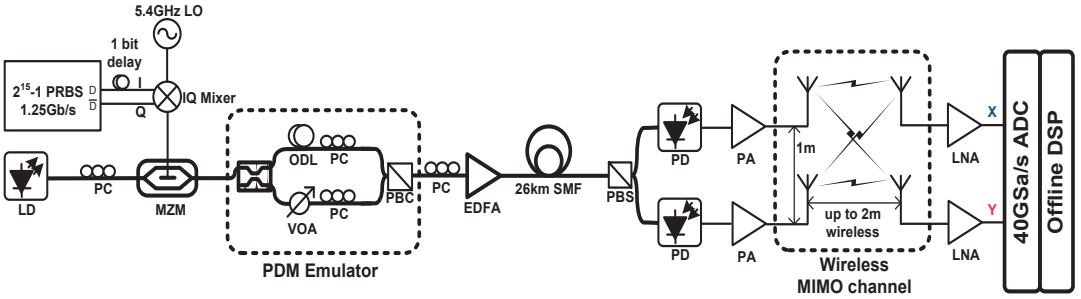

Figure 1. Configuration schematic of the PDM-RoF-MIMO system. LD: laser diode. PC: polarization controller. MZM: Mach-Zehnder modulator. ODL: optical delay line. VOA: variable optical attenuator. PBS: polarization beam splitter. SMF: single mode fiber. PD: photodiode. PA: power amplifier. LNA: low noise amplifier.

II. EXPERIMENT

Fig.1 shows the experimental setup of the PDM-RoF-MIMO system. Two polarization-reversed data streams of 1.25-Gb/s binary pseudo-random bit sequence (PRBS) with a length 2^{15}-1 are generated. The peak-to-peak voltage of the binary signals is approximately 0.8V with minimal waveform overshoots. With 1-bit decorrelation delay introduced to one of the streams, the binary data is mixed with a 5.4GHz local oscillator in an IQ modulator, forming a 2.5-Gb/s QPSK stream. The upconverted signal then is modulated onto an optical carrier at 1549.3nm at a Mach-Zehnder modulator (MZM). The optical signal is launched into a PDM emulator, in which the optical signal is split into two equal copies, which then are aligned with two orthogonal polarizations and combined by a polarization beam combiner (PBC) to form a PDM-RoF signal with a data rate of 5-Gb/s. In the PDM emulator, the two signals are arbitrarily delayed with respect to each other by an optical delay line to decorrelate two optical copies. The polarization state of the output signal from the PDM emulator is controlled by a primary polarization controller (PC) to roughly adjust the polarization in the transmission fiber. A booster EDFA with a gain of ~20dB is cascaded, and then the PDM-RoF QPSK signal is transmitted over a 26km single mode fiber (SMF). At the receiver end, the PDM signal is split into two streams onto two orthogonal polarizations (X and Y), which are detected and amplified by two photodiodes (PDs) and two power amplifiers (PAs) forming the RF inputs of the wireless MIMO channel. Both of the output radio power after the PAs are measured as +5dBm.

The wireless channel consists of two identical transmitting antennas and two identical receiving antennas separated by up to 2m wireless distance. Two transmitting antennas with 4.4dBi directional gains are separated by 1m height, so as two uni-directional receiving antennas. The link losses of straight channel and cross channel are 20dB and 27dB, respectively, so that a ~7dBc lower cross interference is added to the original signal in each receiving antenna.

After undergoing a wireless MIMO channel, the received signals are simultaneously amplified by a low noise amplifier (LNA) and then asynchronously digitized at 40GSa/s using a commercial real-time oscilloscope, with 12-bit analog-to-digital converter (ADC) resolution. All results in the receiver side are based on offline processing of at least 2 million

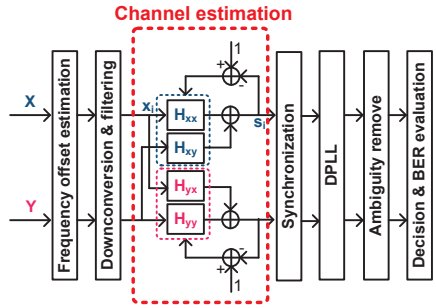

Figure 2. Block diagram of the digital signal processing used in the MIMO signal receiver.

samples on each of the two streams, corresponding to more than 125000 received symbols (250000 bits) for bit-error estimation after digital signal processing. As shown in Fig.2, the two sample streams from the ADC are sent to a digital MIMO demodulator for spatial-correlated channel estimation. The first step is a standard implementation of a RF frequency locking based on a non-decision-directed feed forward algorithm in the frequency domain [11]. After frequency estimation, digital local oscillator operating at the estimated frequency is mixed with two streams and lowpass filtering is performed. The filter shape has noticeable impact on the performance of the receiver; Hamming window and Gaussian filters are used in the experiment. The signals are then down-sampled to a synchronous 1.25G-Sa/s to perform adaptive MIMO channel estimation. The structure of estimator is based on a lattice filter with transfer functions H_{xx}, H_{xy}, H_{yx} and H_{yy} shown in Fig.2, which represents the inverse spatial-correlated matrix of the MIMO channel. Each filter block is implemented in the time domain as a finite impulse response (FIR) filter with optimized number of taps. To realize a preamble-free and channel delay independent estimator, we use the well-proven CMA to perform *blind* filter adaption [12]. CMA is a simple, robust channel estimation algorithm working independent on training sequence or data decision. In essence, the CMA minimizes the time averaged error

$$\varepsilon_{CMA} = \overline{1 - |s_i|^2} \qquad (1)$$

implying the mean distance of equalized symbols s_i from the

constant unit circle in the complex plane. The filter coefficients are adapted according to the algorithm iterations to minimize ε_{CMA}. In our experiment, CMA adaptation works particularly well for spatial-correlated signals with QPSK modulation format. The performance of the algorithm is discussed in section III. After CMA adaptation, the decorrelated output signals are corresponding to two polarizations; the channel impact can be canceled in the blind channel estimator. Subsequently, the symbol timing recovery is achieved by using a cross-correlation based synchronization algorithm. To correct random phase angle rotation of QPSK constellation with respect to the rectilinear desired decision boundaries, a decision-directed digital phase locking loop (DPLL) is implemented on a block of 1000 symbols. In the following, the BER is obtained by direct error counting of 250000bits.

III. Results and Discussion

Fig.3 shows the constellations of the recovered 5-Gb/s PDM-RoF signals in both x and y polarizations (x-pol and y-pol) after 1m wireless MIMO transmission at -11dBm optical power. Without CMA channel estimation, the error vector magnitude (EVM) of constellation clusters are ~30%, which means the QPSK symbols disseminate in a relatively large area due to the cross channel interference. The performance cannot be improved by increasing the transmitting power since the co-increasing interference plays a main role degrading the performance rather than additive noise. Due to the fast time-variant characteristics of the wireless channel, the added interferences fluctuate significantly during the measurement, which results in a requirement of a relatively faster coverage time with respect to the channel fluctuation. The separation between transmitting antennas and receiving antennas also affects the interference level, which shows a closer separation induces lower interference or spatial correlation, vice versa. The small random clusters appearing in the constellation are caused by wireless multipath effect, which corresponds to the various irresolvable paths during the wireless transmission. In the meantime, the digital filter selection also has noticeable effect on the constellation performance. After CMA channel estimation, as shown in the lower row in Fig.3, the constellation clusters dramatically concentrate to smaller clusters. The EVM is ~15% in this case. The multipath effect plays a main role on cluster dissemination and CMA parameters also determine the convergence performance. From Fig.3, it is also shown that the x-pol signal has a slightly better transmission performance than that of y-pol due to the non-identical characteristics between two polarizations.

Another issue noticeable is the necessity of the primary PC in the transmitter. The objective of this PC is to roughly align the two polarizations after fiber transmission with the axis of the PBS in the optical receiver; therefore the polarization dependent channel interference is insignificant. If the primary PC is removed, with the polarization rotating in the fiber, the interference characteristics vary dramatically and consequently, the channel estimation cannot give an identical performance using same parameters. To keep the performance

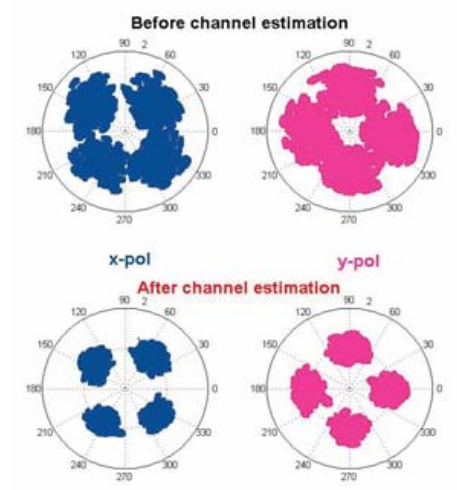

Figure 3. Constellations of the recovered 5-Gb/s x (left column) and y (right column) PDM-RoF signals after 1m wireless MIMO transmission without (upper) and with (lower) CMA channel estimation. 125000 symbols.

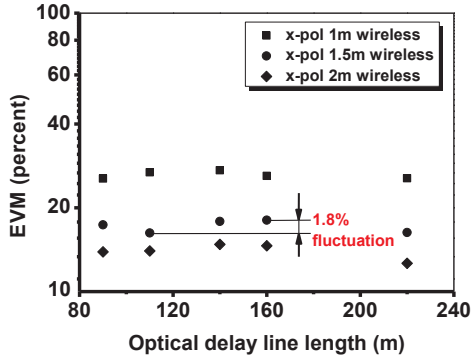

Figure 4. Measured EVM of the demodulated x-polarization QPSK signal versus optical delay between two polarizations with different wireless distances.

of channel estimation stable, the primary PC is preferably kept functional.

Apart from the advantage of non-resorting to preamble or training sequence, the other most significant advantage of using blind CMA adaptation in a MIMO system is it performs consistently with arbitrary change of channel delay. Fig.4 shows the measured EVM of demodulated QPSK signal in the x-polarization against the changing optical delay between two polarizations in the PDM emulator with different wireless transmission distances. A maximal 1.8% EVM fluctuation indicates the algorithm has a constant performance no matter how much delay is introduced in the optical or the wireless links. This property is not possessed by any decision-directed algorithms [8,11].

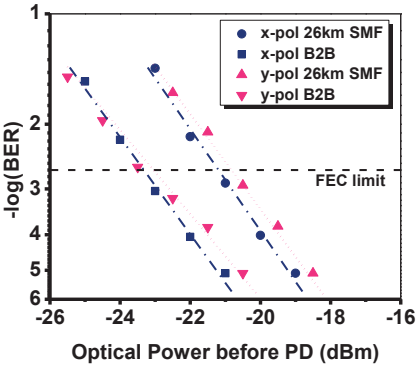

Figure 5. BER performance versus optical power before PD for PDM-RoF signal with 1m wireless MIMO transmission.

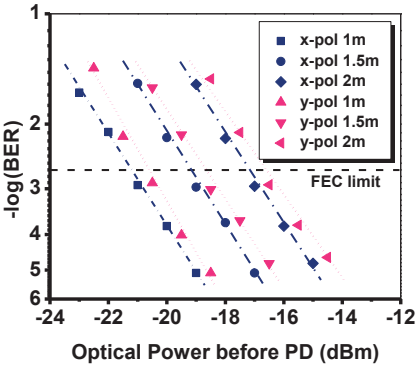

Figure 6. BER performance versus optical power before PD for different wireless transmission distances.

Fig. 5 shows the BER performance as a function of received optical power before the PD in optical B2B and after 26 km SMF and 1m wireless MIMO transmission. The non-identical channel induced performance difference between the x-pol and y-pol branches is ~0.5 dB. 2dB power penalty arisen from fiber dispersion is also observed after 26 km SMF transmission with respect to the B2B case. BER curves for wireless distances of 1m, 1.5m and 2m after 26km fiber transmission are shown in Fig. 6. It indicates ~2dB power penalty between 1m and 1.5m wireless transmission and another ~2dB penalty when the distance goes up to 2m. These penalties are contributed by the increasing cross interference, severer multipath effect and lower signal-to-noise ratio (SNR). Considering the FEC limit at a BER of 2×10^{-3}, it is clearly shown that in all measured distances we are able to achieve transmissions with BER well below this limit. Another issue noticeable is that when received power goes lower, the transmission system turns to noise-limited, where the CMA adaptation has limited equalization capability. So the transmission performance suffers higher degradation with low SNR.

IV. Conclusion

We have presented and demonstrated the first blind MIMO channel estimation of a PDM-RoF signal at 5-Gb/s. The receiver setup as well as the underlying CMA channel adaptation is described in detail and the algorithm performance is analyzed based on the measured results. The blind algorithm shows an advantage of channel delay insensitivity, which significantly decreases the system complexity. We enlarged the channel throughput at 5.4GHz RF band by achieving a spectral efficiency of 4b/s/Hz both in optical and wireless links with PDM and MIMO techniques. Error free PDM-RoF signal over 26km fiber and 1m wireless transmission yields a required received power of -18dBm and 2dB power penalty is observed with respect to B2B case. An up to 2m wireless MIMO transmission performance is studied showing a required received optical power of -14dBm. The results show an increased applicability of highly spectral efficient fiber-wireless systems.

Acknowledgement

This work was supported in part by National Nature Science Foundation of China (NSFC) under grant No. 60736003, 61025004, 61032005 and National 863 Program under grant No. 2009AA01Z222, 2009AA01Z223.

References

[1] A. J. Paulraj, D. A. Gore, R. U. Nabar, and H. Bolcskei, “An overview of MIMO communications - a key to gigabit wireless,” Proc. IEEE, vol. 92, pp. 198–218, Feb. 2004.

[2] W. Fan, A. Ghosh, C. Sankaran, P. Fleming, F. Hsieh, and S. Benes, “Mobile WiMAX systems: performance and evolution,” IEEE Commun. Mag., vol. 46, pp. 41–49, Oct. 2008.

[3] J. Yao, “Microwave photonics,” IEEE J. Lightw. Technol., vol. 27, pp. 314–335, Feb. 2009.

[4] J. Perez, M. Morant, R. Llorente, and J. Marti, “Joint distribution of polarization-multiplexed UWB and WiMAX radio in PON,” IEEE J. Lightw. Technol., vol. 27, pp. 1912–1919, Feb. 2009.

[5] S. L. Jansen, I. Morita, T. C. Schenk, and H. Tanaka, “Long-haul transmission of 16×52.5Gbits/s polarization-division-multiplexed OFDM enabled by MIMO processing,” J. Opt. Netw., vol. 7, pp. 173–182, Feb. 2008.

[6] Y. Han, and G. Li, “Coherent optical communication using polarization multiple-input-multiple-output,” Opt. Expr., vol. 13, pp. 7527–7534, Sep. 2005.

[7] W. Shieh, H. Bao, and Y. Tang, “Coherent optical OFDM: theory and design,” Opt. Expr., vol. 16, pp. 841–859, Jan. 2008.

[8] Y. S. Cho, J. Kim, W. Y. Yang, and C. G. Kang, MIMO-OFDM wireless communications with MATLAB. John Wiley & Sons (Asia), Singapore, 2010.

[9] C. J. Youn, X. Liu, S. Chandrasekhar, Y. Kwon, J. Kim, J. Choe, K. Choi, and E. S. Nam, “An efficient and frequency-offset-tolerant channel estimation and synchronization method for PDM CO-OFDM Transmission,” Proc. ECOC’2010, P4.06, Sep. 2010.

[10] S. Fan, H. Chien, A. Chowdhury, C. Liu, W. Jian, Y. Hsueh, and G. Chang, “A novel Radio-over-Fiber system using the xy-MIMO wireless technique for enhanced radio spectral efficiency,” Proc. ECOC’2010, Th.9.B.1, Sep. 2010.

[11] H. Meyr, M. Moeneclaey, and S. Fechtel, Digital communication receivers: synchronization, channel estimation, and signal processing. John Wiley & Sons (NY), USA, 1997.

[12] C. R. Johnson, P. Schniter, T. J. Endres, J. D. Behm, D. R. Brown, and R. A. Casas, “Blind equalization using the constant modulus criterion: A review,” Proc. IEEE, vol. 86, pp. 1927–1950, Oct. 1998.

Bibliography

[1] J.-i. Kani, F. Bourgart, A. Cui, A. Rafel, M. Campbell, R. Davey, and S. Rodrigues, "Next-Generation PON—Part I: Technology Roadmap and General Requirements," *IEEE Commun. Mag.*, vol. 47, no. 11, pp. 43–49, Nov. 2009.

[2] P. Chanclou, Z. Belfqih, B. Charbonnier, T. Duong, F. Frank, N. Genay, M. Huchard, P. Guignard, L. Guillo, B. Landousies, A. Pizzinat, H. Ramanitra, F. Saliou, S. Durel, P. Urvoas, M. Ouzzif, J. Le Masson, "Access network evolution: optical fibre to the subscribers and impact on the metropolitan and homenetworks," *Comptes Rendus Physique*, vol. 9, Issues 9–10, no. 9-10, pp. 935—946, 2008.

[3] ACMA Report, *Developments in next generation applications and services*, Australian Communications and Media Authority, Nov 2011.

[4] L. Kazovsky, W.-T. Shaw, D. Gutierrez, N. Cheng, and S.-W. Wong, "Next-generation optical access networks," *J. Lightw. Technol.*, vol. 25, no. 11, pp. 3428–3442, Nov. 2007.

[5] R. Gaudino, D. Cardenas, M. Bellec, B. Charbonnier, N. Evanno, P. Guignard, S. Meyer, A. Pizzinat, I. Mollers, and D. Jager, "Perspective in next-generation home networks: Toward optical solutions?," *IEEE Commun. Mag.*, vol. 48, no. 2, pp. 39 –47, feb. 2010.

[6] T. Tokle,M. Serbay, J.B. Jensen, W. Rosenkranz, and P. Jeppesen, "Advanced Modulation Formats for Transmission Systems," in *Optical Fiber Communication/National Fiber Optic Engineers Conference (OFC)*,OMI1, 2008.

[7] J.B. Jensen.,*Multilevel Modulation Formats for Optical Communication Systems*, PhD Thesis, DTU Fotonik, 2009. ISBN 87-92062-26-1.

[8] Peter.J. Winzer, and R-J. Essiambre, "Advanced Modulation Formats for High-Capacity Optical Transport Networks," *J. Lightw. Technol.*, vol. 24, no. 12, pp. 4711–4728, Dec. 2006.

[9] Xiang Zhou and Jianjun Yu , "Multi-Level, Multi-Dimensional Coding for High-Speed and High-Spectral-Efficiency Optical Transmission," *J. Lightw. Technol.*, vol. 27, no. 16, pp. 3641–3653, Aug. 2009.

[10] A.F. Shalash, and K.K. Parhi, "Multidimensional carrierless AM/PM systems for digital subscriber loops," *IEEE Trans. on Comm.*, vol. 47, no.11, pp.1655-1667, 1999.

[11] J. J. Werner,"Tutorial on Carrierless AM/PM- Part I: Fundamentals of digital CAP transmitter," *AT&T Contribution to ANSI X3T9.5 TP/PMD*, June 1992.

[12] J. J. Werner,"Tutorial on Carrierless AM/PM- Part II: Performance of bandwidth efficient line codes," *AT&T Contribution to ANSI X3T9.5 TP/PMD*, Feb. 1993.

[13] B. Whyte,*Multimedia Telecommunication*, Chapman & Hall, 1997.

[14] P.J. Kyees, R.C. McConnell, K. Sistanizadeh,"ADSL: A New Twisted-Pair Access to the Information Highway," *IEEE Commun. Mag.* vol. 33, no.4, pp.52-60, 1995.

[15] T. Collins, *Carrierless Amplitude Phase Modulation, Handbook of Computer Networks: Key Concepts, Data Transmission, and Digital and Optical Networks*, John Wiley and Sons, 2008.

[16] Antonio Caballero, Tien Thang Pham, Jesper B. Jensen, and Idelfonso Tafur Monroy, "Carrierless N-Dimensional Modulation Format for Multiple Service Differentiation in Optical In-home Networks,"*International Photonics Conference (IPO)*, TuM4, 2011.

[17] Xiaosong Tang, I.L.-J. Thng, Xinrong Li,"A new digital approach to design 3D CAP waveforms," *IEEE Trans. on Comm.*, vol.51, no.1, pp. 12– 16,2003.

[18] Paul R. Prucnal, Mario A. Santoro, Ting Rui Fan, "Spread Spectrum Fiber-optic Local Area Network Using Optical Processing," Journal of Lightwave Technology, vol. 4, pp. 547-554, May 1986.

[19] Mikaël Morelle, C. G.-Brugeaud, A.-J. Vergonjanne, J.-P. Cances, "Quality of service differentiation in multimedia 2D optical networks," in *15th European Signal Processing Conference (EUSIPCO)*, 2007.

[20] FP7 Report, *Survey of next generation optical access system concepts*, 2010.

[21] A.F. Shalash and K.K. Parhi,, "Three-Dimensional carrierless AM/PM Line code for the Unshielded Twisted Pair Cables," in *Proceedings of the IEEE ISCAS'96*, 1997.

[22] G.-K. Chang, A. Chowdhury, Z. Jia, H.-C. Chien, M.-F. Huang, J. Yu, and G. Ellinas, "Key technologies of WDM-PON for future converged optical broadband access networks [invited]," *IEEE/OSA J. Opt. Commun. and Networking*, vol. 1, no. 4, pp. C35 –C50, sept. 2009.

[23] T. Kuri, H. Toda, J. Olmos, and K. Kitayama, "Reconfigurable dense wavelength-division-multiplexing millimeter-waveband radio-over-fiber access system technologies," *J. Lightw. Technol.*, vol. 28, no. 16, pp. 2247 –2257, aug. 15, 2010.

[24] Y.-Y. Won, H.-S. Kim, Y.-H. Son, and S.-K. Han, "Full colorless WDM-radio over fiber access network supporting simultaneous transmission of millimeter-wave band and baseband gigabit signals by sideband routing," *J. Lightw. Technol.*, vol. 28, no. 16, pp. 2213 –2218, aug. 15, 2010.

[25] C. Lim, A. Nirmalathas, M. Bakaul, P. Gamage, K.-L. Lee, Y. Yang, D. Novak, and R. Waterhouse, "Fiber-wireless networks and subsystem technologies," *J. Lightw. Technol.*, vol. 28, no. 4, pp. 390–405, 2010.

[26] T. Higashino, K. Miyamoto, K. Tsukamoto, S. Komaki, T. Tashiro, K. Hara, J. Kani, N. Yoshimoto, and K. Iwatsuki,"A New Confguration of Broadband Wireless Access in Heterogeneous Ubiquitous Antenna and Its Experimental Investigation," *PIERS Proceedings*, 2011.

[27] M. Sauer, A. Kobyakov, J.George, "Radio over fiber for picocellular network architectures," *J. Lightw. Technol.*, vol. 25, no. 11, pp. 3301-3320, 2007.

[28] I. Harjula, A. Ramirez, F. Martinez, D. Zorilla, M. Katz, V. Polo, "Practical issues in the combining of MIMO techniques and RoF in OFDM/A systems," *Proc. of the 7th WSEAS*, pp. 244–248 , 2008.

[29] D.D. Falconer, *Carrierless AM/PM" in Bell Laboratories Technical Memorandum*, 1975.

[30] I. Thng, Xinrong Li, Chi Chung Ko, "A new 3D CAP system," *Proceedings of the IEEE Region 10 Conference (TENCON 99)*, vol. 1, pp. 309 - 312, 1999.

[31] Xiaosong Tang; I.L.-J. Thng, "An NS frequency-domain approach for continuous-time design of CAP/ICOM waveform," *IEEE Transactions on Communications*, vol.52, no.12, pp. 2154–2164, Dec. 2004

[32] J. D. Ingham, R. Penty, I. White, and D. Cunningham, "40 Gb/s Carrierless Amplitude and Phase Modulation for Low-Cost Optical Datacommunication Links," in *Optical Fiber Communication/National Fiber Optic Engineers Conference (OFC)*,OThZ3, 2011.

[33] M. Wieckowski, J. B. Jensen, I. Tafur Monroy, J. Siuzdak, and J. P. Turkiewicz, "300 Mbps transmission with 4.6 bit/s/Hz spectral efficiency over 50 m PMMA POF link using RC-LED and multi-level Carrierless amplitude phase modulation," in *Optical Fiber Communication/National Fiber Optic Engineers Conference (OFC)*,NTuB8, 2011.

[34] Roberto Rodes, et.al,"Carrierless amplitude phase modulation of VCSEL with 4bit/s/Hz spectral efficiency for use in WDM-PON," *Optics Express*, vol.19, no.27, 2011.

[35] Roberto Rodes, Marcin Wieckowski, Tien-Thang Pham, Jesper Bevensee Jensen, and Idelfonso Tafur Monroy,"VCSEL-based DWDM PON with 4 bit/s/Hz Spectral Efficiency using Carrierless Amplitude Phase Modulation," in *European Conference and Exposition on Optical Communications (ECOC)*,Mo.2.C.2, 2011.

[36] J. D. Ingham, R. V. Penty, I. H. White and D. G. Cunningham, "Carrierless Amplitude and Phase Modulation for Low-Cost, High-Spectral-Efficiency Optical Datacommunication Links," *Conference on Lasers and Electro-Optics (CLEO) and Quantum Electronics and Laser Science Conference (QELS), 2010*, CThC5, 2010.

[37] J. H. Winters, "On the capacity of radio communications systems with diversity in a Rayleigh fading environments," *IEEE J. Selected Areas Communication* vol.5, no.5, pp. 871–878, Jun 1987.

[38] G. J. Foschini and M. J. Gans, "On limits of wireless communications in a fading environment when using multiple antennas," *Wireless Personal Communications* , vol.6 , pp. 311-335, 1998.

[39] I. E. Telatar, "Capacity of multi-antenna Gaussion channels," *European Trans Communications* , vol.10 , pp. 585-595, 1999.

[40] A. F. Molisch, " MIMO systems with antenna selection - an overview,", *Proceedings Radio and Wireless Conference (RAWCON)*, T2B.1, pp. 167–170, 2003.

[41] H. Sampath, S. Talwar, J. Tellado, V. Erceg, A.Paulraj, "A fourth-generation MIMO-OFDM broadband wireless system: design, performance, and field trial results," *IEEE Comm. Magazine*, vol. 40 , no.9, pp. 143–149, 2002.

[42] H. Bolcskei, " MIMO-OFDM wireless systems: basics, perspectives, and challenges,", *IEEE Wireless Communications*, vol. 13, no.4, pp. 31–37, 2006.

[43] A.J. Paulraj, D.A. Gore, R.U. Nabar, H.Bolcskei, "An overview of MIMO communications - a key to gigabit wireless," *Proceedings of the IEEE* vol. 92, no.2, pp. 198–218, 2004.

[44] S. Nema, et.al, "Integrated DWDM and MIMO-OFDM System for 4G High Capacity Mobile Communication," *Signal Processing an International Journal*, vol. 3, no.5, 2010.

[45] A. Kobyakov, M. Sauer, A. Ng'oma, J.H. Winters, "Effect of Optical Loss and Antenna Separation in 2x2 MIMO Fiber-Radio Systems," *IEEE T. Ant & Prop*, vol. 58, no. 1, 2010.

[46] K. Prince, J. B. Jensen, A. Caballero, X. Yu, T. B. Gibbon, D. Zibar, N. Guerrero Gonzalez, A. V. Osadchiy, and I. Tafur Monroy, "Converged wireline and wireless access over a 78-km deployed fiber long-reach WDM PON," *IEEE Photon. Technol. Lett.*, vol. 21, no. 17, pp. 1274–1276, 2009.

[47] W-T. Shaw, et al., "An Ultra-Scalable Broadband Architecture for Municipal Hybrid Wireless Access Using Optical Grid Network," *Optical Fiber Communication/National Fiber Optic Engineers Conference (OFC)*, OThP2, 2009.

[48] Z. Jia, J. Yu, et al., "Key enabling technologies for optical-wireless networks: optical millimeter-wave generation, wavelength reuse, and architecture," *IEEE Journal of Lightwave Technology*, vol. 25, no.11, pp.3452-3471, (2007).

[49] K. Tsukamoto, T. Nishiumi, T. Yamagami, T. Higashino, R. Kubo, T.Taniguchi, J. Kani, N. Yoshimoto, H. Kimura and K. Iwatsuki, "Convergence of WDM Access and Ubiquitous Antenna Architecture for Broadband Wireless Services," *Proc. 6th PIERS Conf.*, no. 4, pp. 385-389, Apr. 2010.

[50] T. Tashiro, K. Miyamoto, K. Hara, T. Taniguchi, J. Nakagawa, N.Yoshimoto, K. Iwatsuki, T. Nishiumi, T. Higashino, K. Tsukamoto, and S. Komaki, "Broadband Ubiquitous Network Based on RoF-DAS over WDM-PON," *Optical Fiber Communication Conference, OSA Technical Digest*, paper OWT2, 2011.

[51] K. Tsukamoto, T. Iwakuni, K. Miyamoto, T. Higashino, S. Komaki, T. Tashiro, Y. Fukada, J.-I. Kani, N. Yoshimoto, and K. Iwatsuki, "RoF-DAS over WDM-PON Using Bandpass-sampling and Optical TDM Techniques as Universal Entrance Network for Broadband Wireless Access," *Progress In Electromagnetics Research Symposium Proceedings*, pp. 491-495, 2012.

[52] Chun-Ting Lin, Anthony Ng'oma, Wei-Yuan Lee, Chia-Chien Wei, Chih-Yun Wang, Tsung-Hung Lu, Jyehong Chen, Wen-Jr Jiang, and Chun-Hung Ho, "2×2 MIMO radio-over-fiber system at 60 GHz employing frequency domain equalization," *Optics Express*, vol. 20, no. 1, pp. 562–567, 2012.

[53] Sander L. Jansen and Itsuro Morita, "Polarization Division-Multiplexed Coherent Optical OFDM Transmission Enabled by MIMO Processing," *High Spectral Density Optical Communication Technologies Optical and Fiber Communications Reports*, Chapter 8, vol.6, Part 2, pp. 167–178, Springer, 2010.

[54] S.-H. Fan, H.-C. Chien, A. Chowdhury, C. Liu, W. Jian, Y.-T. Hsueh, and G.-K. Chang, "A novel radio-over-fiber system using the xy-MIMO wireless technique for enhanced radio spectral efficiency," in *36th European Conference and Exhibition on Optical Communication (ECOC)*, Paper Th.9.B.1., 2010.

[55] X. Liu and F. Buchali, "Intra-symbol frequency-domain averaging based channel estimation for coherent optical OFDM", *Opt. Express* vol. 16, no. 26, pp. 21944-–21957, 2008.

[56] X. Liu, S. Chandrasekhar, B. Zhu, P. J. Winzer, A. H. Gnauck, and D. W. Peckham, "448-Gb/s reduced-guardinterval CO-OFDM transmission over 2000 km of ultra-large-area fiber and five 80-GHz-Grid ROADMs," *J. Lightwave Technol.* vol. 29, no. 4, pp. 483–490, 2011.

[57] S.L. Jansen, I. Morita, T.C. Schenk, H. Tanaka, "Long-haul transmission of 16×52.5 Gbits/s polarization-division multiplexed OFDM enabled by MIMO processing," *J. Opt. Netw.*, vol. 7, pp. 173-182, 2008.

[58] W. Shieh, H. Bao, and Y. Tang, "Coherent optical OFDM: theory and design," *Optics Express*, vol. 16, pp. 841–859, Jan. 2008.

[59] Y. S. Cho, J. Kim, W. Y. Yang, and C. G. Kang, *MIMO-OFDM wireless communications with MATLAB*, John Wiley & Sons (Asia), Singapore, 2010.

[60] P. Johannisson, H. Wymeersch, M. Sjo¨din, A.S. Tan, E. Agrell, P. Andrekson, M. Karlsson, "Convergence comparison of CMA and ICA for blind polarization demultiplexing of QPSK and 16-QAM signals," *36th European Conference and Exhibition on Optical Communication (ECOC)*, Paper Th.9.A.3., 2010.

[61] Eli Kapon, Alexei Sirbu, "Long-wavelength VCSELs: Power-efficient answer," Nature Photonics 3, pp. 27 – 29, 2009.

[62] J.L. Wei, J.D. Ingham, D.G. Cunningham, R.V. Penty, and I.H. White, "Comparisons between 28 Gb/s NRZ, PAM, CAP and optical OFDM systems for Datacommunication Application," *IEEE Optical Interconnects Conference*, pp.3–4, 2012.

[63] J.L. Wei, L.Geng, D.G. Cunningham, R.V. Penty, and I.H. White, "Comparisons between Gigabit NRZ, CAP and Optical OFDM Systems over FEC Enhanced POF Links using LEDs," *ICTON* , Tu.P.17, 2012.

[64] J. L. Wei, L. Geng, D.G. Cunningham, R.V. Penty, and I. H. White, "Gigabit NRZ, CAP and optical OFDM systems over POF links using LEDs," *Optics Express*, vol. 20, no. 20, pp. 22284-22289, 2012.

[65] Corning Cable System, "Multimode Optical Fiber Selection & Specification," Applications Engineering Notes, AE Note 75, Revision: 11, pp. 1–10, 2012.

[66] Olaf Ziemann, Hans Poisel, Sebastian Randel, Jeffrey Lee, "Polymer optical Fibers for short, shorter and shortest data links," *Optical Fiber Communication/National Fiber Optic Engineers Conference (OFC)* OWB1, 2008.

[67] Davide Visani et. al., "Beyond 1 Gbit/s Transmission Over 1 mm Diameter Plastic Optical Fiber Employing DMT for In-Home Communication Systems," *Journal of Lightwave Tech.*, vol. 29, no.4, pp. 622–628, 2011.

[68] I. Mollers, D. Jager, R.Gaudino, A. Nocivelli, H. Kragl, O. Ziemann, N. Weber, T. Koonen, C. Lezzi, A. Bluschke, S. Randel, "Plastic optical fiber technology for reliable home networking: overview and results of the EU project pof-all," *IEEE Communications Magazine*, vol. 47, no.8, pp. 58–68, 2009.

[69] S.K. Das, T. Ranjan Swain, S.K. Patra,"Impact of in-band crosstalk & crosstalk aware datapath selection in WDM/DWDM networks," *International Conference on Advances in Engineering, Science and Management (ICAESM)*, pp. 180–185, 2012.

[70] Y. Benlachtar, R.Bouziane, P. Milder, R. Koutsoyannis, C.R. Berger, J.C. Hoe, M. Pu¨schel, P.M. Watts, M. Glick, R.I. Killey, "Real-time DSP-based optical OFDM transmission," *23rd Annual Meeting of the IEEE Photonics Society*, pp. 665-666, 2010.

[71] S.C.J. Lee, F. Breyer, D. Cardenas, S. Randel, A.M.J. Koonen, "Real-time gigabit DMT transmission over plastic optical fibre," *Electronics Letters* , vol. 45, no. 25, pp. 1342–1343, 2009.

[72] Anthony Ng'oma, "Radio-over-Fiber Techniques and Applications for Multi-Gb/s In-Building Wireless Communication," *Access Networks and In-house Communications (ANIC)*, paper ATuB1, 2011.

[73] Atsushi Kanno, Keizo Inagaki, Isao Morohashi, Takahide Sakamoto, Toshiaki Kuri, Iwao Hosako, Tetsuya Kawanishi, Yuki Yoshida, and Ken-ichi Kitayama "40 Gb/s W-band (75–110 GHz) 16-QAM radio-over-fiber signal generation and its wireless transmission," *Optics Express*, vol. 19, no. 26, pp. B56-B63, 2011.

[74] Xiaodan Pang, Antonio Caballero, Anton Dogadaev, Valeria Arlunno, Robert Borkowski, Jesper S. Pedersen, Lei Deng, Fotini Karinou, Fabien Roubeau, Darko Zibar, Xianbin Yu, and Idelfonso Tafur Monroy, "100 Gbit/s hybrid optical fiber-wireless link in the W-band (75–110 GHz)," *Optics Express*, vol. 19, no. 25, pp. 24944-24949 , 2011.

[75] L. Deng, D. Liu, X. Pang, X. Zhang, V. Arlunno, Y. Zhao, A. Caballero, A. K. Dogadaev, X. Yu, I. T. Monroy, M. Beltran, and R. Llorente,"42.13 gbit/s 16qam-OFDM photonics-wireless transmission in 75-110 GHz band," *Progress In Electromagnetics Research*, vol. 126, pp. 449-461, 2012.

[76] Atsushi Kanno, Toshiaki Kuri, Iwao Hosako, Tetsuya Kawanishi, Yoshihiro Yasumura, Yuki Yoshida, and Ken-ichi Kitayama ,"Optical and Radio Seemless MIMO transmission with 20-Gbaud QPSK," *38th European Conference and Exhibition on Optical Communication (ECOC)*, Paper We.3.B.2., 2012.

[77] W.Shieh and I. Djordjevic, *OFDM for Optical Communication*, Chapter 1 & 12, Elsevier, 2010.

[78] Pramodini D.V. and A.G. Ananth, "Study of the performance of linear and non-linear narrowband receivers for $2x2$ MIMO systems with STBC multiplexing and Almouti Coding," *International Journal of Electrical and Electronics Engineering Research*, vol. 1, no. 1, pp. 68–83, 2011.

List of Acronyms

1D	1 dimensional
2D	2 dimensional
3D	3 dimensional
4D	4 dimensional
6D	6 dimensional
ANSI	American national standards institute
ADSL	asymmetrical digital subscriber line
ASK	amplitude shift keying
ATM	asynchronous transfer mode
BS	base station
CAP	carrierless amplitude-phase
CDMA	code division multiple access
CMA	constant modulus algorithm
DAS	distributed antenna system
DSP	digital signal processing
DMT	discrete multitone
DQPSK	differential quadrature phase shift keying
DSL	digital subscriber line

DSP	digital signal processing
DWDM	dense wavelength division multiplexing
D8PSK	differential 8-ary phase shift keying
ETSI	European telecommunications standards institute
FTTH	fiber-to-the-home
GPS	global positioning system
HAN	home access network
L/D	levels per dimension
MIMO	multi-input multi-output
MMF	multimode fiber
NGA	next generation access
NGAN	next generation access network
OA	optimization algorithm
OCDMA	optical code division multiple access
ODMA	orthogonal division multiple access
OOFDM	optical OFDM
OOK	on-off keying
PAM	pulse amplitude modulation
PDM	polarization division multiplexing
PMD	polarization mode dispersion
POF	polymer optical fiber
PON	passive optical network
QAM	quadrature amplitude modulation
RAU	remote antenna unit

RC-LEDs	resonant cavity light emitting diodes
RF	radio frequency
RoF	radio-over-fiber
SAC-OCDMA	spectral amplitude coding - optical code division multiple access
SISO	single-input single-output
SMF	single mode fibre
SSMF	standard single mode fibre
WDM	wavelength division multiplexing
WLANs	wireless local area networks
WMANs	wireless metropolitan area networks
x-DSL	x-digital subscriber line